

Alma Mater Studiorum – Università di Bologna

DOTTORATO DI RICERCA IN

Scienze farmacologiche e tossicologiche, dello sviluppo e del movimento umano

Ciclo 29°

Settore Concorsuale di afferenza: 05/E1

Settore Scientifico disciplinare: BIO/10

TITOLO TESI

**Longevity, aging and DNA damage:  
investigation of the role of 53BP1 in the maintenance of genomic stability**

Presentata da: Dott.ssa Eleonora Croco

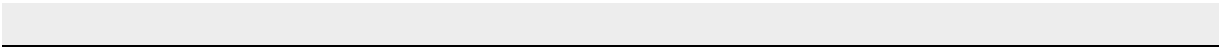
Coordinatore Dottorato

Prof.ssa Patrizia Hrelia

Relatore Prof. Claudio Stefanelli

Co-relatore Dr. Antonello Lorenzini

Esame finale anno 2017



---

*“Nothing in the world has ever been accomplished without passion”*

*(George Wilhelm Friedrich Hegel)*

# CONTENTS

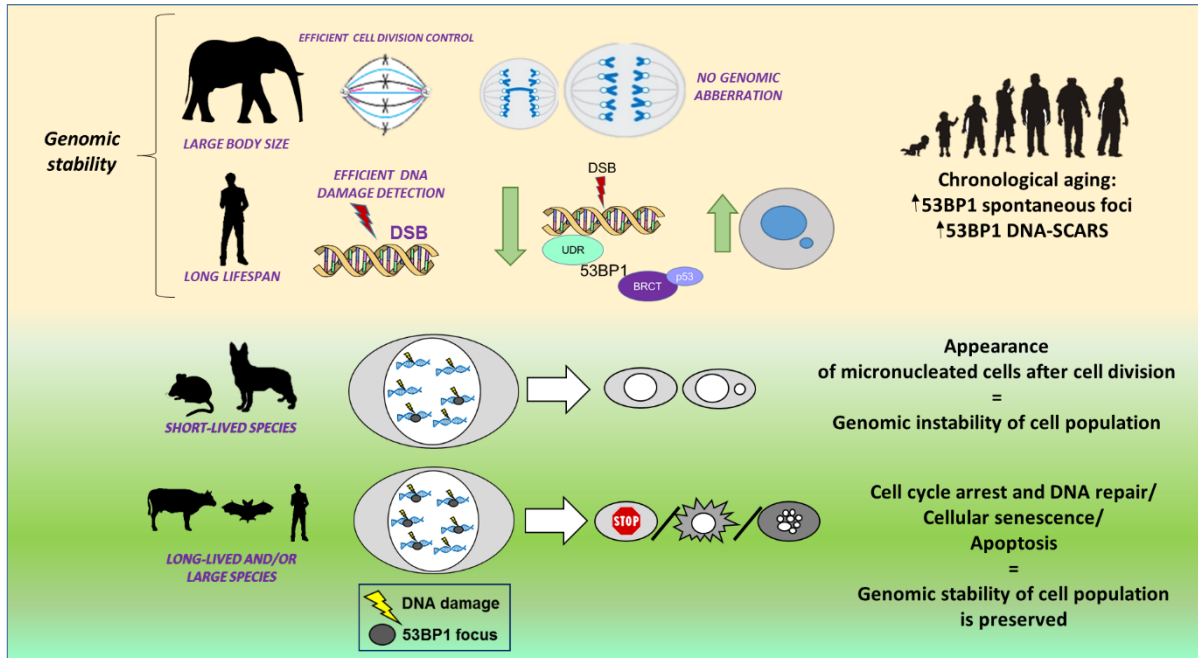
Graphical abstract .....	7
1. Introduction.....	8
1.1 Common features of cellular aging.....	9
1.1.1 Telomere attrition .....	9
1.1.2 Epigenetic alteration. ....	10
1.1.3 Genomic instability.....	11
1.2 Theories of aging.....	12
1.2.1 Free radical theory of aging.....	13
1.2.2 DNA damage theory of aging.....	14
1.3 DNA damage.....	15
1.3.1 DSB, NHEJ PATHWAY and DNA END BINDING ACTIVITY.....	16
1.3.2 Role of 53BP1 in DNA damage recognition.....	18
1.3.3 DNA damage foci.....	21
1.3.4 Micronuclei.....	22
2. Aim of the thesis.....	24
2.1 Project description.....	25
2.1.1 Part I- DNA damage and species longevity: possible role of 53BP1.....	25
2.1.2 Part II- Genetic instability and aging under the scrutiny of comparative biology.....	27
Genomic stability and body mass.....	28
Advantages of the comparative approach.....	29
Analysis of micronucleated erythrocyte frequency across mammals.....	29
2.1.3 Part III- Role of 53BP1 in chronological age.....	30
3. Material and methods.....	32
3.1 Cell culture.....	32
3.2 Freezing and thawing cells.....	34
3.3 Genotoxic treatment.....	34
3.4 Preparation of whole lysates.....	35
3.5 Polyacrylamide gel electrophoresis.....	36

3.6	SDS-PAGE and western blotting.....	36
3.7	Immunofluorescence: foci determination.....	36
3.8	Micronuclei assay.....	37
3.9	DNA synthesis assessment.....	38
3.10	Comet assay.....	39
3.11	Cellular viability assay.....	39
3.12	Cell cycle analysis.....	39
3.13	B-galactosidase assay.....	40
3.14	Annexin V assay.....	40
3.15	CRISPR-CAS9 technology to break down 53BP1 expression.....	41
3.16	Preparative restriction digestion.....	42
3.17	Ligation, electrophoresis and gel recovery of DNA from agarose gels.....	42
3.18	Transformation of competent E. Coli.....	43
3.19	Mini prep.....	43
3.20	Maxi prep.....	43
3.21	Sequencing of plasmids.....	43
3.22	Keratinocytes transfection for stable transformation.....	44
3.23	Clonogenic assay formation.....	44
3.24	Survival assay.....	44
3.25	Microscopy.....	45
3.26	Data analysis and database.....	45
3.27	Statistical analysis.....	45
4.	Results.....	48
4.1	Part I- DNA damage and species longevity: possible role of 53BP1.....	48
4.1.1	Measuring toxicity across the species.....	48
4.1.2	Dose response experiments in 53BP1 foci formation.....	49
4.1.3	53BP1 co-localize with $\gamma$ H2AX after 5 $\mu$ M ETO treatment.....	51
4.1.4	Long lived species exhibit the highest percentage of 53BP1 foci and protein level.....	52
4.1.5	Genotoxic treatment induce 53BP1-PMLnb co-localization and increase of senescence in longer lived species.....	56

4.1.6	Genotoxic stress induce cell cycle arrest in all the species.....	58
4.1.7	Long-lived species induce higher level of apoptosis.....	61
4.1.8	Human DNA generally appears more or equally resistant to fragmentation.....	61
4.1.9	Measuring unresolved damage.....	64
4.1.10	53BP1 foci are inversely correlated with micronuclei abundance.....	66
4.2	Part I- 53BP1 down regulation in keratinocytes cell lines.....	67
4.2.1	53BP1 knock down clone selection.....	67
4.2.2	Stable 53BP1 knock down clone reduces cellular growth.....	69
4.2.3	Down regulation of 53BP1 reduces survival rate in response to damage.....	69
4.2.4	53BP1 down regulation is associate to increased genomic instability.....	70
4.3	Part II- Genetic instability and aging under the scrutiny of comparative biology: a meta-analysis of spontaneous micronuclei frequency.....	72
4.3.1	Body mass and MNEF are inversely correlated.....	72
4.3.2	Residuals and phylogenetically independent contrasts analyses.....	74
4.4	Part II- Role of 53BP1 in chronological age.....	75
4.4.1	Small increase of spontaneous 53BP1 foci in middle and old donors.....	75
4.4.2	Absence of micronuclei increase with chronological age.....	76
4.4.3	Higher rate of DNA-SCARS in old donors.....	77
5.	Conclusion.....	79
6.	List of references.....	87

## Graphical abstract

*In brief:* a comparative biology approach offers a powerful observational point, through which we aimed to explore the possible link between DNA damage and longevity, by investigating the role of 53BP1 protein as a determinant for a long lifespan.



### Highlights:

1. A comparative analysis in five mammalian species of 53BP1 repair foci and micronuclei expression shows an inverse correlation of these two DNA damage markers: higher level of 53BP1 foci are associated to lower incidence of micronuclei formation.
2. By CRISPR-CAS9 methodology, a 53BP1 knock down model, comparable to the difference observed among species, was reproduced: stable downregulation of 53BP1 is associated to lower survival and increase of micronuclei frequency in response to DNA damage.
3. Spontaneous micronuclei (MN) frequency is inversely proportional to adult body mass.
4. 53BP1 as DNA damage marker for the aging process: increased spontaneous 53BP1 foci level and small decrease of repair efficiency are associated to the increase of chronological age, in human donors.

## 1. INTRODUCTION

Aging is a universal and inevitable evolution of life, characterized by global loss of physiological integrity and homeostatic imbalance [1] associated to a progressive decline of tissues and organ functions, to an impaired ability to respond to stress and to an increasing incidence of diseases. All these changes are the results of a side effect of normal metabolism, which is in turn exacerbated by environmental influence and unhealthy lifestyle [2]. The general worsening of the physiological state, which rise up during aging, is considered the primary risk factor for several diseases including neurodegenerative pathologies, diabetes, cardiovascular disorders, and cancer [3]. Therefore, death is a consequence of advancing of age. In the last decades, the improvements in hygiene and social health led significant increase in life expectancy and to a growing number of elderly people worldwide.

So, now more than ever, modern society has to deal with a whole range of social and health problems related to the global population's aging. The need to solve the aging-related problems and the utopian dream of counteracting the effect of time, have prompted the

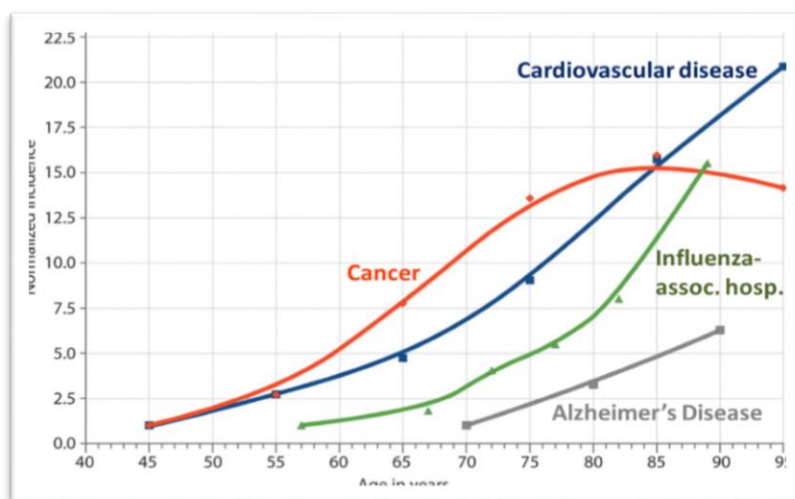


Figure 1: Chronic diseases and aging. Figure from [2]

scientific community to investigate all the phenomena related to aging and, more in general, to longevity. The “systemic” aging can be considered as the resulting effect of all the changes taking place inside our body. In fact, the physiological basis of these phenomena lay in the

progressive lifelong accumulation of deleterious changes that impair the structure of our body at the tissue, cellular and, primarily, molecular level [2]. This is the reason why scientists attempted to find some common features of the aging process and tried to elaborate valuable theories to explain aging; some of them will be explained in the present work.

## 1.1 Common features of cellular aging

Aging research has developed deeply in the last decades and, over this time, a growing knowledge of the molecular and cellular basis of life and disease has been produced. In 2013 a group of scientists, driven by the need to conceptualize the basic and common features of aging, draw up a “list” of nine hallmarks of aging [3]; these hallmarks are: 1) altered intercellular communication; 2) stem cell exhaustion; 3) cellular senescence; 4) mitochondrial dysfunction; 5) deregulated nutrient sensing; 6) loss of proteostasis; 7) telomere attrition; 8) epigenetic alteration; 9) genomic instability. Only the last three will be presented in this thesis.



Figure 2: The hallmarks of aging. Figure from [3]

### 1.1.1 Telomere attrition

Telomeres are specialized structures of terminal repeated sequences of DNA, which lay at the extremity of each chromosome. During every cell division, a small part of the telomeric DNA is inevitably lost, due to the inability of DNA polymerase (which in human is active in the germline and stem cell lines, but not in somatic cells) to replicate the DNA ends. the consequence of this physiological process is the gradual shortening of telomeres, the alteration of the telomeric structure and, consequently, replicative senescence [4][5].

Telomeres can be regenerated by the activation of the telomerase enzyme; for example ectopic expression of telomerase can promote immortalization of primary cell culture, without inducing oncogenic transformation [6]. Telomeres' shortening is a phenomenon occurring both in human and in mice, as a feature of normal aging [7]. In fact, it has been showed that telomerase deficiency in human is associated with premature development of diseases, such as pulmonary fibrosis, dyskeratosis congenita, and aplastic anemia, diseases connected to the loss of the regenerative capacity of different tissues [8]. Experimental evidence support that the same hypothesis is valuable in mice, where telomere length is associated with aging and control of lifespan: mice with shortened or lengthened telomeres exhibit respectively decreased or increased lifespans length [9][10][11].

Since it has become clear that in most cases what it is limiting replicative capacity in vitro is telomere shortening [6], telomere biology has been deeply investigated also across species in cell culture systems [12][13][14]. Stuart *et al.* [15] clearly showed that telomerase activity is low or absent and telomeres are short in long lived and large species and the opposite is true in short and small species. Than it is reasonable to suggest that convergent evolution is at play using short telomere and absence of telomerase activity as a protective mechanisms to limit tumor growth. Larger species, in fact, having more cells, have more potential targets to transformation; additionally, long lived species have more time to accumulate tumor predisposing mutations. This contradiction is clearly summarized into the "Peto's paradox" which states that the risk to develop a tumor per gram of tissue is 3 trillion times smaller in a human than in a mouse [16]. Moreover it has been widely shown that telomerase activity is linked to tumorigenesis, as well: a big percentage of tumors, which generally originate from the transformation of somatic cells, exhibits absence of telomeres shortening and restoration of telomerase activity, with the consequence of unlimited growing capacity and inhibition of replicative senescence.

All these evidence led to the idea that telomere attrition, in mammals, can be considered a common feature of physiological aging.

### 1.1.2 Epigenetic alteration

Conrad Waddington (1905–1975) defined epigenetics as "the branch of biology which studies the causal interactions between genes and their products, which bring the phenotype into being" [17]. More in general epigenetic can be defined as a set of changes which alter the final

outcome of the expression of a locus or a chromosome, without changes in the correspondent DNA sequence. In this context, the idea that many of the epigenetic changes which arise during organisms' development and growth may be involved in the aging process started to spread. For example chromatin remodelling, posttranslational modification of histones, as increased histone H4K16 acetylation, as well as modification of the DNA methylation patterns (H4K20 or H3K4 trimethylation, as well as decreased H3K9 methylation) have been showed to be related to age-associated epigenetic marks [18][19]. In fact some epigenetic markers that are remodelled during reprogramming (like the above mentioned DNA methylations, post-translational modifications of histones and chromatin remodelling) are impaired during aging [20][21][22]. Moreover, cellular differentiation may be also considered an epigenetic phenomenon, largely governed by epigenetic changes, accordingly to Waddington, rather than alterations in genetic inheritance [23]. Thus, epigenetic dysregulation has emerged as one of the key hallmark of the aging process [1]. Studies on the SIRT6, a stress responsive protein deacetylase and mono-ADP ribosyl-transferase enzyme involved in epigenetic changes, showed that its loss of function reduces longevity; on the contrary SIRT6 gain of function was associated to an extended longevity in mice [24][25]. Furthermore, the discovery of the Yamanaka factors, also known as "reprogramming factors" (the transcription factors Oct4 (Pou5f1), Sox2, cMyc, and Klf4), supports the idea that epigenetic changes have a strong influence on lifespan length and opens a new era on the epigenetic studies. Several groups have observed an amelioration of age-associated cellular phenotypes during in vitro cellular reprogramming [26][27][28][29]. It has been also shown that cellular reprogramming obtained by transient expression of Yamanaka factors ameliorated age-associated symptoms, prolonged lifespan in progeroid mice, and improved tissue homeostasis in older mice [30]. Taken all together, these works suggest that understanding epigenetic mechanisms is a fundamental step towards an improvement for the cure of age-related pathologies and for extension healthy lifespan.

### **1.1.3 Genomic instability**

The DNA integrity and stability are constantly challenged by exogenous physical, chemical, and biological agents; but endogenous activity, such as DNA replication, spontaneous hydrolytic reactions and reactive oxygen production, can also represent a source of damage which may impair DNA integrity. Several scientific evidences strengthen the idea of a tight link

between genomic stability and aging. The most important experimental evidence comes from the observation that several progeroid syndromes, such as Werner syndrome, Bloom syndrome, xeroderma pigmentosum, trichothiodystrophy, Cockayne syndrome or Seckel syndrome are characterised by defects on DNA damage repair pathways [31][32][33]. Somatic mutations accumulate within cells from aged humans and model organisms [34]. Other forms of DNA damage can accumulate during aging: Faggioli *et al.* showed an increase of chromosomal aneuploidies in the brain of aged mice [35] and Forsberg *et al.* identified in human an association between aging and the copy-number variations, *in vivo* [36].

Genomic instability can also induce structural and numerical chromosome aberrations in somatic cells which, if not properly repaired, can lead to dangerous outcomes for cell's life.

An investigation on the efficiency of the spindle assembly checkpoint, which is a critical element in regulating chromosome segregation by preventing chromosome mis-segregation and aneuploidy, showed that its efficiency is higher in large species; thus species' longevity does not appear as a key factor [37]. Although this analysis suggests that an increased efficiency of the spindle assembly check point could be more important for evolving large body size than longevity, this does not exclude the possibility that aneuploidy may negatively affect life span. Baker *et al.*, in fact, report that mice with low levels of the spindle assembly checkpoint protein BubR1, display progeroid features, dwarfism, lordokyphosis, and short lifespan [38]. Moreover they showed that transgenic mice overexpressing BubR1 exhibit an increased protection against aneuploidy and cancer, and extended healthy lifespan [39]. All these data together suggest that maintenance of genomic stability is an important feature in order to achieve long lifespan length.

### 1.2 The theories of aging

Multiple theories have been proposed to explain the aging process with significant experimental support, and it is easy to understand that the various theories of aging can overlap at different levels of organization. In the 90's, Kowald and Kirkwood elaborated a theory according to which a "single-factor" process strived for explain the complex mechanism of aging, assuming that a single cause could be responsible for this phenomenon [40]. But in biogerontology there is a growing appreciation that the process of aging is a multifactorial process and that it may not operate in similar fashion in all species [41]. This is probably because different species have evolved different strategies to counteract spontaneous

molecular damage and random malfunctioning of biological machineries. The different efficiency of these strategies could explain the different rate of aging observed across species [42] and why aging is not a universal process [43]. So based on evidence that several mechanisms may interact simultaneously operating at different levels of functional organization, the "single-factor" theory of aging was completely replaced by the vision that aging is the result of a complex multifactorial process, characterized by physiological, genetic and molecular changes that occur over time, as determined by intrinsic, extrinsic (environmental) and stochastic (spontaneous changes within molecules) causes that involve all living species. Therefore, it is possible to speculate that several "single-factor" theories alone can explain just a part of the phenomena, but cannot clarify the aging process in its entirety. Although there are many theories regarding aging, in the present thesis we will deep analyse just two of these theories, which are mostly accredited by the scientific community and useful for the present discussion: 1) free-radicals theory of aging (FRTA); 2) DNA damage theory of aging.

### **1.2.1 Free-radical theory aging**

The free-radical theory of aging is based on the hypothesis that aging is the result of the cellular accumulation of oxidative damage, as a consequence of reactive oxygen species (ROS) released by the mitochondria. We are all living in an environment which leads to ROS production and it has been extensively demonstrated that the concentration of free radicals grows with the increase of metabolic activity [44]. Moreover it is supposed that the individual reactivity or resistance to free radicals stress is improved over time, indeed it is not a pre-determined factor. DNA molecules, proteins and lipids are all possible targets of oxidative damage that occur at cellular level [45]. The FRTA in fact suggests that 1) the production of mitochondrial ROS determines the rate of aging; 2) over time, free radicals are produced faster; 3) with aging, damage caused by ROS production is no longer efficiently repaired. Differences in how different organism handle oxidative damage were also found among the mammalian species. Some authors suggest that long-lived species produce lower levels of ROS when compared to short-lived species; while others demonstrated that rodents under caloric restriction live longer and produce less ROS when compared to controls [46].

Rossini used and tested the FRTA to explain the exceptional longevity of *M. lucifugus* (maximum lifespan= 34 years). In a comparative study, the O<sub>2</sub> consumption and the

production of mitochondrial  $H_2O_2$  in several organs (heart, brain and kidneys) was measured in *M. lucifugus* (little brown bat, long-lived bat) and *Blarina brevicauda* (short-tailed shrew, short-lived). As supposed by the FRTA, *M. lucifugus* produced about half of the amount of  $H_2O_2$  produced by the short-tailed shrew. Rossinni aimed also to observe oxidative damage, due to the high metabolic rate associated with the flight in *M. lucifugus*. Thus, in order to evaluate potential differences in oxidative damage, he measured and compared the  $O_2$  consumption and the production of  $H_2O_2$  in both adults and young individuals (fully developed and able to fly). Surprisingly and against his hypothesis, young individuals had significantly higher levels of  $H_2O_2$  production when compared to adults. The supposition of Rossinni was that lower production of free radicals in adults could be the result of a selection, in the individual, of efficient mitochondria, caused by the selective pressure due to the high energy level required to fly [47].

In invertebrates oxidative damage, in particular the level of superoxide, does not appear to be critical to determine species longevity; instead, in mammals, the effect of oxidative stress on lifespan's length is poorly understood yet, but several authors claimed the potential role of antioxidant treatments as a protection against age-related organ dysfunction and cognitive decline [48]. Despite numerous scientific evidences proving that antioxidants introduced by the diet may reduce the ROS accumulation in rodents without extending lifespan, another study showed that mice with mutations in the superoxide dismutase (SOD) are more prone to develop pathologies and die prematurely. Anyhow, hyper-ubiquitous expression of SOD does not extend lifespan of these animals; therefore, this enzyme does not regulate longevity [49]. Numerous studies showed a link between the dysfunction of the respiratory chain, oxidative damage induced by ROS activity, and aging in the majority of the model organism[50]. All these evidences taken together suggest that oxidative stress is a determinant factor involved in aging.

### 1.2.2 DNA damage theory of aging

For a long time, accumulation of molecular damage has been considered key factor for the aging process [51]. The theory of DNA damage dates back to the late 50's when Failla [52] and Szilard [34] independently hypothesized that accumulation of DNA lesions maybe be the driving force of the aging process. It is now clear that DNA mutations and chromosomal abnormalities increases with age in mice [53] and humans [54], and that longevity is correlated

with the ability to repair the DNA [55]. It is interesting to note that the more serious progeroid syndromes (Werner's syndrome, Hutchinson-Gilford, and Cockayne) originate from mutations which impair genes involved in DNA repair and metabolism [56].

The emerging hypothesis suggest that only certain types of DNA lesions are crucial for aging and this would explain why mutations falling in certain DNA repair genes affect aging, while others do not. A recent study, through an analysis of the genes involved in the DNA repair, showed that genes related to non-homologous repair mechanism are closely associated to aging [57]. In addition, damage to DNA that interfere with transcription appear to contribute to senescence exerting effects on signalling and cellular aging [31].

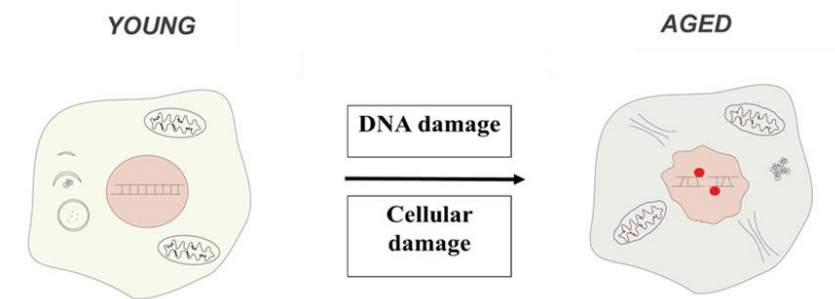


**Figure 3: Schematic representation of cellular aging.** Figure adapted from [58].

Understanding which aspects of DNA biology play a role in aging is still a challenge. Although it is well known that DNA changes over time could play a very important role in aging, the mechanisms which lag behind these changes have to be completely clarified.

### 1.3 DNA damage

DNA is constantly exposed to exogenous and endogenous damaging sources which may threaten DNA molecules, generating several types of DNA lesions. In order to preserve genome integrity, cells have evolved complex mechanisms which allow to point out and detect the presence of the DNA. Connecting to the DNA damage theory of aging, it is possible to hypothesize that the capacity to detect molecular damage is a potential cellular determinant of longevity. Thus, the detection of the presence of damage is a necessary step in order to proceed with repair or, if the damage is irreparable, with other means of damage control, as the induction of cellular senescence or apoptosis. Collectively these mechanisms have been termed as the DNA damage response (DDR). There is a growing evidence that the DDR efficiency can be also modulated by reorganization of the chromatin in answer to DNA damage

[59]. In fact the DDR machinery needs to exploit its function on a molecule, DNA, which is tightly wrapped around histone proteins in the form of chromatin [60]. Albeit chromatin acts as a physical barrier to DNA recognition and repair, it can be modified by some structural changes which take place consequently to DNA damage, such as histone methylation [61] or histone post-translational modifications [62], which in turn can facilitate DDR's function. In the context of the DDR activation, the most documented chromatin modification is the phosphorylation of the histone variant H2AX ( $\gamma$ -H2AX) [63]. Thus, the DNA damage response is a complex scenario where repair proteins are recruited at the lesion's site and chromatin-associated proteins are mobilized to and from DNA breaks [64].

### **1.3.1 DSB, NHEJ pathway and DNA end binding activity**

Among the different types of DNA damage, the most harmful and dangerous lesions are double-strand breaks (DSBs): one unrepaired DSB is sufficient to trigger permanent growth arrest and cell death [65][66][67]. DSB can be induced by endogenous and exogenous causes: physiological causes which include V(D)J recombination and class switch breaks (AID / UNG / EPA); or external factors as ionizing radiations, ROS production, the action of enzymes on the nuclear DNA (including topoisomerase II) and mechanical stress [68]. To repair DSBs, mammals have evolved two major repair pathways: non-homologous end-joining (NHEJ) and homologous recombination (HR). The majority of DSBs in mammals are repaired by NHEJ [69]: in the adult body, the majority of cells, are in G<sub>0</sub> phase and, whereas HR is typically active only during the S and G<sub>2</sub> phases, NHEJ is active throughout the cell cycle [70]. Additionally, NHEJ is significantly faster than homologous recombination [71].

NHEJ can be categorized in two different alternative pathways: 1) the canonical NHEJ (c-NHEJ), which involves core proteins such as Ku70, Ku80, DNA-PKcs, Artemis and the Ligase IV complex (Lig IV, XRCC4, and XLF) [72]; and 2) the alternative NHEJ (alt-NHEJ), also called microhomology-mediated end joining (MMEJ) a DNA-PK-independent repair mechanism, which uses a distinct set of proteins, including but not limited to PARP-1, CtIP, XRCC1, and Ligase III [73][74][75][76][77][78][79]. NHEJ is also regulated by SIRT6 [80] and Werner syndrome proteins [81]. In vertebrates, the Ku heterodimer (composed by Ku70 and Ku80 proteins) is the first proteic complex to be recruited at the DNA damage site; its recruitment to the double strands lesion is a fundamental step in order to activate the NHEJ pathway. Due to its ability to recognize and bind DNA free ends, Ku forms a ring structure at the level of the

damaged DNA free ends [82]; once loaded on the DNA damaged ends, it functions as a scaffold for the assembly of all other proteins involved in the NHEJ pathway.

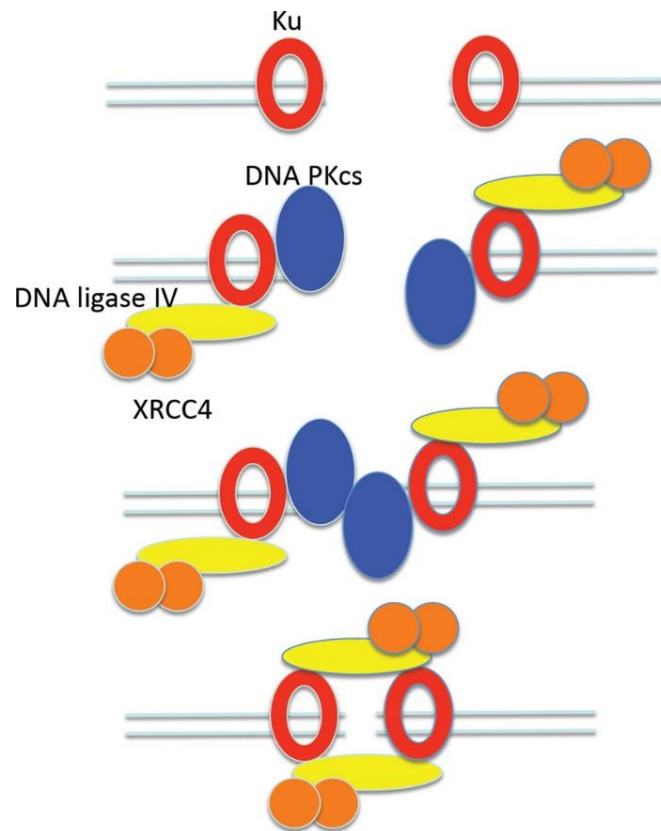


**Figure 4: Model for repair of a DSB by NHEJ.** Figure from [83].

This complex secondarily interacts with the DNA dependent protein kinase (DNA-PKcs) (catalytic subunit), forming the DNA-PKcs complex, necessary for the recruitment of ATM (Ataxia telangiectasia mutated), which in its turn promotes phosphorylation of the H2A histone variant, H2AX, at the site of Ser 139 (called  $\gamma$ -H2AX)[84] and the recruitment of p53 binding protein 1 (53BP1) at cleavage site [85]. DNA-PKcs also induces the phosphorylation of other factors such as Artemis, an enzyme whose 5'  $\rightarrow$  3' single-stranded exonuclease activity is switched to 5' end and 3' endonuclease activity once bound to DNA [86]. The final step of the repair process consists in the ligation of the DNA broken ends through the intervention of LIG4, XRCC4 and XLF (Figure 4) [87].

Thus, efficient detection of the presence of DNA lesion appears to be a fundamental event for a proper cellular answer to DNA damage. Several experimental hypothesis suggest that DNA end-binding activity appears to be more closely related to longevity, than other mechanisms

of genomic surveillance. Stamato and colleagues showed a striking positive relationship between DNA-end binding and species longevity. This is a property which is strictly ascribable to the Ku70/Ku80 protein heterodimer [88]. What made this relationship interesting is the lack of a correlation between DNA-end binding activity with species adult body mass. The underlying hypothesis is that the different abundance of the proteins involved in the early phase of NHEJ (the Ku heterodimer and DNA-PKcs) might likely explain the different binding activities observed across the species [13].

Indeed, other mechanisms of genomic surveillance such as poly(ADP-ribose) polymerase (PARP) activity [89] and the repair of UV induced DNA lesions [90][91], positively correlates both with longevity and body mass; see dedicated reanalysis in [92][15]. For example, mice with loss-of-function mutations in Ku70, Ku80, and SIRT6 each as well as Werner syndrome patients exhibit symptoms of premature aging [93][94][95][96][25][97]. So far, the appearance of accelerated aging in human patients and in mouse models with mutations in genes involved in NHEJ is the strongest evidence supporting the relation which link together impairment of the NHEJ and aging. These mutant studies, however, do not tell us whether NHEJ is affected during normal aging [98].

**1.3.2 Role of 53BP1 and its role in DNA damage recognition**

In the presence of DSBs, 53BP1 is recruited at the level of DNA breaks. 53BP1 is a large DNA damage sensor and oligomeric chromatin reader of 1972 amino acids. It is characterised by the absence of an apparent enzymatic activity and by the presence of several structural domains which can directly interact with DSB-responsive proteins.

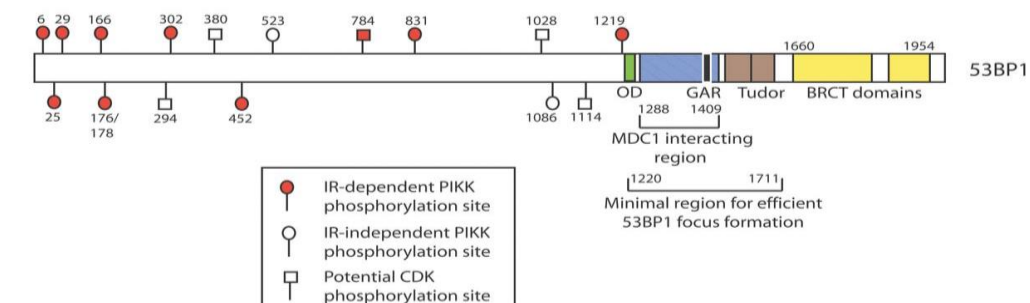


**Figure 5: Domain structure of the mediator/adaptor proteins 53BP1.** Figure adapted from [99].

Among these important structural elements, 53BP1 includes the UDR domain, the BRCA1 carboxy-terminal (BRCT) repeats, the tandem Tudor domains and 28 amino-terminal Ser/Thr-Gln (S/T-Q) sites, which are phosphorylated, at least in part, by the ataxia telangiectasia mutated (ATM) kinase5 [65]. The UDR domain is used for DNA recognition of the damaged site, in order to form nuclear foci (protein agglomerates) in response to a double strand breaks, where it can co-localize with other DNA damage response proteins such as  $\gamma$ -H2AX, Rad50/Mre11/NBS1, BRCA1, and Rad51. The BRCT domain, indeed, is involved in the interaction with p53. Notably, 53BP1 owes its name to the ability to bind p53 and precisely through this interaction it was originally identified [100]. But, while the role of 53BP1 in the DDR pathways has been deeply studied and its contribution completely clarified, 53BP1 involvement to p53-dependent cellular activities remain still undefined. Cuella-Martin *et al.* carefully investigated the influence of 53BP1 activity upon p53-dependent signalling after DNA damage; they demonstrated that 53BP1 stimulates genome-wide p53-dependent gene transactivation and repression events in response to ionizing radiation (IR) and synthetic p53 activation. Overall, these experimental reports suggest that these two functions are structurally separated and independent [101]. In figure 6 53BP1's interactive targets are described in detail.

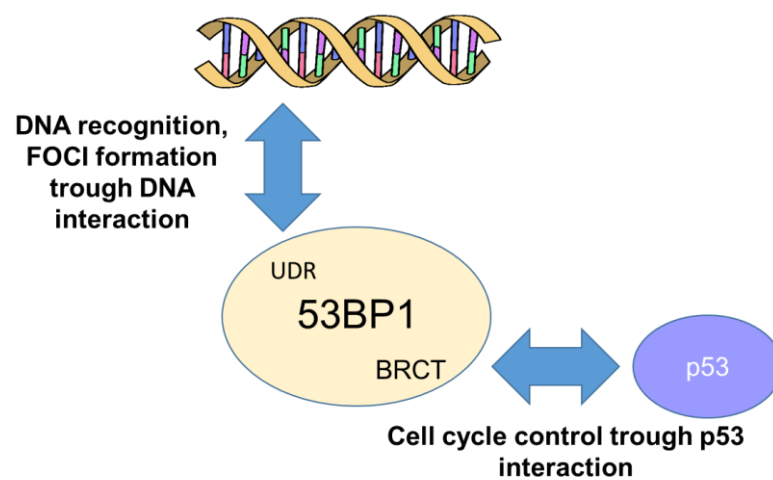


**Figure 6: 53BP1 has two structural and functional domains.** 1) The UDR domain leads 53BP1 to be rapidly relocated at DNA damage site after cellular exposure to ionizing radiation (IR); 2) the tandem BRCT (BRCA1 C terminus) motif, through which 53BP1 directly binds p53 enhancing p53-mediated transcription of reporter genes. These two functions can be fully separated: mutations in the 53BP1 protein sequence can selectively impair its enrichment at nuclear foci or impede p53 binding. When UDR domain is impaired, cells are more sensible to IR displaying a decrease survival. If the BRCT domain is impaired, cells show improved survival after irradiation [85][101].

53BP1-dependent NHEJ is also crucial in the immune system, where it is necessary for immunoglobulin class switch recombination (CSR) and T cell receptor rearrangements [102][103]. It was observed that 53BP1 knockout mice (53BP1<sup>-/-</sup>) have a severe reduction of CSR, thus, results in an over immunodeficiency [104][105]. In order to foster DNA recognition and to promote NHEJ, 53BP1 binds a combination of methylated (H4 Lys20me1/2) and ubiquitinated histone's (H2A ubi-Lys15) epitopes within DSB-associated chromatin [106]. Through the Tudor domain, 53BP1 is recruited to H2AK15 and H4K20 hystones, which are respectively ubiquitylated by RNF8- and mono-dimethylated by RNF168. But the first step towards its recruitment is the formation of the MRE11–RAD50–NBS1 (MRN) complex, which is a sensor of DNA lesion.

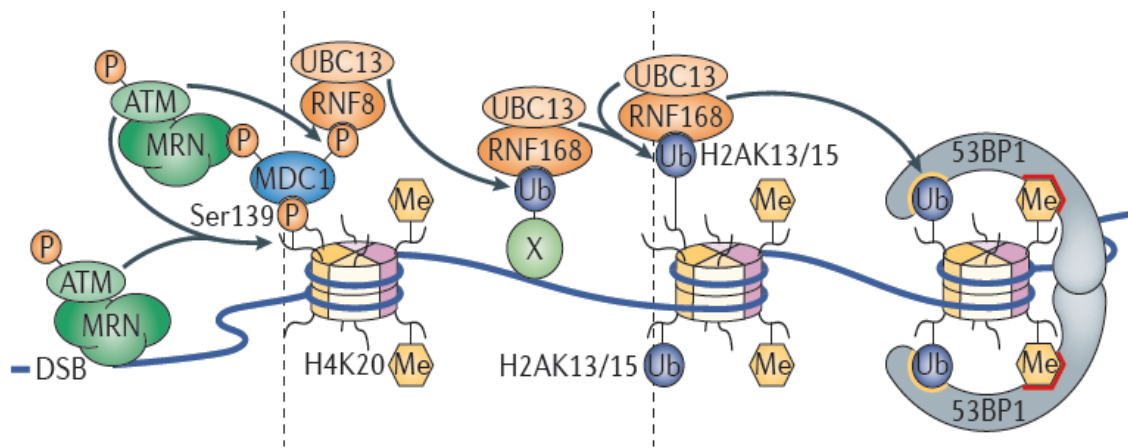


**Figure 7: The signal transduction of 53BP1 pathway.** Figure adapted from [65].

Once MRN complex is aggregated at the level of DSB lesion, it induces auto-phosphorylation of active ataxia-telangiectasia mutated (ATM), which in turn phosphorylates the histone 2A (H2A) variant H2AX at Ser139, in order to generate  $\gamma$ -H2AX.  $\gamma$ -H2AX is in turn recognized by mediator of DNA damage checkpoint protein 1 (MDC1). MDC1 activates a positive feedback loop by recruiting more MRN complexes and activated ATM to the damaged chromatin. This event leads to the recruitment of the E3 ubiquitin ligase RING finger 8 (RNF8) (phosphorylation-dependent). MDC1 linked to RNF8 is recognized by a second E3 ubiquitin ligase, RNF168.[65][85]. This last complex, as previously mentioned, recruits 53BP1 to the DNA damage surrounding chromatin (Figure 5). Moreover, it was found that 53BP1 foci formation is reduced in response to a reduction of the H4K20 methylation [107].

Additionally, 53BP1 possesses tumor suppressor functions. Germline 53BP1 mutations predispose mice to T cell lymphoma, in manner exacerbated by p53 loss [108][109]. Ward *et al.* showed that 53BP1 mice knock out display a higher sensitivity to IR and an increase rate of tumorigenesis [110]. On the whole, these informations track the “portrait” of a key protein, fundamental for the cellular destiny after a DNA damage.

### 1.3.3 DNA damage nuclear foci

As previously mentioned, 53BP1 agglomerates in clusters at double break sites and these clusters are generally called *nuclear foci*. Nuclear foci are agglomerates of DNA damage repair proteins, each with a different but necessary function, which form into the nucleus of stressed cells within minutes after damage. 53BP1 foci, as well as all the different nuclear foci, are easily identifiable through immunofluorescence assays and are universally used as a DNA damage marker [111]. Nowadays very much is known about the role and the kinetics of the DNA damage repair complex

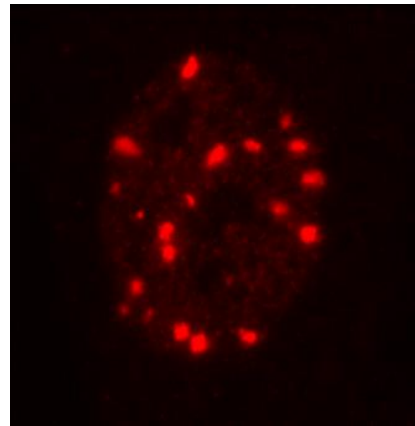


**Figure 8:** Representative image of 53BP1 foci in a human primary fibroblast.

assembly. For example the phosphorylation of the histone variant H2AX ( $\gamma$ -H2AX) and the accumulation of the 53BP1 protein in distinct nuclear foci [112] are widely used as DSBs markers;  $\gamma$ -H2AX phosphorylation promotes the formation of a protein scaffold necessary for the repair of DSBs [113]. Depending on the extent of the damage,  $\gamma$ -H2AX and 53BP1 may co-localize [114] and, since each focus represents a single DSB, their amount is proportional to the intensity of damage [115]. Therefore, nuclear foci represent not only a marker of the presence of DNA damage but also a measure of the damage’s intensity.

Kinetic of nuclear foci, such as 53BP1 foci, can be divided in two temporal phases: 1) early foci which rapidly form after damage and are a sign of an active detection DNA damage system; 2) long lasting foci which, if DNA damage is not properly repaired, can persist for longer time into the nucleus. Moreover, the nuclear location of these persistent foci define two different classes of long lasting foci: 1) if foci localized at the telomeres are called Telomere Dysfunction Induced Foci (TIF) [116]; 2) if foci are localized all over the nucleus, will be called DNA-SCARS (segments of DNA with chromatin alterations) and they can persist for several days after

damage [45]. DNA SCARS, which may include both  $\gamma$ -H2AX and 53BP1, often completely or partially co-localize with PMLnbs (promyelocytic leukemia protein nuclear body) [117][118]. PMLnbs are small dynamic nuclear bodies found in most cell-lines and many tissues. They belong to the nuclear matrix in a structure which has been proposed to regulate many nuclear functions as DNA replication, transcription, or epigenetic silencing [119]. They may also participate to cellular responses to genotoxic stress [120]. Although their biological role is not completely clarified, they are often associated to stress induced senescence [121]. In fact persistent foci are usually abundant in tissues undergoing to genotoxic stress [122] and in senescent tissues of mice and primates [116].

### 1.4.4. Micronuclei



**Figure 9: Representative image of a micronucleated nucleus.**

Another well-known DNA damage marker are micronuclei (MN). MN formation is widely considered as a cytogenetic direct marker of unresolved damage and the analysis of their appearance is used as a measure of the residual genomic instability in a cellular population, after a genotoxic stress. MN are defined as small, round, DNA containing cytoplasmic bodies derived by loss of nuclear material, not incorporated into the nucleus of a daughter cell after an aberrant mitosis [123] [124] (fig 8). Thus, MN can be constituted by different nuclear portions: acentric chromosomes, chromatid fragments or whole chromosomes. MN generation is strictly connected to the action of chemical or physical agents which induce, *in vivo* and *in vitro*, genotoxic stress. Mutagenic agents can be classified into (1) clastogenic agents, able to give rise to or induce disruption or breakages of chromosomes, leading to chromosomal deletion, insertion or rearrangements or (2) aneugens agents, that damage the mitotic spindle or the centromere of a whole chromosomes [125]. Both mutagenic mechanisms lead to a separation of portion of chromatin from the main nucleus, in favour of the formation of a new structure similar to the main nucleus, but independent and smaller when compared to it [126]. Fenech *et al.* draw a list of characteristics which need to be applied in order to correctly identify MN. Thus MN, must 1) be round or oval shaped 2) to lay close to the main nucleus 3) have a

diameter between  $1/3$  and  $1/16$  of the diameter of the main nucleus 4) have the same staining intensity and the same appearance of the latter [127] (see Figure 9). Because cell division is necessary for the generation of MN, it is recommended that MN are scored by the cytokinesis block micronucleus (CBMN) assay developed by Fenech and Morley [128]. Therefore, the presence of micronuclei in the cellular cytoplasm is considered an indicators of genetic damage.

---

## *2. AIM OF THE THESIS*

In mammals, species lifespan can vary by more than 100 fold (shrew 2 years, bowhead whale 211 years). It would be plausible to think that differences in lifespan may reflect structural differences between species at the cellular level by influencing fundamental processes. The DNA damage theory of aging, mentioned above, postulates that accumulation of mutations over time is one driving force of the aging process; additionally one may ask whether accumulation of DNA damage could also have determined the average lifespan of a species, during evolution. Accordingly, less efficient repair systems of a given species could leave more frequently unsolved damages in the cellular population, thus leading to increased genomic instability, which in turn would decrease the overall longevity of the species. This hypothesis is supported by the observation that a positive correlation exists between longevity and the ability to repair damage in model organism [55]. In addition, it has been shown that the abundance of proteins like Ku80 and DNA-PKcs, which are directly involved in DNA end-binding during DSB repair, correlates with the longevity of certain species [13].

This thesis aims at further verification of the hypothesis that the efficiency of DNA damage repair, which likely contributes to the individual aging process, is also suited to explain the big difference in longevity observed in different mammalian species. Specifically, I intended to test whether long-lived species have more efficient cellular DNA repair machineries and investigated potential differences among five mammalian species, with respect to DNA damage-repair and the maintenance of genomic stability in response to low and high genotoxic damage.

53BP1 is widely known as a key regulator and orchestrator of the cellular response to double strand break damage: on one hand it is directly recruited on the DNA damage site and on the other hand it regulates cellular responses through its direct interaction with p53. Thus, 53BP1 should be investigated to assess the efficiency of the DNA damage response in the comparative experimental model. In addition, formation of micronuclei should be monitored to evaluate long-term effects of genotoxic stress in these different species. And finally, similar experiments should be applied to cultures of primary skin fibroblasts from human donors of

different age to explore a potential association between DNA damage, senescence markers and the chronological age.

## 2.1 Project description

The project has been structured in three parts, each investigating the same theme from different observational point of view: interspecies longevity, *in vitro* studies (PART I); interspecies longevity, *in vivo* studies (PART II) and intraspecies longevity *ex vivo* and *in vitro* studies (PART III).

### 2.1.1 PART I- DNA damage detection by 53BP1: relationship to species longevity

Croco E., Marchionni S., Bocchini M., Angeloni C., Stamato T., Stefanelli C., Hrelia S., Sell C., Lorenzini A.

#### Abstract

In order to examine potential differences in genomic stability, we have challenged fibroblasts derived from five different mammalian species of variable longevity with the genotoxic agents, etoposide and neocarzinostatin. We report that cells from longer-lived species exhibit more tumor protein p53 binding protein 1 (53BP1) foci for a given degree of DNA damage relative to shorter-lived species. The presence of a greater number of 53BP1 foci was associated with decreased DNA fragmentation and a lower percentage of cells exhibiting micronuclei. These data suggest that cells from longer-lived species have an enhanced DNA damage response. We propose that the number of 53BP1 foci that form in response to damage reflects the intrinsic capacity of cells to detect and respond to DNA harms.

#### INTRODUCTION

Double-strand breaks (DSBs) are the most harmful DNA lesions a cell can encounter. In mammals, non-homologous end-joining (NHEJ) is the cellular mechanism responsible for repairing the majority of DSBs [69]. This is because NHEJ is much faster than homologous recombination (HR) [71] and it is active throughout the cell cycle, whereas HR is typically active only during the S and G2 phases [70]. Moreover, the majority of cells in the adult body are in G0. At the sites of DSBs, nuclear foci of phosphorylated histone H2AX ( $\gamma$ -H2AX) and tumor protein p53 binding protein 1 (53BP1) can be detected by immunofluorescence and are widely used as DNA damage markers since their abundance has been reported to correlate very closely with the degree of genotoxic insult [reviewed in [129]. 53BP1 accumulates in DNA

damage foci after the occurrence of DSBs in order to facilitate NHEJ repair [130]. Previous works had shown that 53BP1 is involved in activation of the DNA damage response during the G<sub>1</sub>, S, and G<sub>2</sub> phases of the cell cycle [131][132][133].

We have previously observed an unexpected difference in the formation of DNA damage foci between human and mouse cells following exposure to the same concentration of neocarzinostatin (NCS). Despite similar exposure to the DNA-damaging agent, human cells exhibited a significantly greater number of 53BP1 foci compared with mouse cells. The greater abundance of foci in human cells correlated inversely with the appearance of micronuclei, which represent the presence of severe genomic damage [134]. We have also reported an impressive correlation between mammalian longevity and the capacity of nuclear proteins to bind DNA ends, which appears to be largely dependent on increased expression of the evolutionarily highly conserved heterodimer Ku80/Ku70 [13]. The DNA end-binding assay represents the accumulation of proteins required for the initial DNA damage recognition, a necessary step before a cell can proceed with repair, cell cycle arrest or apoptosis. These data persuaded us to conduct a deeper investigation into the relationship between the appearance of markers of DNA damage and mammalian longevity.

To this end, we have compared fibroblast cells from mouse (maximum life span, 4 y; weight, 20.5 g), cow (maximum life span, 20 y; weight, 750 Kg), dog (maximum life span, 24 y; weight, 40.0 Kg), little brown bat (maximum life span, 34 y; weight, 10.0 g), and human (maximum life span, 122 y; weight, 62.0 Kg) in their response to the genotoxic insult caused by etoposide (ETO) and neocarzinostatin (NCS). ETO is a poison that binds reversibly to topoisomerase II $\alpha$ / $\beta$  to block re-ligation of cleaved DNA strands, causing DSBs [135] while NCS is a macromolecular chromoprotein antibiotic that causes single- and double-strand breaks [136]. Our experimental approach was based on the assumption that the biological mechanisms that facilitate longevity are cell autonomous and thus will be reflected in fundamental cellular processes. Consequently, these mechanisms can be studied in cell culture away from the complexity of the whole organism. For example, using a cell culture approach, Dostàl and colleagues have demonstrated that long-lived rodent species are more efficient in excluding Cadmium that is known for disturbing DNA base excision and mismatch repair [137].

With the present work, we propose that quantitative, species-specific differences in 53BP1 foci formation observed following exposure to genotoxic agents correlate with differences in

lifespan and adult body mass, suggesting a new interpretation of nuclear foci as markers of a species' ability to detect and mitigate DNA damage to ensure genomic stability.

### **2.1.2 PART II- Genetic instability and aging under the scrutiny of comparative biology: a meta-analysis of spontaneous micronuclei frequency**

Eleonora Croco, Silvia Marchionni, Antonello Lorenzini.

The idea that accumulation of DNA damage may be responsible for the aging process dates back to the late 1950s [52][34]. The key aspects of this theory are twofold: the idea that damage accumulates with time and the fact that damage to the DNA is of fundamental importance. The first concept is easily explainable if we look at many of the lifeless objects of our daily life that, after a period of service, accumulate some sort of damage (cars, buildings, etc.). These objects are designed to last for a specified time and they maintain themselves well for that period. However, damage eventually appears and accumulates due to intrinsic failure of their parts, harmful extrinsic factors, and lack of proper maintenance and repair. The result is a period of good function followed by a gradual decline. Biological systems are similar: there is a period of low mortality up to a point, followed by a gradual decline in fitness and increased mortality. Linking this concept to longevity, each species possesses an intrinsic design that ensures functionality for the life span of that species. Repair of DNA damage is critical to that design.

The second concept, that damage to the DNA is of fundamental importance, is also readily understandable thanks to a recent scientific breakthrough. Gibson and colleagues, having created the first synthetic life form through the synthesis of a 1.08-megabase-pair mycoplasma genome, have de facto demonstrated that DNA has a master role in the hierarchy of organic molecules [138]. DNA damage will, in fact, carry consequences at any level of biological organization or function (RNA, protein, metabolism, etc.).

Szilard, in his theory paper "On the nature of the aging process", discussed "hits" to chromosomes that render genes inactive[34]. However, genetic instability may also be obtained in the absence of actual damage to the DNA molecule. Aneugens, for example, are substances that cause genetic instability by simply interfering with chromosome segregation. Genetic, genomic, or chromosome instability are thus broader terminologies that are being used progressively more in gerontology [139].

Many observations and theoretical considerations support a role for genetic instability in aging. In rats, for example, inducing DNA damage with a single dose of ionizing radiation at a young age (6 weeks) shortens average life span by 10% for a dose of 1 Gy and 25% for a 3-Gy dose [140]. The very existence of more than 150 genes involved in DNA damage repair attests to the importance of DNA integrity in sustaining life [141]. Following this reasoning, the perturbation of one such repair gene should, to some degree, negatively affect life span. In support of this, the Ku heterodimer, comprising the Ku70 and Ku80 polypeptides, is critical for double-strand break (DSB) repair. Double mutants, as well as mutants of either Ku component, display an approximate 66% reduction in life span, with signs of early aging [96]. Despite a dramatic effect of the mutant Ku on life span, not all data are supportive of the theory. Kaya and colleagues, for example, have monitored a mutant of *Saccharomyces cerevisiae* that accumulates high levels of mutations. Whereas old wild-type cells with few mutations were dying, young mutant cells with many more mutations continued budding [142]. In conclusion, although the DNA damage accumulation theory is among the “oldest” of the aging theories, discussion of its true relevance is still very active among gerontologists.

### **Genomic stability and body mass**

The somatic mutation theory of aging predicts that long-lived species will have superior genomic stability. In fact, if alterations at the level of DNA are supposed to be responsible for the aging process, these alterations must accumulate at a lower rate in longer-lived species. With similar reasoning, we can hypothesize that genomic stability will also be positively related to adult body mass. In fact, two species with similar longevity but different adult body mass will differ in their total number of cells in adulthood. Consequently, the number of total cellular divisions that the genome must sustain, from the creation of the zygote onward, can be very different. Additionally, body mass is positively correlated with longevity among mammals, birds, amphibians, and reptiles [143]. In the multitude of cellular mechanisms involved in preserving genomic stability, some will be more essential in order to guarantee longevity, while others will be more essential in order to guarantee the development of greater body mass. For example, we have found that the capacity to bind DNA ends (a capacity of the Ku heterodimer) correlates with longevity, but not with body mass in 12 mammalian species [13]. In contrast, we have found that the efficiency of the spindle assembly checkpoint correlates strictly with body mass and more loosely with longevity in six species of mammals

[144]. The efficiency of excision repair after UV damage and the activity of Parp, an enzyme involved in single-strand break (SSB) repair, are other examples where a correlation is found both with longevity and body mass [89][92][91][15].

### **Advantages of the comparative approach**

Life span studies may be extremely long lasting, being clearly linked to the life span of the tested species. Rats and mice, which require at least three to four years of study, are the most studied mammals in the laboratory. Nonetheless, these two rodents are not the best representation of the aging process in mammals since their longevity lay at the lowest extreme of the vast range of life spans exhibited by this class. Maximum longevity in mammals spans 100-fold, from 2.1 years for the forest shrew to 211 years for the bowhead whale (data from the AnAge database; [145]). Comparing characteristics of species known to differ significantly in longevity represents a unique and powerful approach to aging studies [146]. Comparative cellular biology also gives the potential to manipulate the environment and challenge cells with different stressors to monitor their differential reactivity (reviewed in [15]). In a recent and comprehensive review, Moskalev and colleagues analyzed evidence for and against the DNA damage theory cataloguing studies based on Koch-like criteria [34]. The authors concluded, in part, that comparative biology data are thus far scarce in the literature (both for and against the theory). In the present article, we will demonstrate to the gerontological community that comparative biology data are readily available and may need only to be extracted from the literature. To this end, we conducted a meta-analysis on spontaneous in vivo micronuclei (MN) frequency in mammalian erythrocytes of species with different longevity and body mass. Our aim was to search for a possible relationship between these two parameters (longevity and body mass) and the propensity to this type of genomic instability.

### **Analysis of micronucleated erythrocyte frequency across mammals**

MN are small cellular bodies containing genomic material enclosed in nuclear membranes. These small bodies are produced during mitosis when a whole chromosome or chromosome fragment is left behind by the mitotic spindle and fails to be incorporated into either one of the daughter cell nuclei. The spontaneous or induced formation of MN is used as a cytogenetic test using different cellular substrates: epithelial cells from mouth swab, lymphocytes from blood, and erythrocytes from blood, bone marrow, or spleen [147][148]. Erythrocytes are

particularly useful since they naturally expel the nucleus during maturation, but do not expel the MN [149]. With staining such as Giemsa or acridine orange, micronucleated erythrocytes (MNE) are scored to assess the possibility of genotoxicity *in vivo* [150]. Observing MN in bone marrow erythrocytes may testify to recent genotoxic damage, while the presence of MN in circulating erythrocytes is an indication of chronic exposure [151]. If the aging process is seen as an accumulation of damage, then it may be likened to a chronic exposure. Consequently, we have screened the literature for reports on the spontaneous frequency of MN in circulating erythrocytes in different species of mammals.

### **2.1.3 PART III- 53BP1, DNA DAMAGE AND CHRONOLOGICAL AGE**

The aging process is accompanied by an accumulation of cellular damage, which compromises the viability and function of cells and tissues. Dermal fibroblasts are mostly quiescent cells that are regularly exposed to environmental stimuli, thus these cells provide a paradigmatic model of long-term cellular adaptation to exogenous stress [152]. One of the biggest goal in the aging field is to find markers which can be applied for early identification of aging process. Human diploid fibroblasts have been used as the election model for *in vitro*-studies of cellular aging, but so far, only a small amount of information about the aging process of these cells in their physiological tissue environment, i.e. the dermis , is known [153]. Since DNA damage markers can be easily identified and studied, the major part of these studies attempted to find an association between their expression and aging. In a recent study, numbers of 53BP1 foci in dermal fibroblasts were also positively associated with the age of the donor [154]. Fibroblasts in the dermis of aged baboons exhibit accumulation of nuclear foci positive for 53BP1. Many of these foci are co-localised with telomere markers suggesting they indicate telomere dysfunction [155]. Micronuclei numbers were shown to be higher at older age in lymphocytes (reviewed in [156]) and buccal cells [147]. However, an inverse relation between the number of 53BP1 foci and micronuclei has also been described between mouse and human cells [134]. In our work [157] a wide cohort of individuals with different chronological age was tested, *in vitro*, for the presence of two DNA damage markers: MN and 53BP1 foci formation. The expression of these two markers was investigated in untreated and rotenone treated primary fibroblasts from 100 donors. No association between micronuclei and chronological age was found; DNA damage foci of cultured fibroblasts are significantly associated with chronological age, but not with biological age, of donors.

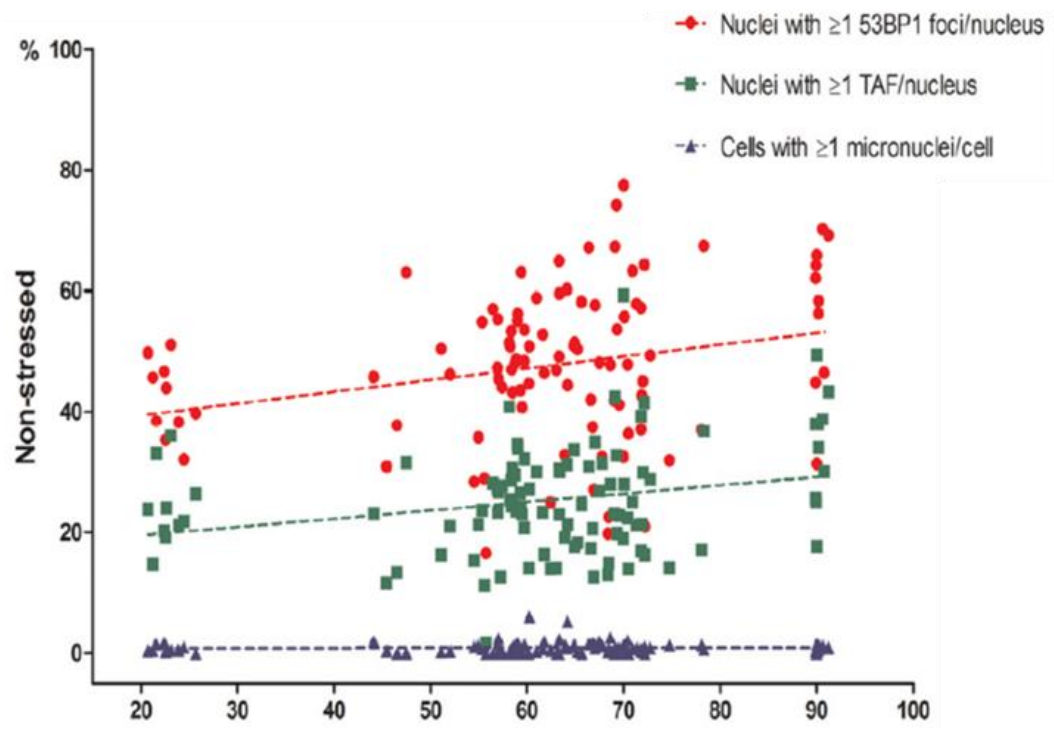


Figure 10: 53BP1 foci dependent on chronological age. Figure adapted from [157].

### 3. MATERIAL AND METHODS

#### 3.1 Cell culture

All fibroblast strains and lines used are described in Table 1. Fibroblast strains from mouse, little brown bat, dog, and cow were established as previously described [158]. Adult human fibroblasts were obtained from Claudio Franceschi (DIMES, University of Bologna).

Fibroblasts from mammals species were maintained in Minimum Essential Medium (MEM) with Earle's Salts and L-glutamine containing 10% fetal bovine serum (FBS), MEM vitamins and amino acids, and penicillin-streptomycin (all from Sigma Aldrich, St. Louis, Mo). Fibroblasts were passaged weekly, washing them twice with PBS 1X and using Trypsin-no EDTA 1X for detaching the cell layers. The number of cells were counted using the Burker chamber and they were seeded according to the standard cell density (10.000/cm<sup>2</sup>). Cumulative population doubling (PD) was determined as previously described [159].

Skin fibroblast from 15 human female donors were used in the present study. They were aged 20, 23, 25, 26, 26, 40, 41, 42, 43, 49, 60, 62, 63, 64 and 67 years, thus covering a wide age spectrum 20 – 67 years. They were divided into three different chronological age groups, each with five biological replicates: “young” (20–30 years), “middle aged” (40–50 years) and “old” (60–70 years). All these strains were provided from Prof. Boege (Uniklinik, University of Düsseldorf).

HaSK-pw keratinocytes (KT) (characterised by Petra Boucamp, German Cancer Research Center, Heidelberg, Germany), spontaneously immortalized keratinocytes, described in [160], were kindly provided from Prof. Boege (Uniklinik, University of Düsseldorf). They were maintained in FAD II medium, a 3:1 mixture of DMEM and Ham's F12 medium supplemented with 10% FBS, 24 ng/ml Adenin, 1 ng/ml hEGF, 0.4 µg/ml hydrocortisone, and 5 µg/ml insuline. The KT cell line was authenticated by short tandem repeat (STR) profiling confirming its uniqueness. KT were passaged 1:5 every three days, in order to avoid high confluence level.

TAB.1 Cell culture strains and lines

<b>STRAIN NAME</b>	<b>SPECIES</b>	<b>COMMON NAME (strain)</b>	<b>ORIGIN (Age)</b>	<b>EXPERIMENTS</b>
MEF	Mus musculus	Mouse	Embryo, F	FOCI, MN,
M3M	Mus musculus	Mouse	Adult (3 months), F	FOCI ETO, MN, WB, MTT
M2W	Mus musculus	Mouse	Young (2 weeks), F	FOCI ETO, MN, WB, MTT
3T3	Mus musculus	Mouse	Embryo (Immortalized)	FOCI NCS, MN, COMET
YA35CF	Homo sapiens	Human	Adult (25 years), F	FOCI, MN, WB, MTT
IMR90	Homo sapiens	Human	Embryo, F	FOCI, MN, COMET, WB
WI38	Homo sapiens	Human	Embryo, F	FOCI, MN
B#1	Bos taurus	Cow	Young (about 6 months), F	FOCI, MN, COMET, MTT
D#1	Canis familiaris	Dog (Beagle)	Young adult, F	FOCI, MN, COMET, MTT
D#BAS	Canis familiaris	Dog (Basset hound)	Young adult, F	WB, MTT
LBB#4B	Myotis lucifugus	Little Brown Bat	Young adult, (immortalized), F	FOCI, MN, COMET, MTT
KT	Homo sapiens	Human	Immortalized, KT	GENOME EDITING, MN, SURVIVAL ASSAY, CFA
F20-F67	Homo sapiens	Human	Adult, F	FOCI IRRADIATION, MN

All cell strains were maintained at 37°C in a humidified atmosphere containing 5% CO<sub>2</sub>. With the exception of the immortalized 3T3 mouse line and keratinocytes, little brown bat strains that had undergone spontaneous immortalization, lines displayed cellular senescence and were used for all experiments at approximately the first half way through their replicative lifespan.

### **3.2 Freezing and Thawing of cells**

In order to freeze cells, they were collected, counted and cellular suspension was centrifuged at 300 x g for 5 minutes. The cellular pellet was suspended, according to the standard cellular density, in freezing medium (FBS 70%; complete MEM 20%; DMSO 10%), previously prepared and stored at 2°-8°C until its use. The suspension was transferred into crio-tubes. After an overnight passage at -80°C, tubes were transferred into liquid nitrogen for long term storage.

For thawing cells, tubes from liquid nitrogen were warmed in the water bath at 37°C for 1 minute. Cells were mixed and suspended in 5-10mL of fresh MEM and seeded in T25 or T75 flask. The day after, fresh new medium was added.

### **3.3 Genotoxic treatment**

Two different type of genotoxic treatment were performed 1) radiomimetic treatment, ETO and NCS treatment; 2) ionizing radiation (IR) treatment.

- 1) For the chemical treatment, cells were treated with ETO and NCS (both from Sigma Aldrich, St. Louis, Mo). The majority of the experiments were performed on S phase synchronized cells and when unsynchronized cells were used, this is specified. S phase was chosen as the most appropriate time for exposure to genotoxic stress, accordingly to a previous study where differences in susceptibility to genotoxic damage were determined between human and mouse cells, showing that susceptibility is most apparent in S-G<sub>2</sub> [134]. Additionally, topoisomerase II inhibitors are most effective during DNA replication in S phase [161]. Cultures were initially arrested in G<sub>0</sub> by serum starvation for 48 hours (h) in serum-free medium. Cells were then stimulated to enter the cell cycle by the addition of fresh complete medium with 10% FBS. For each species, the time following FBS stimulation required for entry into S phase was defined by cell cycle analysis (data not shown). Mouse and bat cells were stimulated in complete medium with 10% FBS for 16 h; dog, cow, and human for 18 h. Once synchronized, cells were treated in complete serum-free medium to avoid the potential for interference of serum on drug bioavailability. Unsynchronized cells were used only on initial dose response experiments (Figure 14 and 15). Dose ranging from 5 µM to 100 µM of ETO and ranging from 0.13 µM to 1.35 µM of NCS were used.

- 2) IR treatment was performed by the use of the Gulmay's machine, available at a separate facility of the University of Dusseldorf. All the IR experiments were performed on unsynchronized cells, under the same condition of voltage (150kV) and amperage (15mA). Time exposure is described in Tab. 2.

---

 TAB.2 Ionizing radiation settings
 

---

<b>Gy</b>	<b>TIME</b>
1	1'23"
4	5'33"

---

### 3.4 Preparation of whole cells lysates

Cell whole lysates from fibroblasts derived from mouse, little brown bat, dog, cow and human were prepared by adding ice-cold RIPA buffer (50mM Tris, 150mM NaCl, 1% NP-40, 0.1% SDS, 0.5% sodium deoxycholate, 1mM PMSF, 1 µg/mL leupeptin, 1 µg/mL pepstatin). Lysates were collected and protein amount was dosed by using DC protein assay (5000111, Bio-Rad kit), based on a modification of the Lowry's method. A standard curve was prepared by obtaining 3-5 standards of protein (Bovine Serum Albumine, BSA), containing from 0.2 mg/ml to about 1.5 mg/ml protein. For the dosage, samples were prepared according to manufacturers' instructions. Then, to determine protein concentration absorbance was read at 750 nm.

To collect whole lysates from primary fibroblasts from young, middle, old donors and for KT (wild type and knock down) pellets were resuspended in 2X lysis buffer (250 mM Tris-HCl, pH 6.8, 2% glycerol, 4% SDS, 20 mM DTT, 1.4 M urea, 20 mM EDTA, 2 mM PMSF, 5 mM pefa block, 0.04% bromphenol blue) in a volume sufficient to get a final density of  $1 \times 10^5$  cells/ 20 µl. Thus, lysates were homogenized by ultrasound (10 s at 20% power).

All samples where boiled (100°C, 5 min). 50 micrograms of cell extracts or 30 µl of warm aliquots were loaded onto SDS-polyacrylamide gels.

### **3.5 Polyacrylamide gel electrophoresis**

Electrophoresis was performed in 1x TGS buffer running buffer at voltage of 90-160V.

### **3.6 DS-PAGE and Western blotting**

After separation, proteins were electrophoretically transferred from the gel to a nitrocellulose membrane by the tank-blot method. Therefore the nitrocellulose membrane was activated in MeOH for 1min, washed in H<sub>2</sub>O and equilibrated in transfer buffer (48 mM Tris, 39 mM glycine, 0-20 % methanol, pH ~9.2), while the gel was equilibrated for at least 20 min in transfer buffer. After transfer, the nitrocellulose membranes were blocked for 1 h in 5% bovine serum albumin (BSA) or Milk in Tris-buffered saline containing 0.1% Tween-20 (TBST). Membranes were incubated with 5% BSA or Milk TBST primary antibody shaking overnight and then were incubated for 1 h with goat anti-mouse-HRP or goat anti-rabbit-HRP (Cell Signalling, Billerica, Ma) in 5% BSA or Milk TBS-T. Blots were washed in TBS-T and incubated with Clarity™ Western ECL substrate (Bio Rad, Hercules, Ca) for 5 minutes before developing. Densitometry measurements were captured using the ChemiDoc station and software (Bio Rad, Hercules, Ca). All densitometric measurements were normalized to loading controls.

### **3.7 Immunofluorescence: foci determination**

Fibroblasts were seeded onto glass coverslips, and treated with ETO or NCS at varying concentrations for 6 or 2 h respectively. Cells were fixed at the indicated times after the beginning of damage in 3,7 % paraformaldehyde for 10 minutes and permeabilized in 0.5% Triton X-100 in PBS for 15 minutes. Cells were washed three times in PBS and blocked for 1 hour in 5% goat serum 1% BSA in PBS containing Tween-20 (PBST) (blocking solution), after which they were incubated with primary antibody in 0,1% blocking solution buffer for 1 h at room temperature in a humidified chamber. All the antibodies used are listed in Tab. 3.

53BP1 antibody (NB 100-304) binds, in tested species, epitopes with homologies that range between 90% and 92% compared to the human epitope. Anti- $\gamma$ H2AX antibody, used for human and mouse, binds an epitope with a homology of 90% between these two species. Slides were washed three times in blocking solution and incubated with secondary antibody in 0,1% blocking solution for 1 h. Cells were washed three times, stained with DAPI, and mounted with Vectashield mounting medium (Vector Laboratories, Burlingame, Ca) before

visualizing. Images were captured using an Olympus BX61 fluorescence microscope (Tokyo, Japan) equipped with a Hamamatsu ORCA-ER camera (Hamamatsu City, Japan) or an Olympus IX50 equipped with a Diagnostic Instruments 9.0 Monochrome - 6 camera (Sterling Heights, Mi). Clearly identifiable 53BP1 or  $\gamma$ H2AX foci inside the nucleus were counted as positive foci. Nuclei were scored as containing: 53BP1 foci ( $F < 5$ ;  $5 \leq F < 20$ ;  $F \geq 20$ ). Nuclei with fewer than 5 foci were considered foci-negative because this number of foci was common in untreated cells. Overlapping and/or contiguous 53BP1 and PML foci were scored in co-localization experiments.

### 3.8 Micronuclei assay

Unsynchronized cells or cells synchronized in S phase, as previously described, were treated with ETO or NCS at varying concentrations for 6 or 2 h, respectively; or with IR at different grade of irradiation. At the times indicated in each figures, cells were fixed in 4% paraformaldehyde for 10 minutes and permeabilized in 0.2% Triton X-100 in PBS for 1 minute. Fixed cells were stained with DAPI and washed with PBS. Cells were mounted with Vectashield and scored using fluorescence microscopy as above. Micronuclei, defined as DAPI-positive bodies that were morphologically identical but smaller than the nucleus, were scored according to Thomas and Fenech [127]. Cells were considered micronucleus-positive if they contained, at least, one micronucleus.

## MATERIAL AND METHODS

TAB.1 Antibodies' list

EPITOPE	COMPANY
53BP1, NB 100-304	Novus Biologicals, Littleton Co
anti- $\beta$ -actin, A5441	Sigma Aldrich, St. Louis, Mo
Nek4 (2631C1a), sc-81332	Santa Cruz Biotechnology, Dallas, Tex
cyclin A (H-432), sc-751	Santa Cruz Biotechnology, Dallas, Tex
Calnexin, #PA5-34665	Thermo Fisher Scientific, Ma
anti-mouse-HRP or goat anti-rabbit-HRP	Cell Signalling, Billerica, Ma
$\gamma$ -H2AX ,05-636, clone JBW301,	Merck Millipore, Billerica, Ma
PML Antibody (PG-M3), sc-966	Santa Cruz, Dallas, Tex
AlexaFlour555-conjugated goat anti rabbit, #4413S	Cell Signaling, Danvers, Ma
AlexaFluor488-conjugated goat anti-mouse, #4408S	Cell Signaling, Danvers, Ma
anti-BrdU , clone BU20A	eBioscience, San Diego, Ca

### 3.9 DNA synthesis assessment

Fibroblasts were seeded onto glass coverslips, synchronized as described above, and treated with 5 $\mu$ M ETO for 6 h. 10 $\mu$ M Bromodeoxyuridine (BrdU) pulse, with different lapse of time, was performed to assess DNA synthesis. Cells were fixed at the desired time point, as previously described, and were treated with 1M HCl for 45 minutes at room temperature. HCl was then neutralized with borate buffer and cells were washed once in PBS and blocked for 30 minutes in 4% BSA in PBST. Cells were incubated with an anti-BrdU antibody in 1% BSA-PBST buffer for 2 h at 37°C in a humidified chamber. Slides were then washed three times in PBST and incubated in AlexaFluor488-conjugated goat anti-mouse secondary antibody in 1% BSA-PBST for 1 h to label BrdU incorporation.

### 3.10 Comet assay

The microgel electrophoretic technique was performed utilizing the neutral lysis method which detects DSBs [162]. From a population of synchronized cells, a single-cell suspension was prepared by trypsin disaggregation. Disaggregated cells were counted and treated with 50  $\mu$ M ETO and 1.35  $\mu$ M NCS, respectively for 60 and 30 minutes, at room temperature and were then re-suspended in 1% low-melting agarose. The low-melting cellular suspension was seeded onto slides and cells were lysed by placing the slides in a humid chamber at 37°C with 2% SDS, 0.05M EDTA, 0.5 mg/ml proteinase K for at least 18 h. Lysis was performed under neutral conditions to detect DSBs. After lysis, slides were washed two times in 0.5X TBE buffer. Electrophoresis was carried out at 30 v/cm for 15 minutes in 0.5X TBE buffer. For visualization of DNA damage, slides were stained with DAPI and observed using fluorescence microscopy as described above. Cells with DNA damage appeared as comets. One hundred comets were scored for each species and each time point, and analysed with Open Comet [163] image analysis software. Individual comet images were scored for several features including tail length and percentage DNA in tail.

### 3.11 Cellular viability assay

Fibroblast viability was evaluated in terms of mitochondrial activity, by conversion of the dye MTT to insoluble formazan [164]. Cells were seeded in 96-well plates and treated with 5 and 50  $\mu$ M of ETO and 0.13 and 1.35  $\mu$ M of NCS for 6 and 2 h, respectively. At the times indicated (24, 48 and 72h), cells were washed with PBS and incubated in MTT (5 mg/mL) in PBS for 2 h. After removal of MTT, formazan crystals were dissolved with DMSO (all from Sigma Aldrich, St. Louis, Mo) and the amount of formazan was measured at  $\lambda = 570$  nm (ref.  $\lambda = 690$  nm) with a spectrophotometer (Victor<sup>2</sup> Multilabel Counter, PerkinElmer, Waltham, Ma). All experiments were repeated at least two times, with each comprising an evaluation of five wells per treatment. Mitochondrial activity in treated cells was calculated as a percentage relative to control cells according to the formula: (absorbance of treated fibroblasts/absorbance of untreated fibroblasts)  $\times$  100.

### 3.12 Cell cycle analysis

Cells were harvested by trypsinization, washed in PBS, and fixed overnight in 70% ethanol at 4 °C. Ethanol was removed by centrifugation and cells were washed with PBS, then

resuspended and incubated 30 minutes at room temperature in Guava Cell Cycle Reagent containing propidium iodide. Cells were analyzed for DNA content on a Guava EasyCyte Mini flow cytometer using the Guava Cell Cycle program (Guava Technologies, Hayward CA).

### **3.13 Beta-gal assay**

B-galactosidase assay detects senescent cells in a given population by staining the  $\beta$ -galactosidase activity. Providing to the cells an exogenous substrate, X-gal, this will be lysed by the enzyme causing the blue colour of senescent cells, appreciable at the microscope. Human (y#18) and mouse primary fibroblasts were synchronized in G0 for 48 hours by serum-free starvation and then fresh complete medium was added for 18 and 16 hours, respectively in human and mouse, to induce entry in S phase. Once synchronized, cells were treated with 0,13  $\mu$ M of neocarzinostatin (LD-NCS) in serum-free medium for 2 hours. Then LD-NCS was removed, cultures were washed, complete fresh medium was added to the culture plates and cells were incubated for 24 hours. At this time point, fibroblasts were washed twice with PBS1X and processed according to manufacturer's instructions (Senescence Cells Histochemical Staining Kit, CS0030-1KT Sigma Aldrich, St. Louis, Mo.) After staining, all the samples were washed three times with PBS1X and incubated for 48 hours. To avoid acidification of the medium due to CO<sub>2</sub> exposition, which can inhibit Beta-gal activity, plates were carefully sealed during incubation. For each sample a total number of 200 cells was counted. The percentage of senescent cells was determined by scoring the number of cells blue staining positive for the beta-gal assay, on total number.

### **3.14 Annexin V assay**

Annexin V assay allows detection of apoptotic and necrotic cells in a given cellular population. This assay includes the evaluation of Annexin V, a probe which binds to phosphatidylserine exposed on the external membrane of apoptotic cells, and 7-AAD, a cell impermeant dye, as an indicator of membrane structural integrity. 7-AAD is excluded from live, healthy cells and early apoptotic cells, but permeates in late-stage apoptotic and dead cells. For the evaluation of the presence of apoptotic cells, unsynchronized primary human and mouse fibroblast were used. Fibroblasts were seeded and, one day later, were treated with 100  $\mu$ M Etoposide (HD-ETO) for 30 minutes in serum-free medium. After treatment, the medium containing Etoposide was removed, cells were washed and fresh medium was added. Then, cells were

incubated for 24 and 48 hours. At different time points cells were collected, centrifuged and resuspended with Guava Nexin Reagent (4500-0450, Merck Millipore, Billerica, Ma). Analysis of the samples was performed with Guava easyCyte 5HT Millipore cytofluorimeter (Merck Millipore, Billerica, Ma). Early apoptotic cells (Annexin V (+) 7-AAD (-)) were gated and scored in untreated and treated samples.

### 3.15 CRISPR-CAS9 technology to break down 53BP1 expression.

The type II prokaryotic CRISPR (clustered regularly interspaced short palindromic repeats)/Cas is an adaptive microbial immune system, evolved in order to face phages' infections. It has been recently demonstrated that CRISPR nuclease system is able to facilitate genome editing in mammalian cells [165]; in fact it facilitates cleavage at the DNA level, with the help of RNA-guided site-specific. With this approach, it is possible change the target sequence by addressing the DSB at the genomic locus supposed to be edited. The DSBs, induced by nuclease activity, can be repaired by nonhomologous end-joining (NHEJ) or homology-directed repair (HDR); NHEJ's repair choice might efficiently introduce insertion/deletion mutations of various lengths which may disrupt the translational reading frame of the coding sequence [166]. Knockdown of 53BP1 gene has been programmed by disrupting the transduction of the protein by introducing a DSB at the start codon site (ATG triplet, as shown in Figure 11).

TTCCATTCCAGGGGAGCAGATGGACCCTACTGG AAGTCAGTTGGATTTCAGATTCTCTCAGCA

**Figure 11: 53BP1 sequence from the start codon.**

From database (<http://crispr.mit.edu/>) two guide RNAs (gRNA) have been designed:

**53BP1-AUG\_fw** *caccGGGGAGCAGATGGACCCTAC*

**53BP1-AUG\_rv** *aaacGTAGGGTCCATCTGCTCCCC*

53BP1 gRNA was cloned inside the pM U6\_gRNA plasmid, using the restriction site BbsI (Figure 12).

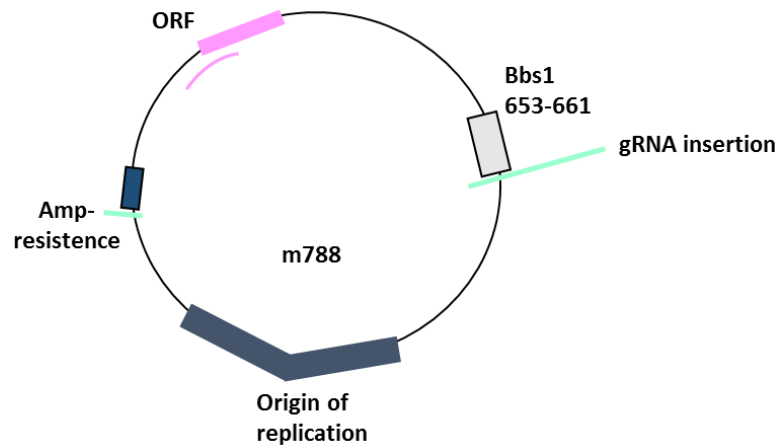


**Figure 12: pM U6\_gRNA plasmid sequence.**

### **3.16 Preparative restriction digestion**

Prior to the gRNA insertion into the linearized plasmid, a preparative restriction digestion was used to open the vector. 2 µg of plasmid DNA were digested by restriction enzyme (BbsI) in the appropriate buffer for 1 h at 37°C. DNA was then separated by agarose gel electrophoresis. And the DNA bands were cut from the gel. DNA was extracted from the gel using a gel extraction kit according to manufacturer's instruction.

### **3.17 Ligation, electrophoresis and gel recovery of DNA from agarose gels**

The Quick Ligation kit (NEB), to ligate gRNA fragments and the plasmid, was used according to manufacturer's instructions. Ligation was performed for 10 minutes at RT and then transferred to 4°C before transformation. After ligation, DNA fragments were separated by agarose gel electrophoresis, accordingly to their molecular size. 1% agarose gel was prepared by melting agarose in 1X TAE buffer. EtBr was added to a final concentration of 1 µg/ml. For electrophoresis, samples mixed with appropriate volume of 6X DNA loading buffer, were loaded onto a gel placed in a proper chamber was covered with 1X TAE buffer. Electrophoresis was performed at 120 V for 40 minutes. To check for the length of the inserted DNA fragment into the plasmid vector and its correct orientation another analytical restriction digestion was performed.

### 3.18 Transformation of competent *E. coli*

In order to transform competent *E. coli*, an aliquot of cells (DH5 $\alpha$ ) (0.2 ml) was mixed with ligation reaction mixture, previously prepared (2  $\mu$ l), and incubated for 30 minutes on ice. To open the membrane pores and let the ligation construct enter the cell, DH5 $\alpha$  were heat shocked at 42°C for 30 sec and immediately transferred to 4°C. LB-media (0.5 ml, warm) was added to the cells, mixed and suspension was incubated for 1 h at 37°C under vigorous shaking (250 rpm). Then, transformed cells were plated on LB-agar plates containing 50  $\mu$ g/ml ampicillin and allowed to grow not less than 24 h, at 37°C.

### 3.19 Miniprep

Single and well isolated colonies were picked from the selection plate and inoculated in 2.5 ml TB selective medium (50  $\mu$ g/ml ampicillin). Selected colonies were incubated overnight at 37°C, under shaking. Transformed *E. coli* cultures were pelleted; pellets, from each colony, were mixed with lysis solution (0.2 N NaOH, 1% SDS), neutralized with NH<sub>4</sub>OAc (7.5 M) and kept on ice (10 minutes) to precipitate genomic DNA. By the addition of 2-propanol, plasmid DNA was precipitated from the supernatant. Thus, DNA pellets were air dried and resuspended in TE containing RNaseA (50  $\mu$ g/ml). In order to check the size and the sequence of plasmids, isolated DNA undergone restriction digestions and consequent sequencing.

### 3.20 Maxiprep

Plasmid with the right size and sequence, were selected to perform a large scale plasmid isolation. Transformed *E. coli* were inoculated in a primary culture of 3 ml selective TB selective medium (50  $\mu$ g/ml ampicillin) and incubated for approximately 8 h at 37°C under shaking. After a small incubation, starter cultures were diluted into 250 ml selection TB medium and grown on large scale overnight under the conditions mentioned above. Bacterial cells were harvested and plasmid DNA's purification was performed using QIAGEN Plasmid Maxi Kit according to the manufacturer's protocol. Then for each sample, DNA concentration was determined spectrophotometrically.

### 3.21 Sequencing of plasmids

Sequencing of the constructs was performed by the BMFZ (Biologisch-Medizinisches Forschungszentrum) of the Heinrich-Heine-University Düsseldorf (Germany).

**3.22 Keratinocytes transfection for a stable transformation**

Prior to transformation, cells were seeded and splitted on day before transfection at 1:4 and 4/5 dilution, respectively. Cells were transfected with 1 µg of 53BP1 knock down maxi prep and Cas-9-RFP tagged (to select transfected clones) were used for keratinocytes transfection with the transfection Kit (301425, QIAGEN, Hilden, Germany). Procedure were carried out according to the manufacturer's protocol. Stable transgenic cell clones were selected 48 h after transfection and maintained in selective medium containing 100 mg/ml hygromycin. Approximately three weeks later, only red clones were selected.

**3.23 Clonogenic Assay Formation Assay (CFA)**

Untreated cells were seeded, in triplicate, in petri dishes at a final density of 1000 cells/plate. Cells were incubated until they have formed colonies that were of a substantially good size to be scored. The right colony size is defined as a cluster of cells of, at least, 50 cells. After discarding medium, cells were at first washed with PBS1X and then fixed for 30 minutes at room temperature with pre-iced methanol 100%. 0, 5% crystal violet solution was added to the samples, which were incubated at room temperature for 5 minutes. In order to remove crystal violet, plates were immersed in tap water and then they were allowed to dry at room temperature up to a few days. The number of colonies were counted by a stereomicroscope [167].

**3.24 Survival Assay**

Survival efficiency was tested on keratinocytes wild type (KT WT) and 53BP1 knock down (53BP1 KD). Cells were seeded 24h prior irradiation and then were irradiated with two different doses of ionizing radiation (IR), 1Gy and 4 Gy respectively. After treatment with IR, cells were collected, counted and seeded in duplicate on a culture dish (Petri dish) at a final density of 240.000 cells/dish. After treatment cells were incubated and allowed to grow for 7 days. After 7 days, cells were stained with 0,5% of crystal violet solution, as described for CFA. Crystal violet was dissolved in acetic acid 100% for 5 minutes. Solved crystal violet was collected and absorbance was read at the spectofotometer (495 nm). Untreated and treated samples were analysed and results are an average of 4 independent experiments.

### 3.25 Microscopy

Images were captured using an Olympus BX61 fluorescence microscope (Tokyo, Japan) equipped with a Hamamatsu ORCA-ER camera (Hamamatsu City, Japan) or an Olympus IX50 equipped with a Diagnostic Instruments 9.0 Monochrome - 6 camera (Sterling Heights, Mi).

### 3.26 Data analysis and database

Spontaneous MNE frequency (MNEF) for 65 mammals data were collected through a systematic PubMed search. MNEF is known to be higher in erythrocytes of developing organisms and to decrease to a certain level in adult life [168]. Additionally, studies performed in mice [169] and humans [156] show that during aging there is again an increase in MNEF. According to Sato et al., this increase is not observed, or observed only very late in life, in some strains of mice [194]. In light of these considerations, we collected data only for adult animals for which the approximate age was specified (47 species) and which are reported in Tab.3. Additionally body mass (BM) and maximum longevity (ML) values are shown as taken from the AnAge Database [145]. More detail about selection can be found in [170].

### 3.27 Statistical analysis

All results are expressed as the mean  $\pm$  s.e.m, unless specified. Differences between species, treatment or time point were evaluated using ANOVA, followed by Tukey's Multiple Comparison Test (\* *p value* < 0.05, \*\* *p value* < 0.01, \*\*\* *p value* < 0.001) using Graphpad Software Inc (La Jolla, Ca), unless specified. Maximum human longevity is 122 years. In the figures captions and in the correlation analysis it is adjusted to 90 years to account for the fact that, for the others species, only small cohorts were used to determine maximum life span, and 90 years seems a more realistic estimate for a random sample of humans.

## MATERIAL AND METHODS

MAMMALS	n	MNEF (MNE/10000 TE)	MAXIMUM LONGEVITY (years)	BODY MASS (Kg)	REFERENCES
<i>Alouatta palliata</i>	2	3,00	24,0	7,00	Zuniga, 2005
<i>Antilope cervicapra</i>	1	1,50	23,9	37,50	Zuniga, 1996
<i>Apodemus flavicollis</i>	18	17,40	4,5	0,03	Abramsson,1997
<i>Apodemus sylvaticus</i>	12	13,30	6,3	0,02	Abramsson,1997
<i>Ateles geoffroyi</i>	20	0,67	47,1	7,20	Zuniga,2005
<i>Bos Taurus</i>	43	1,28	20,0	750,00	Cristaldi, 2004
<i>Canis familiaris</i>	16	1,22	24,0	40,00	Zuniga, 1996
<i>Capra falconeri</i>	1	0,00	19,1	41,00	Zuniga, 1996
<i>Capra hircus</i>	13	0,80	20,8	61,00	Zuniga, 1996
<i>Cavia porcellus</i>	10	0,30	12,0	0,72	Zuniga, 1996
<i>Cebuella pygmaea (Callithrix pygmaea)</i>	1	10,00	18,6	0,12	Zuniga, 2005
<i>Cebus albifrons</i>	4	20,50	40,4	2,46	Zuniga, 2001
<i>Cercopithecus aethiops (Chlorocebus aethiops)</i>	4	0,40	30,8	5,62	Zuniga, 2005
<i>Clethrionomys glareolus</i>	24	4,00	4,9	0,09	Abramsson,1997
<i>Cryptotis parva</i>	10	24,30	3,5	0,05	Meier, 1999
<i>Didelphis virginiana</i>	3	1,30	6,6	3,00	Zuniga, 2001
<i>Equus asinus</i>	9	1,70	47,0	165,00	Zuniga, 1996
<i>Equus burchelli (Equus zebra)</i>	1	1,20	33,2	296,00	Zuniga, 1996
<i>Equus caballus</i>	27	2,64	57,0	300,00	Cristaldi, 2004
<i>Felis domesticus</i>	64	8,52	30,0	3,90	Zuniga, 1996
<i>Felis ruffus (Lynx rufus)</i>	1	0,50	32,3	8,60	Zuniga, 1996
<i>Felis yagouaroundi</i>	1	4,50	18,6	7,00	Zuniga, 1996
<i>Gazella thomsoni</i>	1	4,00	20,0	25,00	Zuniga, 1996
<i>Giraffa Camelopardalis</i>	1	0,00	39,5	800,00	Zuniga, 2001
<i>Gorilla gorilla</i>	2	0,90	55,4	139,84	Zuniga, 1996
<i>Homo sapiens</i>	14	0,40	122,5	62,03	Zuniga, 2005
<i>Lama glama glama</i>	2	3,50	28,9	140,00	Zuniga, 1996
<i>Macaca fascicularis</i>	2	0,00	39,0	6,36	Zuniga, 2005
<i>Macaca mulatta</i>	1	2,60	40,0	8,23	Zuniga, 1996
<i>Mandrillus sphinx</i>	1	1,00	40,0	23,00	Zuniga, 2005
<i>Mephitis mephitis</i>	1	2,50	13,9	3,50	Zuniga, 1996
<i>Meriones unguiculatus</i>	8	9,40	6,3	0,05	Zuniga, 1996
<i>Mesocricetus auratus</i>	11	6,30	3,9	0,10	Zuniga, 1996
<i>Microtus agrestis</i>	24	1,20	4,8	0,05	Abramsson,1997
<i>Mus musculus</i>	22	15,20	4,0	0,02	Abramsson,1997
<i>Odocoileus virginianus</i>	5	2,30	23,0	87,00	Zuniga, 1996
<i>Oryctolagus cuniculus</i>	12	1,96	9,0	1,80	Ramirez, 1999
<i>Ovis aries</i>	5	0,80	22,8	80,00	Zuniga, 1996
<i>Pan troglodytes</i>	1	2,00	59,4	44,98	Zuniga, 2005
<i>Panthera leo</i>	2	0,60	27,0	175,00	Zuniga, 1996
<i>Peromyscus leucopus</i>	10	0,00	8,0	0,02	Meier, 1999
<i>Pongo pygmaeus</i>	2	0,50	59,0	64,47	Zuniga, 1996
<i>Rattus norvegicus</i>	10	2,20	3,8	0,30	Zuniga, 1996
<i>Saguinus midas</i>	1	4,00	21,0	0,55	Zuniga, 2005
<i>Sciurus aureogaster</i>	4	3,50	23,6	0,60	Zuniga, 2000
<i>Sus scrofa</i>	55	3,77	27,0	130,00	Cristaldi, 2004
<i>Tamias americana (Mazama temama)</i>	1	4,00	17,1	33,00	Zuniga, 1996

**Table 4. Data used in the meta-analysis.** All data were used for Figure 37 A, B, C. Only data highlighted were used for figure 37 D, E, F and for figure 38; only data highlighted with  $n \geq 3$  were used for figure 37 G, H, I; MNEF, MicroNucleated Erythrocytes Frequency; MNE, MicroNucleated Erythrocytes; TE, Total Erythrocytes (micronucleated and not)[171][172][173][174][148][175].

## 4. RESULTS

### 4.1 PART I- DNA damage detection by 53BP1: relationship to species longevity

#### 4.1.1 Measuring toxicity across the species

The comparative approach performed in the present study arises from the hypothesis that differences in lifespan may reflect structural cellular differences. This experimental investigation, in fact, aimed to test whether the efficiency of DNA damage repair may also explain the big difference in longevity, observed across mammalian species. The selection of mammalian species enrolled in the present experimental model was carried out on the basis of two fundamental features for an analysis in biogerontology: species should cover wide variation in body size mass and lifespan length. Primary skin fibroblast from mouse, cow, dog, bat and human were challenged with two radiomimetic drugs: ETO and NCS.

*In primis*, it was necessary to monitor cell survival and, eventually, to register metabolic differences in response to the two selected genotoxic damaging agents. A comparison of metabolic activity measures was performed.

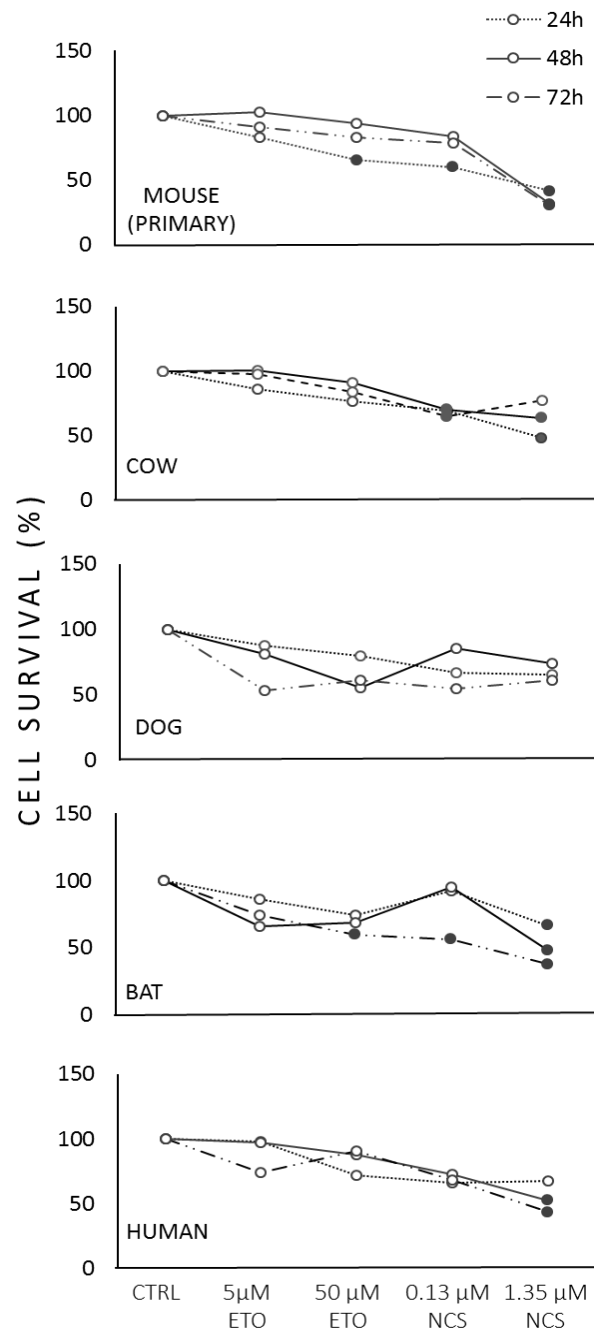


**Figure 13: MTT assay to measure toxicity.** Fibroblast viability was evaluated with the colorimetric MTT assay in untreated (CTRL) and treated cells (5µM and 50µM ETO; 0.13 µM and 1.35 µM NCS) at 24, 48 and 72h after the beginning of treatment. Statistical analysis compares treated to untreated controls, for each species. ● = *p* value < 0.05; ○ = *p* value > 0.05.

The MTT assay gives a measure of metabolic activity as the cellular capacity to convert MTT to formazan (Figure 13) at 24, 48 and 72h after damage across all the five species. Low doses treatments (5  $\mu\text{M}$  ETO or 0.13  $\mu\text{M}$  NCS) induce a low cytotoxic effect in all species and did not cause a significant reduction in MTT activity, whereas doses 10 times higher did.

#### 4.1.2 Dose response experiments in 53BP1 foci formation

To assess the efficiency of the DNA damage response in the comparative experimental model, the role of 53BP1 was investigated across the five species.

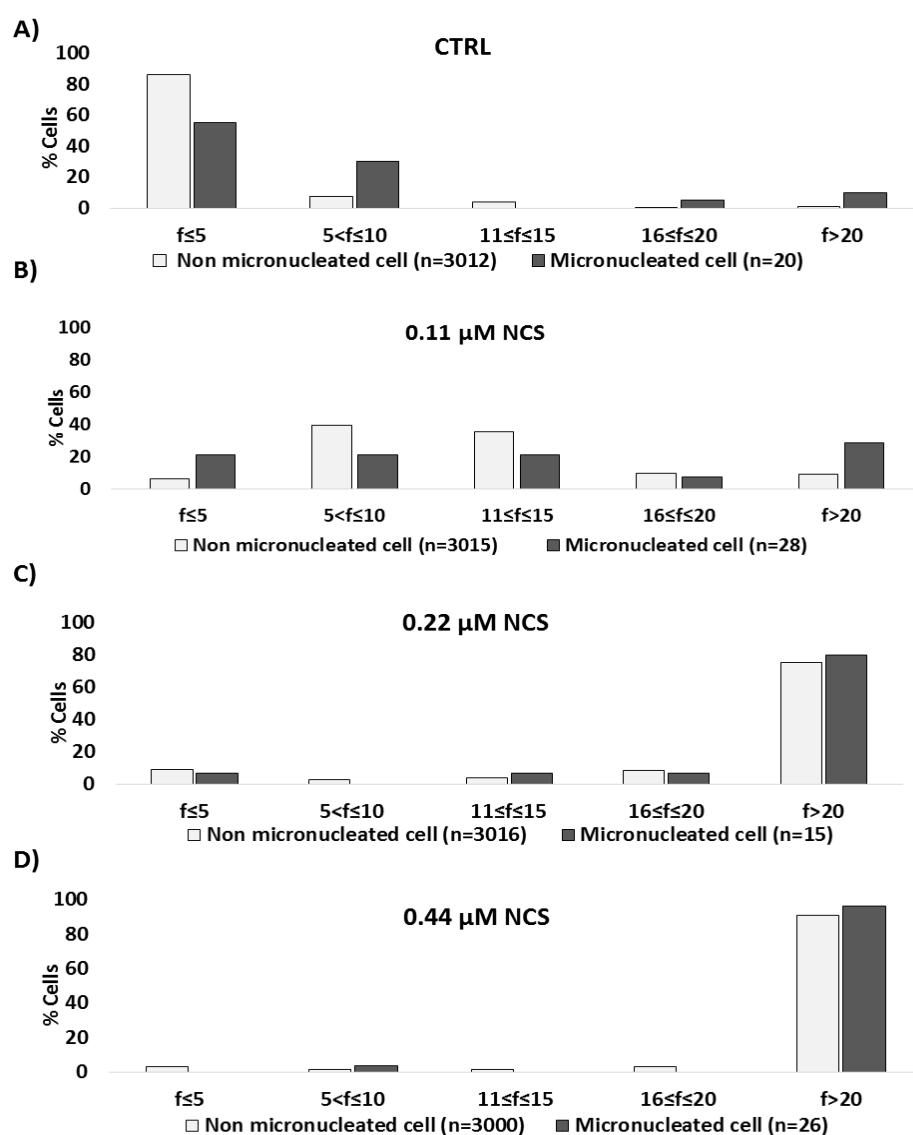


**Figure 14: Dose-response relationship of 53BP1 foci in unsynchronized cells.** 53BP1 foci were scored 24h after damage both in non micronucleated (light grey bars) and micronucleated cells (dark grey bars) after treatment with increasing concentration of NCS (A-D).

53BP1, as previously mentioned, is a DNA damage marker and sensor, which rapidly accumulates at DNA damage site. Agglomerate of 53BP1 protein are called foci and their abundance is directly proportional to the intensity of damage. Thus, to determine time and concentrations that would yield a not maximized 53BP1 foci response, preliminary experiments with increasing concentration of genotoxics were performed. Human fibroblasts (IMR90) were treated for two hours with increasing doses of NCS (CTRL, A; 0.11  $\mu$ M, B; 0.22  $\mu$ M, C; 0.44  $\mu$ M, D) and then fixed 24h after the beginning of damage. Fixed cells were prepared for immunofluorescence to detect 53BP1 and  $\gamma$ -H2AX foci. Data report of an experiment on human cells showed that already at a low concentration of NCS (0.22  $\mu$ M) the 53BP1 foci response is maximized (i.e. the vast majority of the nuclei have more than twenty 53BP1 foci each). Similar dose response experiments were performed for ETO (Figure 21).

Thus, the majority of the experiments were carried out using the lowest concentration able to elicit a significant response. A second comparison was performed between mouse (3T3) and human (IMR90) unsynchronized cells. Untreated cells (A, C) and cells treated (B, D) with 1.35  $\mu$ M NCS, for 2h, were fixed 72h after the beginning of damage. At the highest concentration used for NCS (1.35  $\mu$ M), while the response of the most responsive species (human) was totally maximized, the response of mouse cells were still intermediate (Figure 15).

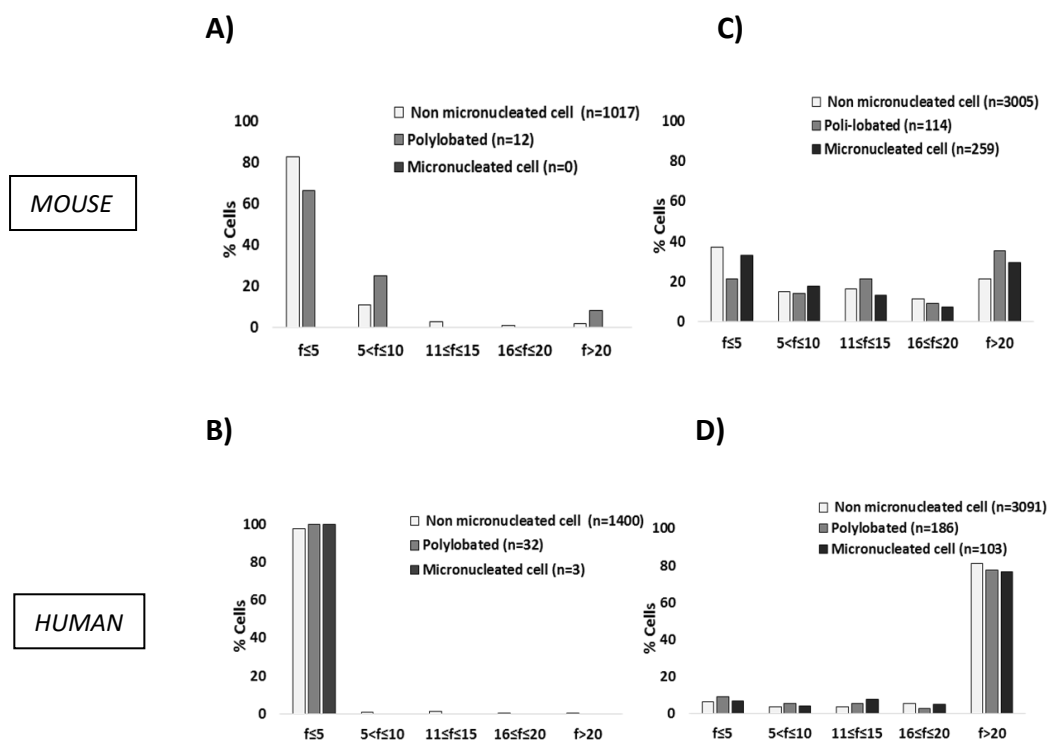


**Figure 15: High NCS doses induce massive 53BP1 foci formation in human but not in mouse.** Fixed cells were prepared for immunofluorescence. A) and B) untreated cells from mouse and human; C) and D) cells treated with 1.35  $\mu$ M NCS from mouse and human respectively. 53BP1 foci (f) were scored in three categories of cells represented in: 1) Non micronucleated cells (nuclei with regular shape); 2) Polylobated (nuclei with irregular shape and nuclear bud); 3) Micronucleated cells (nuclei with regular or irregular shape with MN and nuclei with mitotic crisis).

#### 4.1.3 53BP1 co-localize with $\gamma$ -H2AX after 5 $\mu$ M ETO treatment.

Since published data suggest that long lived species have a better Ku70-Ku80 DNA-end binding capacity [13], we speculated that long-lived species could be more efficient in detecting and, possibly, repairing DNA DSBs. To prove that treatments used were able to elicit DSBs, a co-immunostaining experiments for 53BP1 and  $\gamma$ -H2AX was performed. The co-localization of 53BP1 and  $\gamma$ -H2AX is, in fact, a widely accepted marker of the presence of a DSB [112]. Figure 16.A shows that, with 5  $\mu$ M ETO treatment, 53BP1 foci co-localize with  $\gamma$ -H2AX foci in the vast majority of cases in both mouse primary and human cells. Between 1, 2 and 10 h after the beginning of treatment, every hundred 53BP1 foci, more than eighty 53BP1 foci co-localized with  $\gamma$ -H2AX in both species (Figure 16.B).

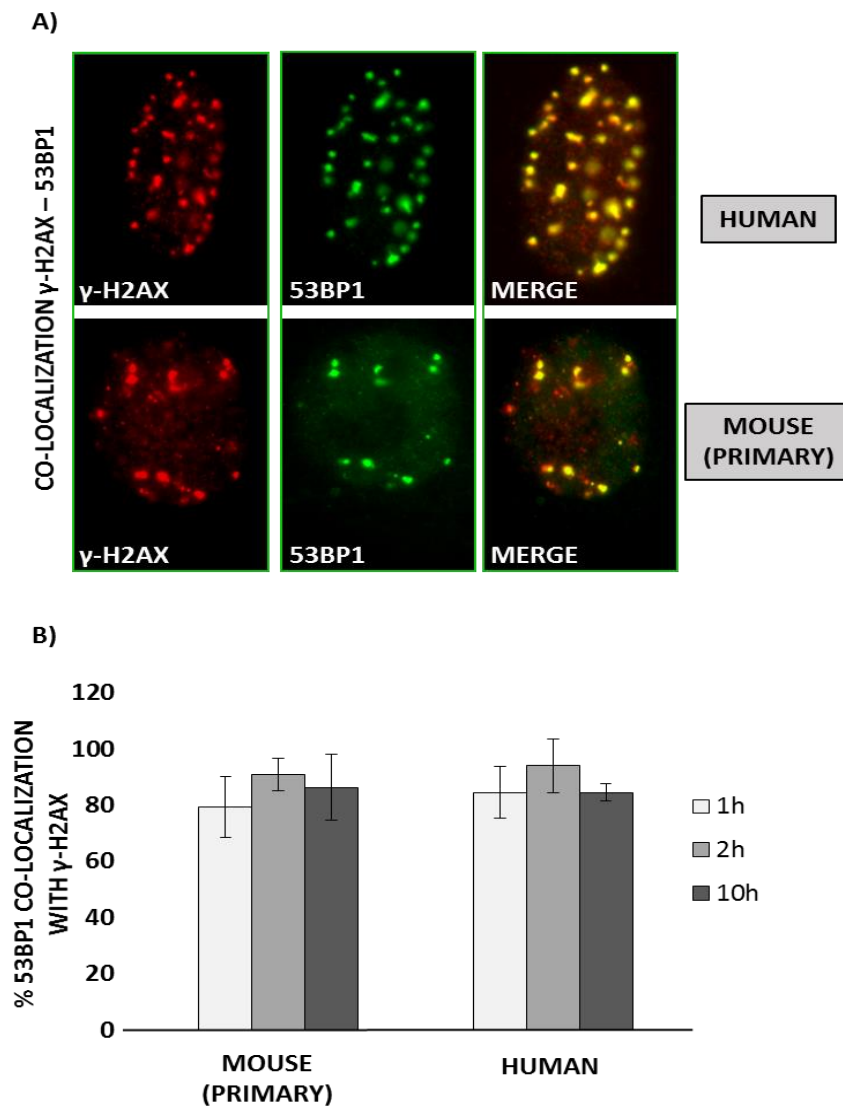


**Figure 16. 53BP1 and  $\gamma$ -H2AX co-localize in the presence of DSBs.** A) Representative immunofluorescence of nuclei in fibroblasts stressed with 5 $\mu$ M ETO treatment ( $\gamma$ -H2AX in red, 53BP1 in green, merge in yellow). B) 53BP1 co-localization with  $\gamma$ -H2AX in nuclear foci 1, 2 and 10 h after the beginning of 5 $\mu$ M ETO treatment. Statistical analysis: T-Student test followed by paired test. Shown are means  $\pm$  sd of two independent experiments.

#### 4.1.4 Long-lived species exhibit the highest percentage of 53BP1 foci and protein level.

In order to assess if differences in the efficiency of DNA damage detection machineries could be a driving force of the evolution of longevity, 53BP1 appearance was investigated in a comparative model. Synchronized primary fibroblasts from five different mammalian species (mouse, cow, dog, bat, human), were exposed to either 5  $\mu$ M ETO or 0.13  $\mu$ M NCS during S phase and were monitored at specific time intervals, from two hours up to three days after the beginning of damage. Cells were scored for 53BP1 foci, which were grouped into:  $f < 5$ ,

$5 \leq f < 20$  foci and  $f \geq 20$  foci per nucleus. The histogram bars show the percent of nuclei with 53BP1 foci  $\geq 5$  (obtained summing  $5 \leq f < 20$  and  $f > 20$ ). Figure 17 (A and B) shows a time-course analysis after 5  $\mu$ M ETO treatment. The time course analysis revealed a peak in 53BP1 foci formation between 2 and 10 h in all species (Figure 17), followed by a gradual decline in the percentage of foci-positive nuclei.

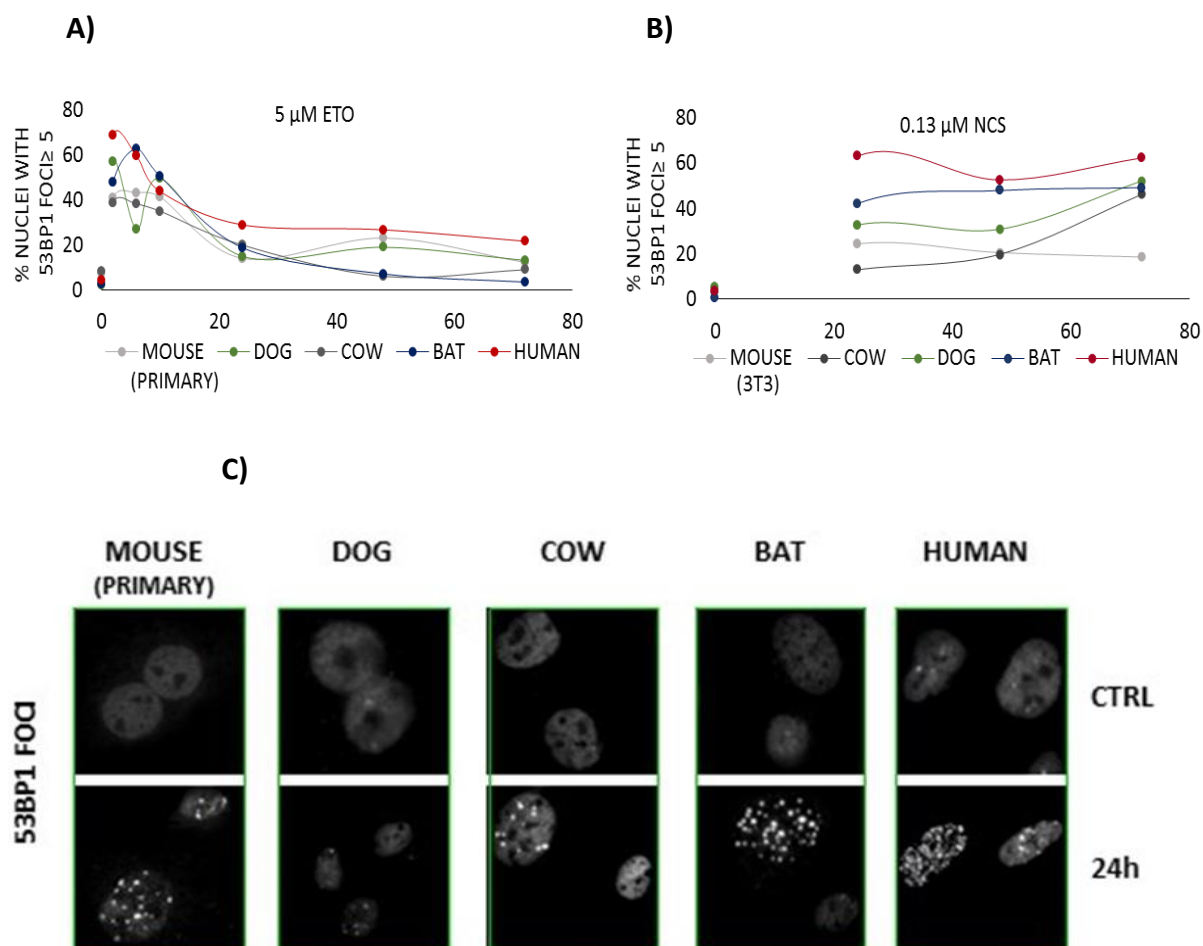


**Figure 17. 53BP1 foci formation kinetic is similar in all the species.** Time course curve shows the trend of foci formation after 5 $\mu$ M ETO (A) or 0,13  $\mu$ M NCS (B) treatment, in all species, from 0 to 72 h. C) Representative immunofluorescence image of 53BP1 foci formation in untreated (CTRL) and 5 $\mu$ M ETO treated human cells, observed 24h after the beginning of damage.

Interestingly, longer-lived species showed a higher percentage of nuclei with more than five 53BP1 foci. Human cells, derived from the longest-lived species, exhibited the highest percentage of foci when compared to all other species, with statistical significance observed consistently at 2 and 24 h from the beginning of damage (Figure 18.A and B). More interesting, human cells seemed to retain a higher number of foci over time.

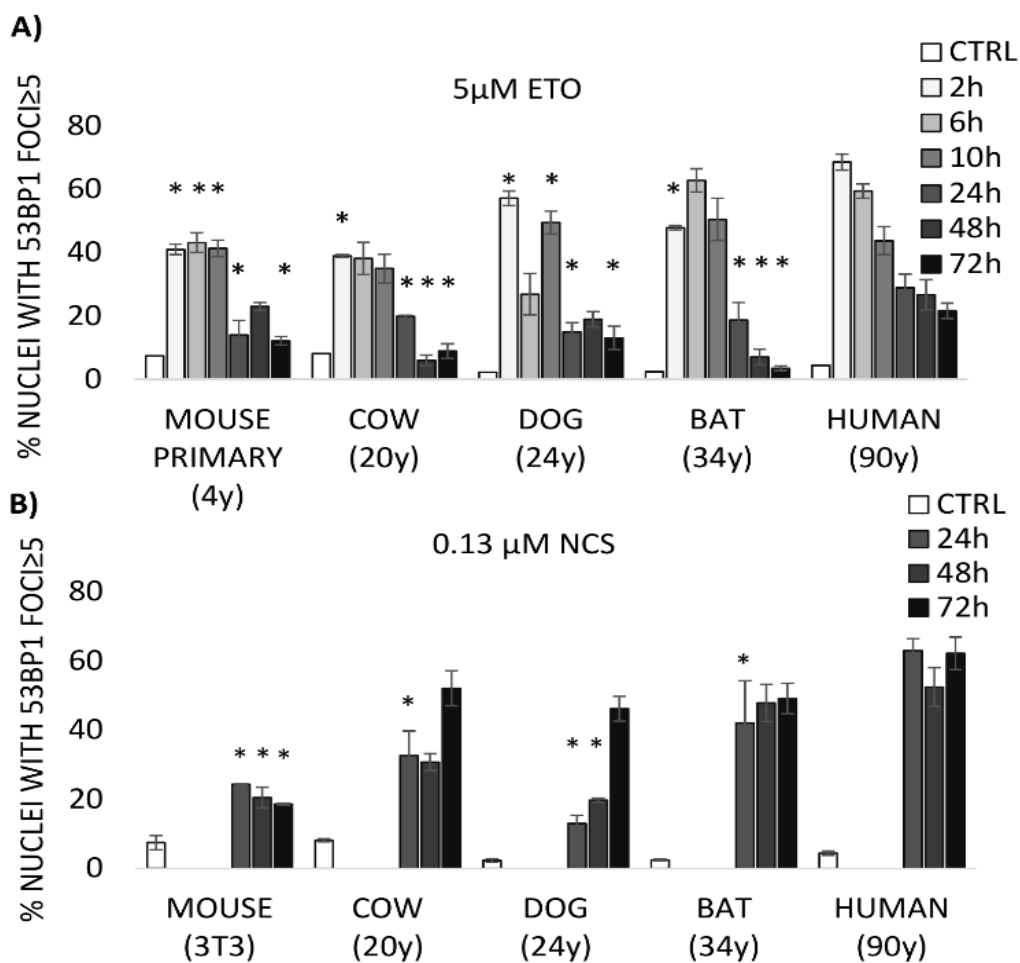


**Figure 18. Longer lived species recruit 53BP1 in nuclear foci at a higher rate.** A) Untreated (CTRL) and 5 μM ETO treated cells were fixed either during and right after treatment at the following time points: 2, 6, 10, 24, 48 and 72 h following the beginning; B) Untreated (CTRL) 0.13 μM NCS treated cells were fixed at 24, 48 and 72 h. The respective maximum life span of each species is reported in parenthesis in years (y). From 200 to 400 cells were scored twice for each sample, from 2 to 6 independent experiments. Statistical significance is referred to the comparison of all the species to the equivalent time point in human.

As previously showed, 24 h were required for visible foci to form in treated with 1.5 μg/mL of NCS (0.13 μM) [134]. Accordingly, foci were scored from 24 to 72 h after the beginning of damage with this agent. Similar to results with 5 μM ETO treatment, longer-lived species exhibited a higher percentage of cells with more than five foci per nucleus in response to 0.13 μM NCS. Human cells showed the highest percentage of cells with more than five 53BP1 foci (Figure 18.A and B). At the opposite, both primary and immortalized 3T3 mouse cells exhibited the lowest foci response among the studied species; mouse and cow response were

comparable only in the case of ETO treatment. Following genotoxic stress, the steady state level of the 53BP1 protein was also assessed. Independently from treatment time, whole lysates show a multiband pattern of 53BP1, suggesting the existence of different modifications of the protein (Figure 19).

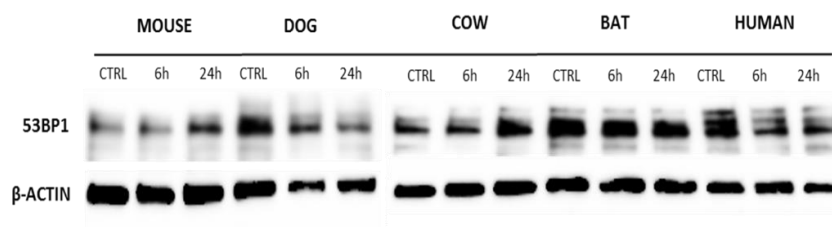


**Figure 19. 53BP1 protein expression in response to DNA damage.** A) Immunoblot analysis in fibroblasts for 53BP1 in lysates from untreated (CTRL) or 5 $\mu$ M ETO treated (+) for 6 h, harvested at 6 or 24 h after genotoxic treatment.

Densitometric analysis of multiple experiments is shown in Figure 19. It appears that protein levels do not change substantially during the 24 h following the beginning of 5  $\mu$ M ETO treatment (except for the 24 h time point in dog cells, figure 20). This suggests that 53BP1 is a constitutive protein. Mouse and dog cells have significantly lower level compared with human cells. More generally, the larger and/or longer-lived species (cow, bat and human) appear to possess higher 53BP1 protein amount although these differences are always below one fold (Figure 20).

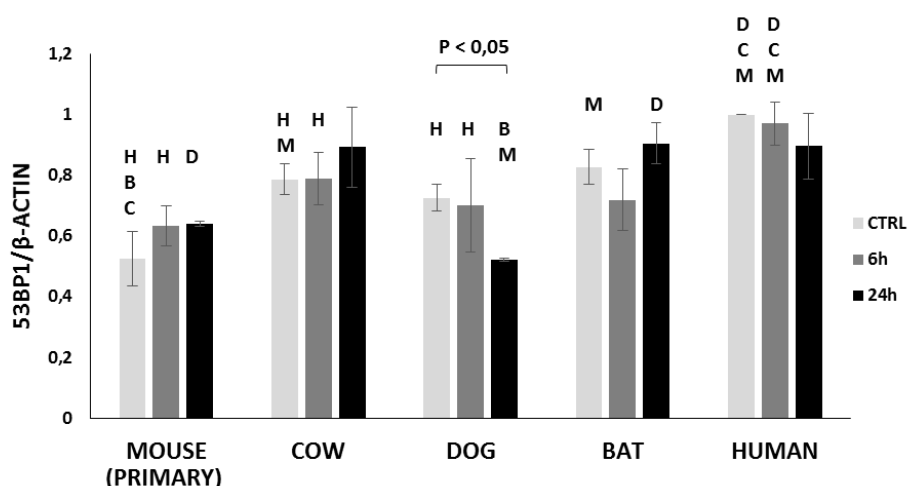


**Figure 20. 53BP1 protein expression after DNA damage.** Quantification of 53BP1 signal, normalized over actin signal, is representative of two or more independent experiments in untreated (CTRL) and 5 $\mu$ M ETO treated in fibroblasts. Statistical analysis: T-Student test followed by paired test (two tailed). The data from a single species were compared to each individual species for the same treatment time, and, inside a single species. CTRL values were compared with 6 and 24 h time points. Significant difference ( $p$  value < 0,05) between pairs of species is indicated by the presence of a squared bracket or by the initials of each species (M = mouse; D = dog; C = cow; B = bat; H = human).

#### **4.1.5 Genotoxic treatments induce 53BP1-PMLnb co-localization and increase of senescence in long-lived species**

Detection of the presence of damage is a necessary step in order to proceed with repair. But when damage is irreparable, cells respond to DNA stress with other means of damage control: primarily, cell division can be inhibited through the activities of the tumor suppressor p53, in order to prevent the genomic instability; or cellular senescence can be induced. The latter process is well known as stress-induced senescence (SIS): it takes place in response to a variety of stressors that include DNA damage, changes in the structure of the heterochromatin, strong mitogenic signals resulting from the expression of oncogenes or exposure to strong genotoxic stressors [121]. Recently, nuclear markers of senescence has been identified as DNA Segments of Chromatin Reinforcing Senescence (abbreviated in SCARS). DNA-SCARS, as suggested by Rodier and colleagues, are long-lasting foci where co-localization of 53BP1 and Promyelocytic leukemia protein (PML) nuclear body (nb) takes place [121]. In support of this interpretation and to test if, in the present experimental model, treatments performed with genotoxics induced also DNA-SCARS formation, PMLnb and 53BP1 were co-stained through an immune-fluorescence on human cells. Human fibroblasts were treated, during S phase, with increasing doses of ETO (5, 50, 100  $\mu$ M) for 6h. Cells were then fixed at 24h, 48h and 72h after the beginning of damage. Figure 21 shows that, even with at low concentration of genotoxic treatment, a significant increase in the percentage of PML nuclear body contiguous to 53BP1 foci is observable at 72h after the beginning of treatment. Since, 53BP1 foci formation assay (Figure 18.A and B) showed that all the five species, and in particular human, retained 53BP1 agglomerates for long time after damage (72h), we could hypothesize DNA-SCARS are induced after low and higher genotoxic treatments.

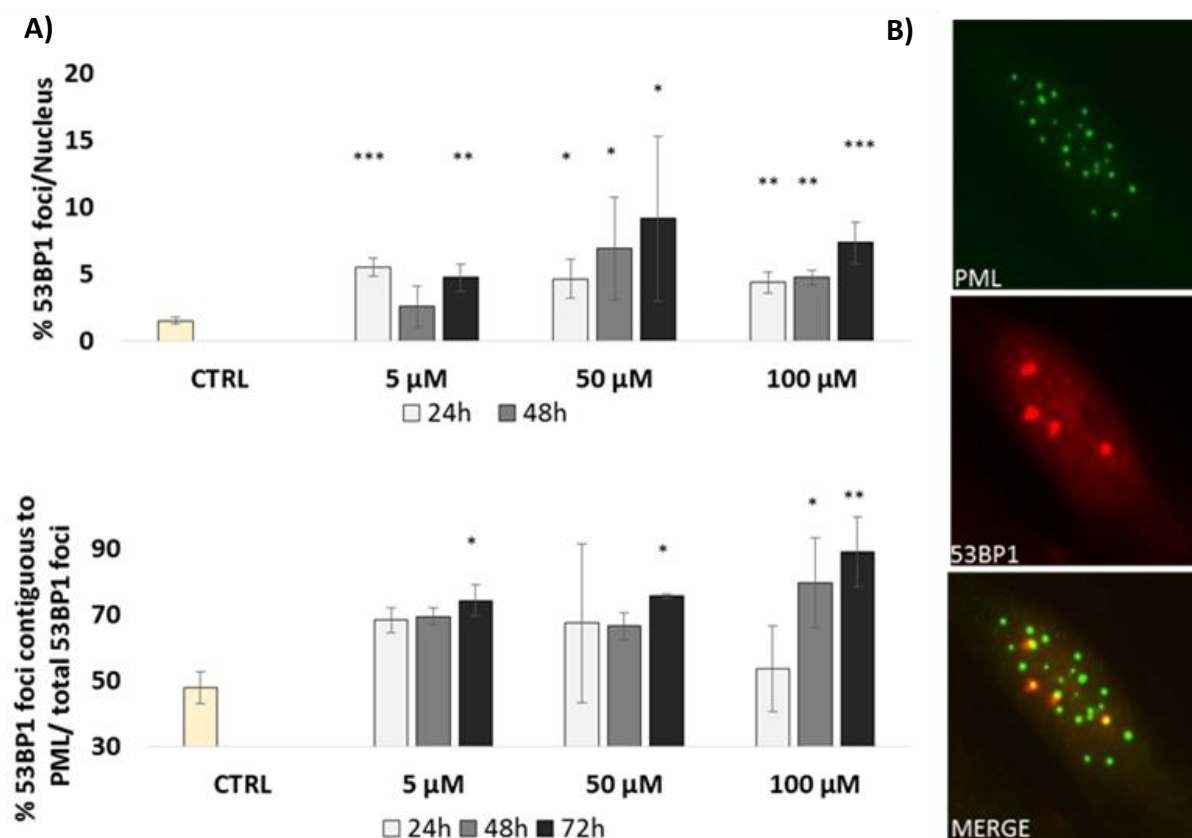


**Figure 21. Genotoxic damage induces co-localization of 53BP1 with PMLnb.** 53BP1 foci per nucleus and percent of 53BP1 foci contiguous to PMLnb were scored in 50 nuclei for each experimental condition and time point experiments in untreated (CTRL) and 5μM ETO treated in fibroblasts (A). Graphs represent two independent experiments. Statistical analysis: T-Student test followed by paired test (two tailed); *p* value < 0.05. B) Representative immunofluorescence of contiguous PML/53BP1 foci.

Additionally, the hypothesis that long-lived species are able to induce more efficiently senescence was tested and  $\beta$ -gal activity has been measured in human and mouse fibroblasts, challenged with a genotoxic stimulus (0.13  $\mu$ M NCS). Senescence-associated (beta)-galactosidase ( $\beta$ -gal) is widely used as a biomarker of replicative senescence [176]. In both species,  $\beta$ -gal activity was measured 24h after NCS treatment. Data report shows a similar rate of senescence in untreated cells but a stronger induction of senescence in human (long living species), suggesting that longer lived species are better equipped in activating all the mechanism which may protect cells from genomic instability (Figure 22).

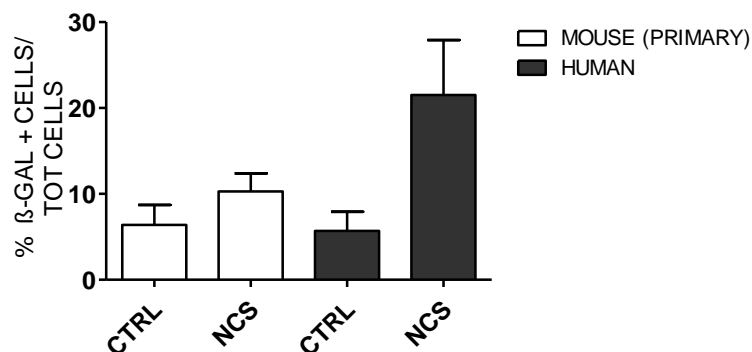


**Figure 22: β-gal activity increases in human cells after high dose genotoxic treatment.** Mouse and human fibroblast were treated with low doses of NCS and tested for β-gal activity, 24h after damage.

#### 4.1.6 Genotoxic stress induce cell cycle arrest in all the species

DDR is a complex pathway which exploits its activity by controlling the cell cycle progression as well. In order to give to the cell sufficient time to repair DNA damage, cell cycle is usually slowed down after a genotoxic insult. With respect to cell cycle control in response to DNA damage, DNA content was measured in mouse, dog, cow, and human cells (Figure 23). On a Guava EasyCyte Mini flow cytometer, cell cycle progression was monitored in  $G_0$  synchronized cells (48 h of serum starvation), and stimulated to enter into the S-phase by adding fresh regular growth medium. Cells in S-phase were treated with 5 $\mu$ M ETO for 6 h in serum free medium. Cells were harvested by trypsinization and fixed overnight in 70% ethanol at 4 °C. Fixed cells were prepared for cell cycle analysis by addition of Guava Cell Cycle Reagent containing propidium iodide. Cytofluorimetric analysis revealed a significant shift in the cell cycle profile in all four species tested. In treated cells, between 2 and 6h after damage, an increase of percentage of cells in the S and  $G_2$  phases of the cell cycle was observed, especially  $G_2$  for mouse and S for dog, cow, and human (Figure 23).

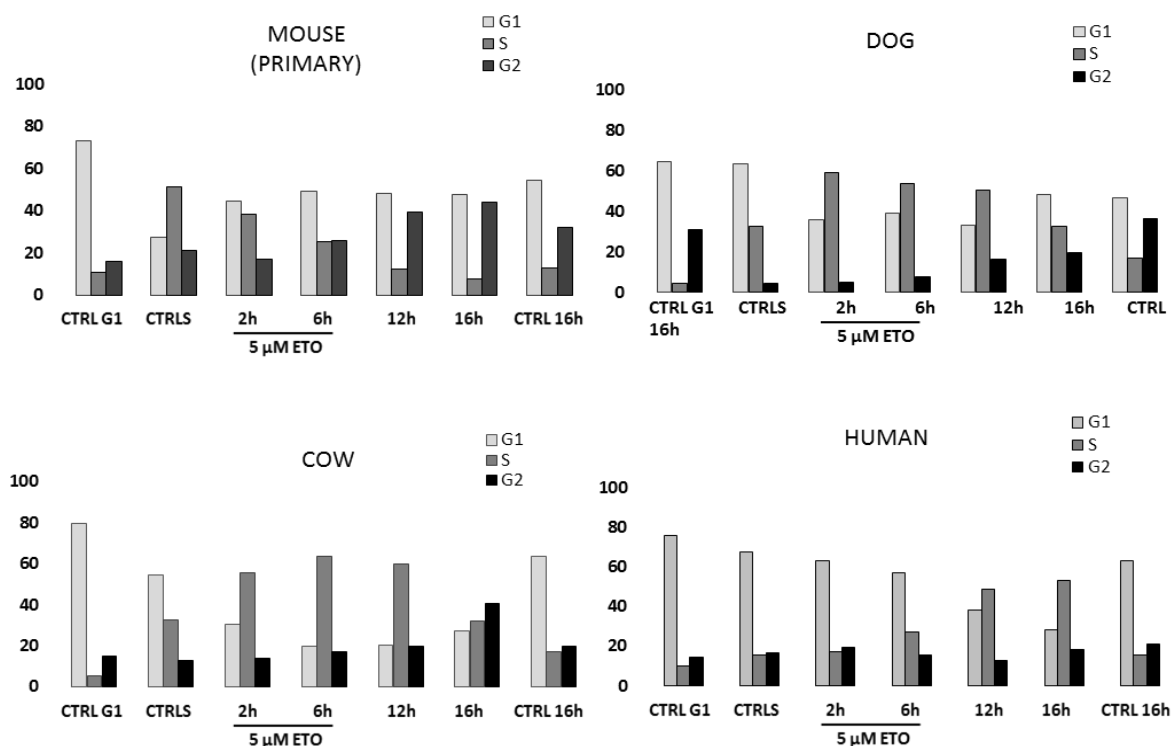


**Figure 23. Influence of DNA damage on species cell cycle.** Synchronized fibroblasts from four mammal species, were treated for 6 hours with 5 μM ETO. Synchronized population was analyzed at different time after damage and up to 16h.

Moreover, Cyclin A and Nek 4 expression was examined through western blot analysis in species for which antibodies with conserved epitopes were available. Both of them in fact, are markers used in order to highlight cell cycle progression in a cellular population. Increased expression in cyclin A, in all treated cells, confirmed a larger proportion of cells in G2 arrest. (Figure 24).

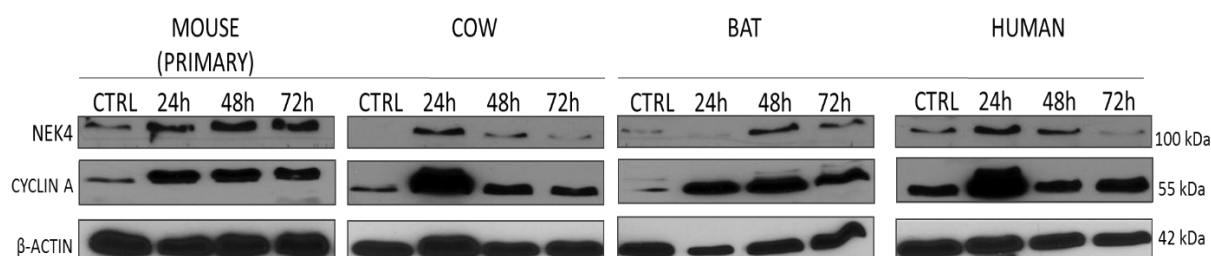


**Figure 24. Immunoblot analysis for NEK4 and CYCLIN A after DNA damage.** Lysates from untreated cultures (CTRL) or from cultures treated with 5 μM ETO for 6 hours, were collected at 24, 48 and 72 h after the beginning of the genotoxic treatment. Membranes were exposed for different intervals to obtain optimal signals. Actin and ponceau staining (protein) were used as loading controls.

This was evident in all species, but especially pronounced in human and cow. In addition, the expression of Nek 4, a recently described regulator of both DNA-PK association with DNA damage and entry into senescence [177], also increased following damage.

To further observe differences in the efficiency of cell cycle arrest following damage, we exposed mouse and human cells to 5  $\mu$ M ETO and pulsed them with BrdU. Cells were analyzed for the percentage of cells synthesizing DNA (BrdU-positive nuclei) and the percentage that harbor BrdU-positive 53BP1 foci (BrdU staining only in damage foci) at time points from 14 to 72 h after the beginning of damage (Figure 25). For the 14 and 24 h time-points, the cultures were pulsed with BrdU for 3 h at 10 h from the beginning of treatment; the 72 h time-point was pulsed for 3 h at 24 h from the beginning of treatment. At 14 h, human cell populations contained a lower percentage of cells synthesizing DNA compared with mouse cells, but a similar percentage of cells with BrdU foci.

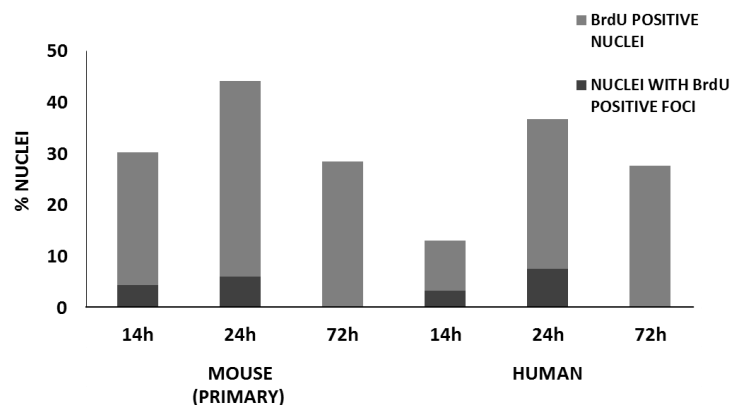


**Figure 25. DNA synthesis after DNA damage in mouse and human cells.** Cell populations were analyzed for the percentage of cells synthesizing DNA (BrdU positive throughout the nucleus; BrdU/TOT) and the percentage of cells that harbor BrdU-positive 53BP1 foci (% Nuclei with BrdU Foci) at 14, 24 and 72 h after the beginning of 5 $\mu$ M ETO treatment.

At 24 h, the percentage of cells incorporating BrdU increased for both species, indicating progression through the cell cycle. Again, the human population had a lower percentage of cells incorporating BrdU, but a higher percentage of BrdU in foci, suggesting a more active repair (Figure 25).

#### 4.1.7 Long-lived species induce higher level of apoptosis

An additional mechanism owned by cells to protect DNA integrity, when DNA damage is irreparable, is the induction of apoptosis. To assess whether induction of apoptosis was similar among the species, Annexin V assay was performed in unsynchronized untreated and treated (100  $\mu$ M ETO) fibroblasts. Cells were treated and then allowed to recover for 24 and 48 hours after damage, both untreated and treated samples. Controls value for each species are indicated as 1 and values from treated samples were normalized over control.

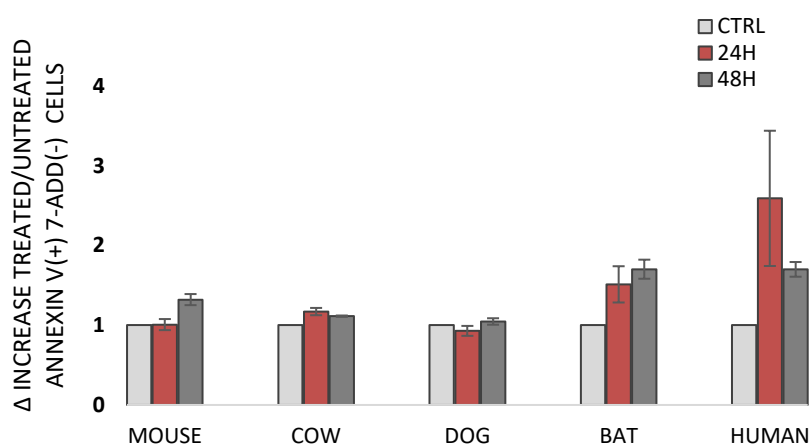


**Figure 26. Long-lived species induce higher level of apoptosis.** Fibroblasts from mouse, cow, dog, bat and human were treated with 100  $\mu$ M ETO and allowed to recover for 24 and 48h. Data represents a ratio of treated/ untreated samples. Annexin V(+) 7-AAD(-) cells were scored as early apoptotic. Shown are means  $\pm$  s.e.m of two independent experiments.

Data report values of the ratio of treated over untreated cells Annexin V(+) and 7-AAD(-), which represents the portion of cellular population in an early apoptotic state. Graph shows that longer lived species (human and bat) induce higher level of apoptosis at both time points (24 and 48 hours after damage) (Figure 26).

#### 4.1.8 Human DNA generally appears more or equally resistant to fragmentation

Overall, data collected on cell cycle control and 53BP1 foci formation addressed simple questions to answer: are long-lived more prone to DNA damage, when compared to short lived species? Are long-lived species more fragile when challenged with a genotoxic stress? In order to investigate this hypothesis, DNA fragility was evaluated after genotoxic stress by

## RESULTS

comet assay. For DNA damage detection at the individual cell level, the comet assay was performed under neutral conditions, which allowed recognition of DSB. Comet tails obtained with the 5  $\mu\text{M}$  ETO and 0.13  $\mu\text{M}$  NCS, concentration used in long-term experiments, were too short to show significant differences (data not reported). Thus, higher doses of ETO and NCS were used for comet assays. Figure 28 shows data from cells treated with 50  $\mu\text{M}$  ETO and 1.35  $\mu\text{M}$  NCS for 60 and 30 minutes, respectively. Genotoxic treatments resulted in DNA fragmentation and the appearance of comet tails.

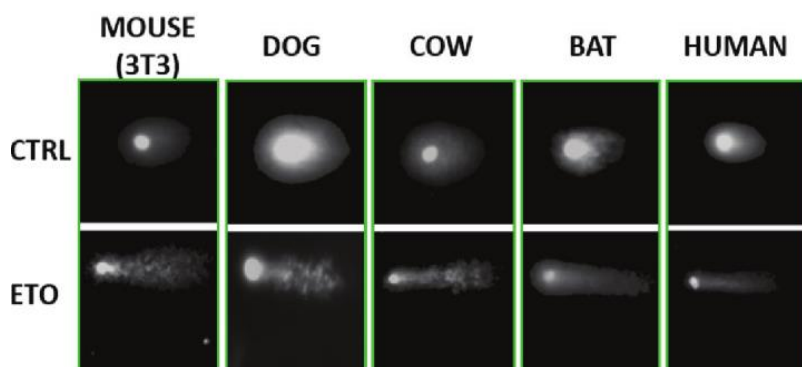


**Figure 27.** Representative comets of untreated and high dose treated fibroblasts.

Percentage of DNA in comet tails and tail moments (measures obtained by multiplying tail length by percentage DNA in tail) were analysed for all the five species, and data are shown as fold increase over untreated. After both treatments, we observed a significant increase in the percentage of tail DNA in all species. Although the results of the two measure of DNA damage (percent tail DNA and tail moment) did not overlap, cells from the mouse, the shortest-lived species in the panel, had significantly greater DNA fragmentation in all instances. The longest-lived species (human) and the largest (cow) exhibited the least amount of damage in the comet assay (Figure 28).

Since DNA damage repair is activated within minutes of damage [178], it is possible to hypothesise that difference observed among species are a consequence of faster repair mechanisms, rather than chromatin structural strength.

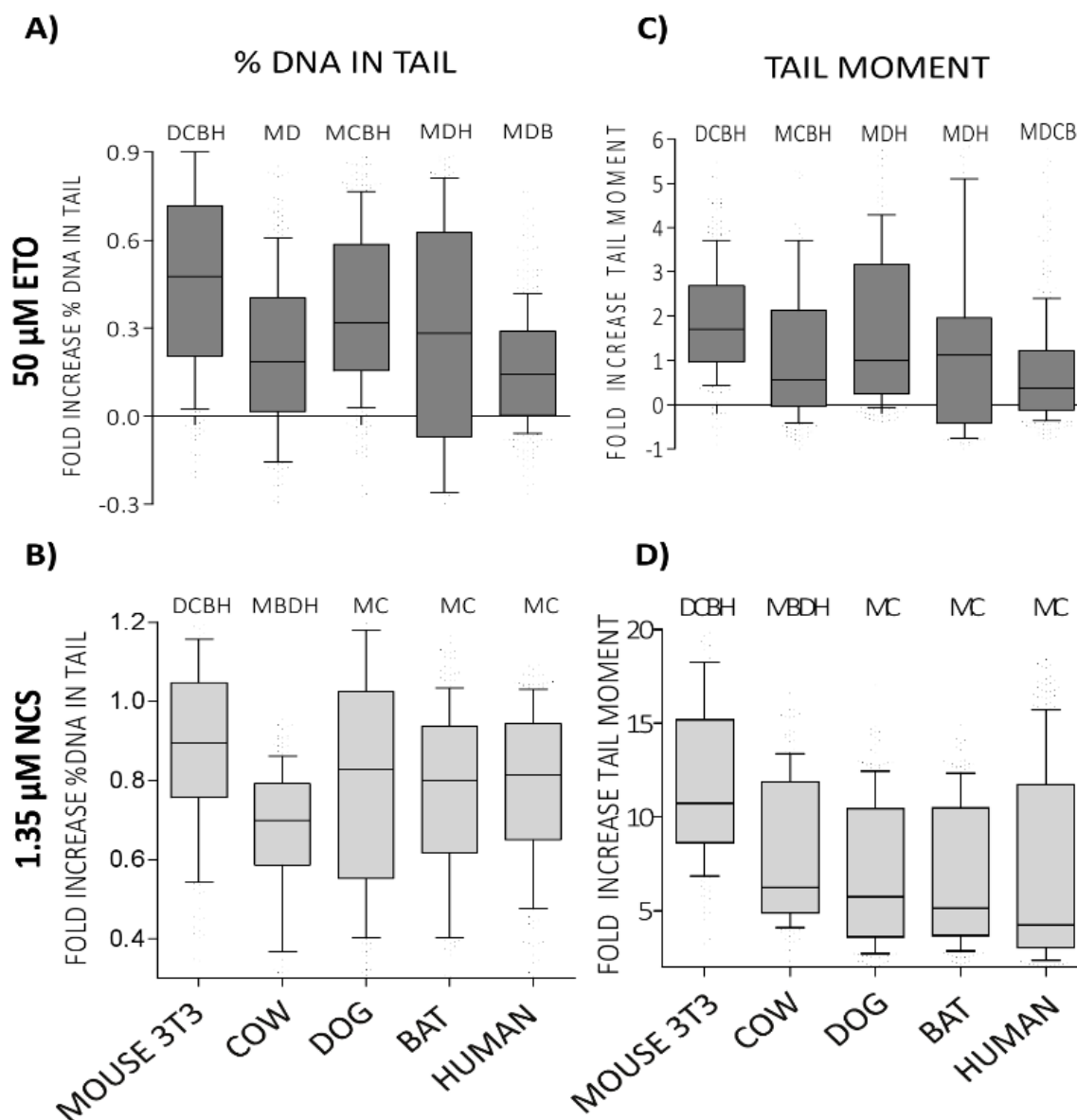


**Figure 28. Human DNA generally appears more or equally resistant to fragmentation when compared to other species.** Quantification of percent DNA in comets tails (A-B) and quantification of Tail moment (C-D) after 50 $\mu$ M ETO and 1.35 $\mu$ M NCS are presented in a box plot showing means  $\pm$  s.e.m and whiskers representing 10-90 percentile. For both treatments, data were obtained from two independent experiments. Statistical analysis: Kruskal-Wallis analysis. The data from a single species was compared to each individual species. Significant difference ( $p$  value  $< 0, 0001$ ) between pairs of species is indicated by the presence of the initials above the box plot for each species (M = mouse; D = dog; C = cow; B = bat; H = human). G) Representative comets of untreated (CTRL) and 50 $\mu$ M ETO treated fibroblasts.

#### **4.1.9 Measuring unresolved damage**

MN are widely considered a direct cytogenetic marker of unresolved damage. They originate, as a consequence of aberrant mitosis, from chromosome fragments or whole chromosomes that lag behind at anaphase [127]. To evaluate long-term effects of genotoxic stress in these different species and the amount of unresolved damage in each species after genotoxic stress, micronuclei formation was scored at 0, 24, 48 and 72 h after the beginning of damage. All cells were synchronized in G<sub>0</sub> phase by 48 h incubation in serum free medium. Cells were then stimulated to enter into the S-phase by adding complete growth medium (10% FBS) as described in materials and methods. Cells in S-phase were treated in serum free medium with 5 μM ETO (A), 0.13 μM NCS (B) or 5 μM ETO with a BrdU pulse (C, cells were pulsed with BrdU for all the length of the treatment); cells were washed and fed with growth medium and allowed to recover from damage. MN were scored on a minimum of 400 cells. Surprisingly, it was observed that shorter-lived species have a higher percentage of nuclei with ≥1 micronuclei. In particular, mouse, the shortest-lived and the smallest species, showed the highest percentage of micronuclei at all time points both after 5 μM ETO and 0.13 μM NCS treatments (Figure 29.A and 29.B, respectively). As a demonstration that micronuclei arise only in cycling cells, MN were also scored in BrdU-positive cells (Figure 29.C).

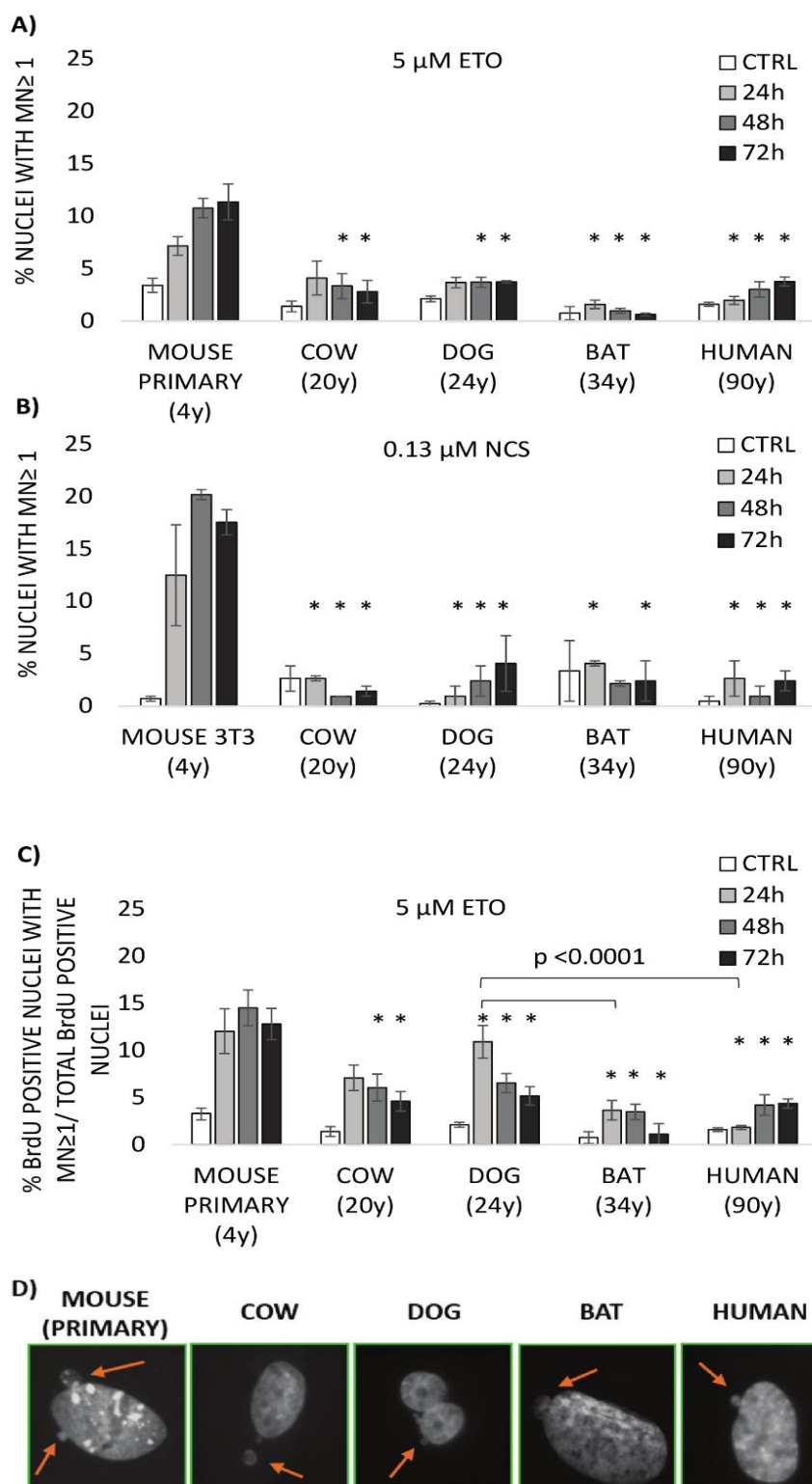


**Figure 29: Short-lived species have higher percentage of Micronuclei (MN).** MN were scored at 24, 48 and 72 h after the beginning of the ETO (A) and NCS (B) treatments. Means were calculated from two to six experiments. MN were also scored in BrdU+ cells (C). In all instances, untreated cells (CTRL) are cells at 24 h past complete growth medium addition. The respective maximum life span of each species is reported in parenthesis in years (y). D) Dapi staining for a representation of MN in all the analysed species.

#### 4.1.10 53BP1 foci are inversely correlated with micronuclei abundance

To interpret the relationship between 53BP1 foci, micronuclei and lifespan, the data for 53BP1 foci formation and micronuclei were plotted with species longevity. We used data from the 72 h time point following the beginning of NCS exposure, since this treatment produces the highest number of long lasting foci interpretable as DNA-SCARS. Micronuclei are inversely related to long-lasting foci ( $R^2=0.868$ ;  $p=0.021$ ; Figure 30.A).

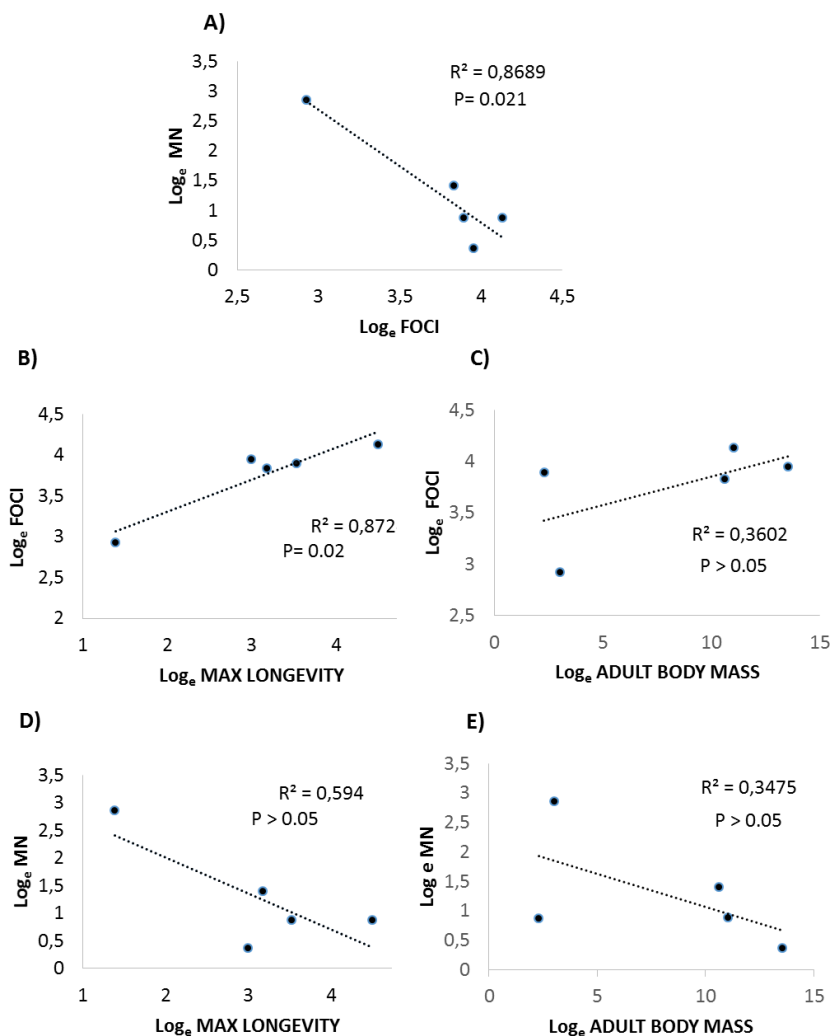


**Figure 30. Correlations of 53BP1 foci and MN with maximum life span and adult body mass.** Correlations were examined using data collected at 72 h after the beginning of  $0.13\mu\text{M}$  NCS treatment for both 53BP1 Foci and MN. Panel A contains the inverse correlation between 53BP1 foci and MN. Panels (B) and (C) contain positive correlations between 53BP1 foci and longevity and body mass respectively. Panels (D) and (E) contain the negative correlation between MN and longevity and body mass respectively. All values were natural logarithm transformed. Coefficient of determinations and  $p$  values are shown.

Additionally, while long-lasting foci were strongly and positively related with longevity ( $R^2=0.87$ ;  $p=0.020$ ; Supp. Figure 9.B), micronuclei were negatively related ( $R^2=0.59$ ), although this relationship did not reach significance in this data set (Supp. Figure 9.D). Like maximum life span, body mass was also positively related with long-lasting foci ( $R^2=0.36$ ; Supp. Figure 9.C) and negatively related with micronuclei ( $R^2=0.35$ ; Supp. Figure 9.E), although neither association reached significance in this data set. These data suggest that both longevity and body mass are related to genome surveillance and stability, but that longevity is more strongly related than body mass.

## 4.2 PART 2- 53BP1 Knock down clones

### 4.2.1 53BP1 knock down clone selection

Analysis of the expression of 53BP1 foci together with MN formation among the species showed an inverse association between these two DNA damage markers: a lower amount of 53BP1 foci is associated to a higher genomic instability, measured as the increase of MN formation. To investigate the contribution of 53BP1 in the mechanism underlying the differences in MN formation, accordingly to a genotoxic stress, 53BP1 knock down clones were generated. By CRISPR-CAS9 technology approach, 8 different knock down clones were isolated from transfection of isogenic keratinocytes cells and one was selected for the present study. Figure 31 shows the keratinocytes wild type (WT) and the eight 53BP1 knock down clones (1-8). The clone number 3 (red rectangle) was selected for the present experimental thesis.

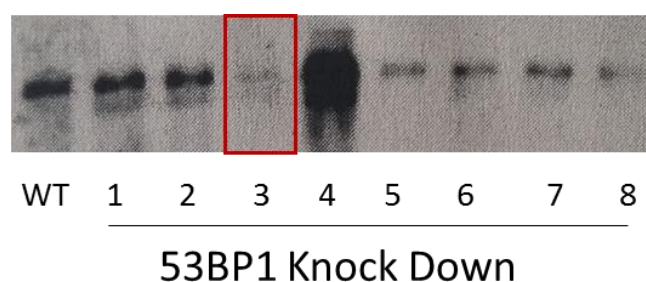


**Figure 31.** Immunoblot represents keratinocytes: one wild type sample (WT) and 53BP1 knock down clones (1-8). Eight clones were isolated from transfection and clone n° 3 (red rectangle) was selected (53BP1 KD), studied and characterized.

All the experiment concerning 53BP1 knock down clones were performed at “Central Institute of Clinical Chemistry and Laboratory Medicine”, University of Düsseldorf.

Further immunoblot analysis, from whole cell lysates, showed that the 53BP1 levels were reduced of around the 40-50% in 53BP1 KD (Figure 32).

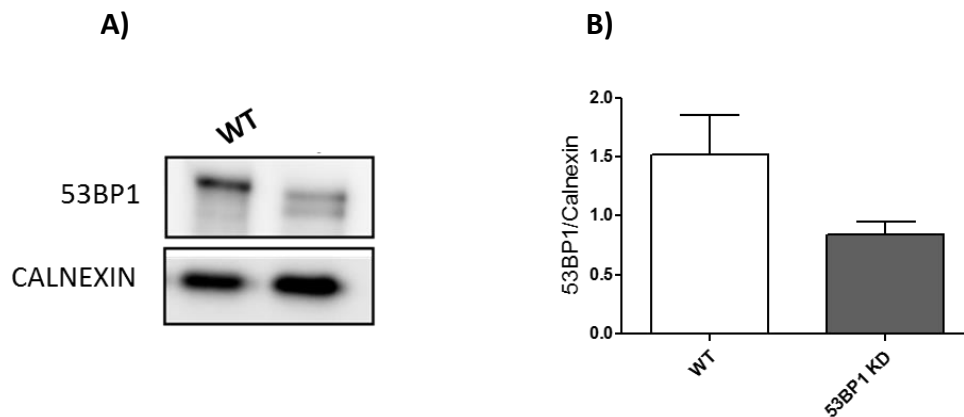
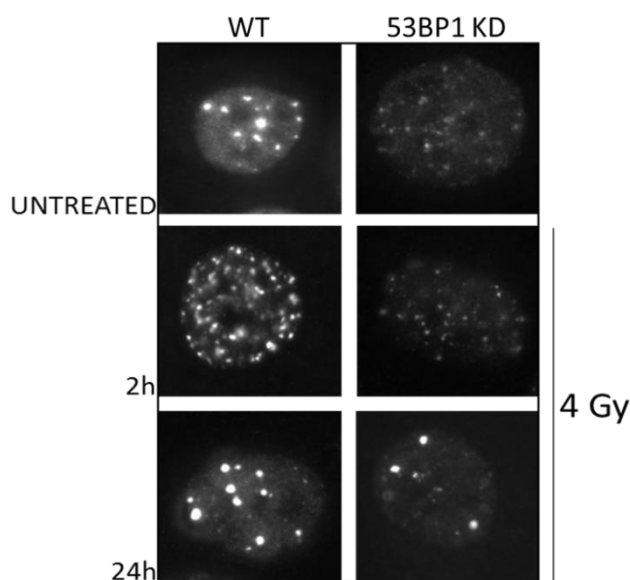


**Figure 32: CRISPR-CAS9 approach to reduce 53BP1 level.** A) Immunoblot analysis shows wild type (WT) and 53BP1 knock down (53BP1 KD) keratinocytes cell lines. B) Signal quantification of 53BP1/calnexin (loading control), in three measurements. Signal quantification was performed with ImageJ software. Shown are the means +/- s.e.m.

53BP1's knockdown was also confirmed by immunofluorescence analysis (Figure 33). Despite lower level of 53BP1, 53BP1 KD clone is still able to respond to genotoxic lesions, as observed in the immunofluorescence of untreated and 4 Gy IR treated cells (Figure 33). 53BP1 stable down regulation could be interpreted as a condition which is miming the physiological

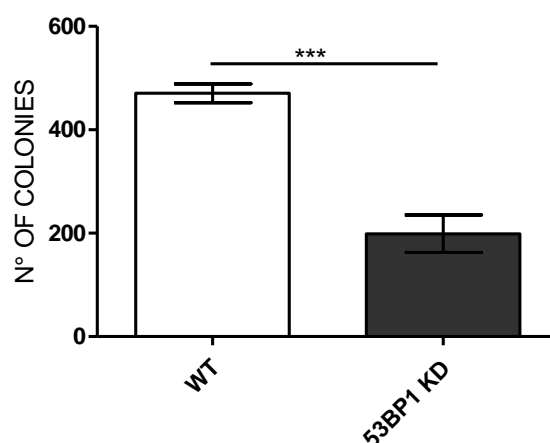


differences found among the species. Therefore, assuming that this approach may reflect differences observed across the species (i.e. mouse and human) in the comparative approach, in terms of 53BP1 abundance, several cellular responses were further investigated to fully characterize 53BP1 KD clone.

**Figure 33: Representative immune-fluorescence of WT and 53BP1 KD.** Untreated and treated cells were stained with 53BP1 probe. Cells irradiated with 4 Gy dose, were fixed at 2 or 24h after irradiation.

#### 4.2.2 Stable 53BP1 knock down clone reduces cellular growth

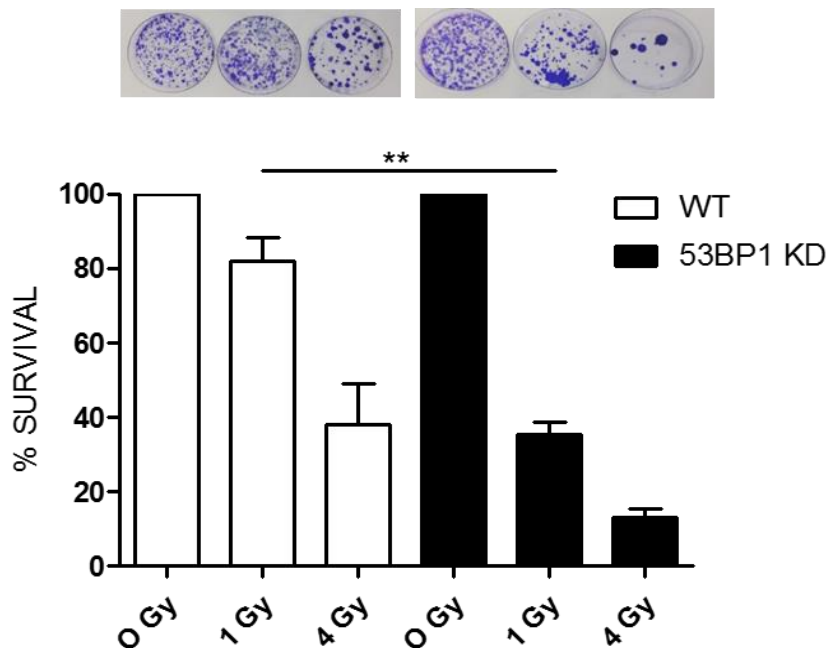
CFA is a useful method to test the survival efficiency of a cell line, in other words it measures the ability of cells of a certain cellular population to divide and form colonies after a cytotoxic or genotoxic treatment. Here, the CFA approach was used to measure clonogenic growth efficiency to determine if down regulation of 53BP1 could impair growth of untreated cell lines. WT and 53BP1 KD clones were seeded at standard density and incubated for 2-3 weeks. Prior to count, colonies are allowed to reach the size of approximately 50 cells. Colonies with less than 50 cells were not scored. Figure 34 shows that the growth efficiency is reduced in 53BP1 KD controls, when compared to the WT. This outcome is consistent with data on 53BP1 MCF-7 knock out, showed in [101].



**Figure 34: Reduced survival in untreated 53BP1 KD clones.** WT and 53BP1 KD were seeded and grown for 2-3 weeks. Shown are the means  $\pm$  s.e.m. of two independent experiments. Statistical analysis: T-Student test followed by paired test. *p* value < 0,001.

#### 4.2.3 Down regulation of 53BP1 reduces survival rate in response to damage

53BP1 is a well-known DNA damage sensor and marker. 53BP1 interacts with p53, regulating cellular DNA damage pathways p53-dependent [101]. These pathways involve the cell cycle regulation and survival. We aimed to evaluate how survival rate changed after ionizing radiation, in WT and 53BP1 KD. Keratinocytes from wild type and knock down were seeded at the same cellular density one day prior irradiation, which was performed at two different doses, 1 and 4 Gy. 7 days after irradiation cells were fixed, stained and analysed.



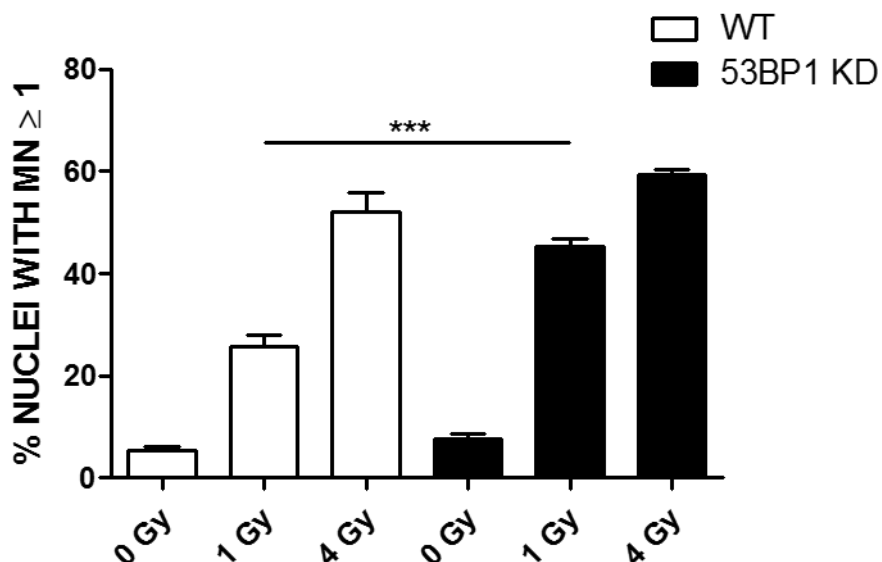
**Figure 35: 53BP1 KD shows a lower survival rate after IR.** Wild type and 53BP1 KD clones were irradiated with 1 and 4 Gy doses and allowed to recover for 7 days. Means  $\pm$  s.e.m of three independent experiments are represented in the graph. For each experiment, samples were seeded in duplicate, and each duplicate read 5 times. Statistical analysis was performed comparing the % survival in WT and 53BP1 KD for each experimental condition. Statistical analysis: T-Student test followed by paired test. *p* value < 0,01.

Figure 35 shows the percentage of survival of treated samples compared to untreated, whose value was fixed as 100% of survival. In both cell lines, low and high doses treatment induce a decrease of the survival of treated cells when compared to the respective control. A comparison between the WT and 53BP1 KD clone, for each treatment showed that 1 Gy irradiation induces a significant reduction of the survival rate in 53BP1 KD clones; while differences between WT and knock down are lower at 4 Gy irradiation. Experimental data suggest that 53BP1 is at play in the cellular processes activated in order to survive to a genotoxic damage.

#### 4.2.4 53BP1 down regulation is associated to increased genomic instability

In order to assess if 53BP1 directly contribute to the process which lead to MN formation in response to double strand breaks, MN were blindly scored in WT and 53BP1 KD clones, in untreated and treated cells. Cells were seeded one day prior to treatment, treated with 1 and 4 Gy irradiation and then allowed to recover for 24h. Therefore, since the aim of this experimentation was to directly evaluate the presence unresolved damage, MN were scored,

approximately after the first division; in other words, 24h after damage. In a preliminary experiment, MN were also scored at 72 hours after damage, but the related data are not included in the present analysis; it is plausible to speculate that, in a cell line with a high proliferation rate, analysis at 72 hours can lead to an inaccurate estimation of MN numbers. In fact, due to activation of cellular pathway (i.e cell cycle arrest, apoptosis) in response to DNA damage, some micronuclei can be lost or misunderstood with mitotic crisis.



**Figure 36: MN formation increases after IR in 53BP1 KD clones.** WT and 53BP1 KD clones were irradiated with 1 and 4 Gy. MN were scored 24h, twice, in 500 cells. Means  $\pm$  s.e.m. of three blind independent experiments are represented in the graph. Statistical analysis was performed comparing the % MN in WT and 53BP1 KD for each experimental condition. Statistical analysis: T-Student test followed by paired test. *p* value < 0,001.

53BP1 KD clones, compared to WT, showed an increase of % of MN in all the three conditions (0, 1, 4 Gy), but differences are statistical significant only at 1 Gy. Since isogenic cells were chosen and differences, between wild type and knockdown clones, lay exclusively in the different amount of 53BP1 level, it is possible to state that 53BP1's down regulation is directly responsible of the mechanism leading to an increasing number of MN in response to a DSB damage: lower 53BP1 protein levels are strictly connected to higher genomic instability. Moreover, the experimental model achieved by CRISPR-CAS9 technology, is a challenging approach: no other 53BP1 stable knockdown models are available in non-transformed cells.

### **4.3 PART II- Genetic instability and aging under the scrutiny of comparative biology: a meta-analysis of spontaneous micronuclei frequency**

#### **4.3.1 Body mass and MNEF are inversely correlated**

In order to test if spontaneous micronuclei frequency is associated to longevity in mammals, a comparative meta-analysis of pre-existing data has been performed. As a first step, a correlation analysis between the log<sub>10</sub> transformed values of MNEF, body mass and maximum longevity for all 47 species reported in Tab.4, was performed. The comparisons between these data could be weakened by factors related to peculiar differences in the circulatory systems of the species and to different modalities of erythropoiesis. For example, polychromatic erythrocytes (immature erythrocytes) are absent in the peripheral blood of some species [172]. A major problem was represented by the capacity of the spleen, in some species, to selectively eliminate MNE. This issue could be eliminated analysing micronuclei in reticulocytes that are not eliminated by the spleen even in species with a filtering organ [151][179]. Unfortunately, the available data on micronucleated reticulocytes are extremely scarce in comparison with the available data on mature erythrocytes. Udrouiu has addressed the spleen filtration issue using data from haematological studies, histological investigations of the spleen, MN analyses before and after splenectomy, and comparisons between MN frequency in peripheral blood versus bone marrow [180]. Using this classification and other studies to better discriminate between species of the same family or genus [175][148][174], we have selected species suitable for the MNE test (highlighted in Table 3). As a result, the species cohort decreased to 21.

To allow logarithmic transformation, 0.5 points was added to each MNEF value (in all figures, the abbreviation log<sub>10</sub> MNEF implies this addition). Correlations were done between log<sub>10</sub> values calculating R<sup>2</sup> and the significance of the regression line using Microsoft Excel software (Microsoft Corporation, Redmond, Washington, USA). Comparative analysis was performed as suggest by Speakman [181]. Although the values are highly dispersed, trend lines show an inverse and highly significant relationship of MNEF with both body mass and maximum longevity (Figure 37, A and B respectively). A scatter plot of the relationship between maximum longevity and adult body mass for the selected species is shown in Figure 37.C.

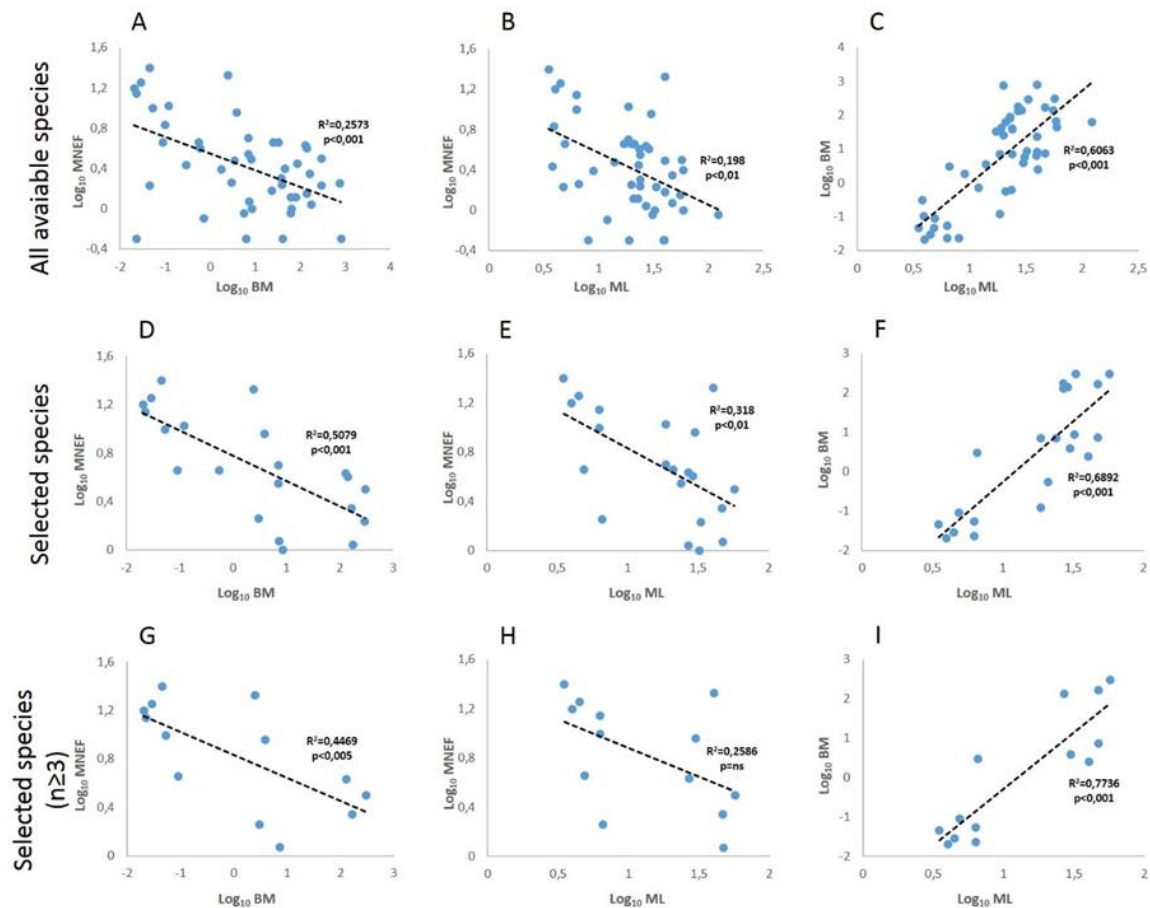


**Figure 37. Correlations between log<sub>10</sub> micronucleated erythrocyte frequency (MNEF) versus log<sub>10</sub> body mass (BM) and log<sub>10</sub> maximum longevity (ML) and correlation between log<sub>10</sub> BM versus log<sub>10</sub> ML.** In A, B, C, are reported the correlations for all species reported in Table 1, n=47. In D, E, F are reported the correlations for species judged suitable for the MNE test (highlighted in Table 1), n=21. In G, H, I are reported the correlations for species judged suitable for the MNE test (highlighted in Table 3) with n ≥ 3, n=13. Linear regression, coefficient of determination (R<sup>2</sup>), and significance value (p) are shown.

A second set of analysis was performed only on species without a micronucleated erythrocytes filtering spleen. Although the cohort size was necessarily smaller, the correlation between MNEF and body mass as well as that between MNEF and maximum longevity improved (Figure 37.D and 37.E respectively). This suggests that any potential link between MNEF as a measure of genomic stability and body mass or maximum longevity may be partially hidden if the filter action of the spleen is not taken into account.

A third set of analysis was performed only for species for which the number of replicates was above or equal three. In this last analysis, the significance of the relationship between body mass e MNEF was not abolished (Fig. 37.G); on the opposite, the significance of the relationship between longevity and MNEF was lost (Fig. 37.H). This analysis underline the

existence of a tighter relation between body mass and MNEF, in comparison to the one between maximum longevity and MNEF.

#### 4.3.2 Residuals and phylogenetically independent contrasts analyses

In approaching the residuals and the phylogenetically independent contrasts analyses, we considered more relevant the issue of micronucleated erythrocytes removal by the spleen filtrating action than the issue of the low n value for some of the considered species. Consequently, to avoid performing these analyses on a too small cohort, we decided to eliminate the species where the spleen has a filtrating action and, at the same time, to keep in also species with an  $n < 3$ . Proceeding in this way, these analyses were conducted on 21 species (see Table 3, highlighted data add ref paper). The first analysis shows the correlation between the residual of MNEF and the residual of body mass, in both cases controlling for maximum longevity (Fig. 38.A), and the correlation between the residual of MNEF and the residual of maximum longevity, in both cases controlling for body mass (Fig. 38.B).

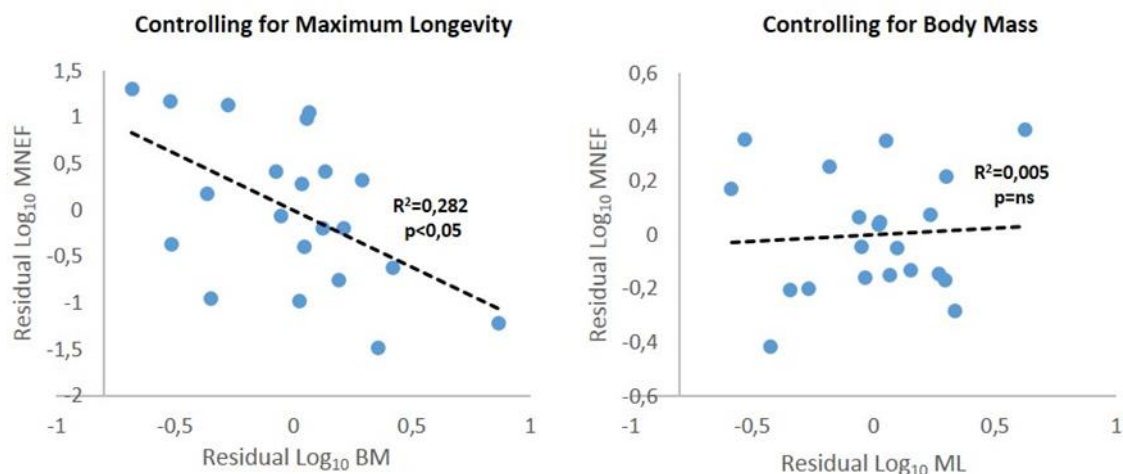


**Figure 38. Analysis of residuals.** Regression plot using the residual approach: Residual of log<sub>10</sub> MNEF versus residual of log<sub>10</sub> body mass (BM) controlling for log<sub>10</sub> maximum longevity (A); Residual of log<sub>10</sub> MNEF versus residual of log<sub>10</sub> maximum longevity (ML) controlling for log<sub>10</sub> body mass (B). Linear regression, coefficient of determination (R<sup>2</sup>), and significance value (p) are shown.

Since the relationship with body mass remains significant, while that with longevity does not, this analysis suggests, as for the preceding correlations, that the determinant factor is body mass.

#### 4.4 PART III- Role of 53BP1 in chronological age

##### 4.4.1 Small increase of spontaneous 53BP1 foci in middle and old donors

It has been showed that human fibroblasts exhibit a decline in DNA double strand breaks (DSB) repair pathways [182] and a gradual decline of DSB repair capacity was observed in nucleated peripheral blood cells of old human donors [183]. Based on these evidence, I aimed to test if the efficiency in sensing DNA damage and repair ability, measured by 53BP1 foci formation, is impaired during the aging process. To address this question, fibroblasts from three donors groups characterised by different chronological age were treated with a low dose of ionizing radiation (1 Gy). All the experiments on three donors groups were performed at the “Central Institute of Clinical Chemistry and Laboratory Medicine”, University of Dusseldorf. All cells used were at a low passage in culture, far from replicative senescence. Irradiated cells were allowed to recover for 2, 24, 48 and 72 hours after damage. Figure 39 shows a time-course analysis after 1 Gy irradiation, where the same 53BP1 foci formation kinetic was observed in the three donors groups (Figure 18.A), similar to the kinetic observed in the comparative experimental assay across the species: the 53BP1 foci formation peak, observed at 2 hours after damage, is followed by a gradual decline in the percentage of 53BP1 foci positive nuclei (Figure 39).

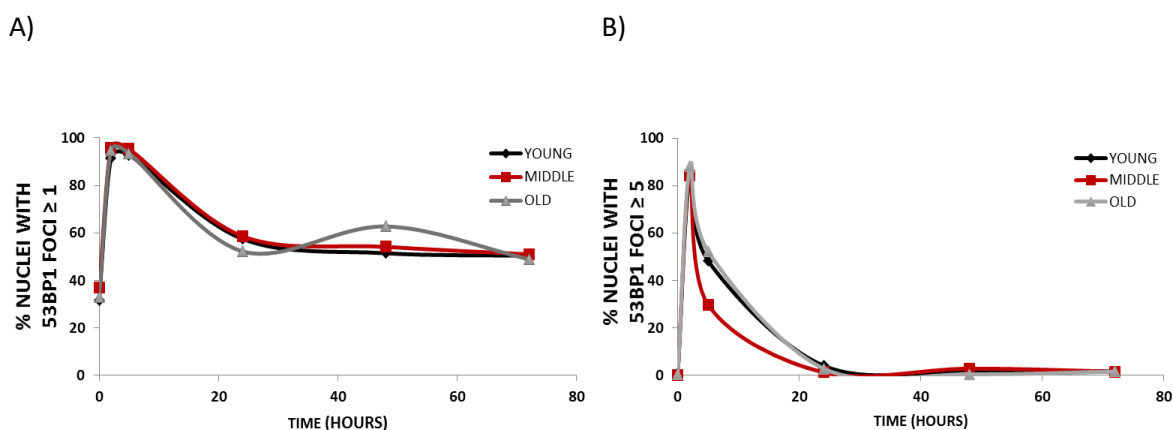


**Figure 39: 53BP1 foci formation kinetic in young, middle and old donors.** 53BP1 formation was monitored from 2 up to 72h after 1 Gy irradiation. Foci were grouped in  $F \geq 1$  (A) or  $F \geq 5$  (B).

In figure 40, a bar graph shows the percentage of 53BP1 foci recruited for each donor group scored, for each sample, on a total of 100 cells. Data report a small increase of 53BP1 foci associated to an increase of chronological age (Fig 40.B), in untreated cells although not significant. Noteworthy is that Kalfalah *et al.* [143], using the same cell strains, have reported a significant increase in untreated fibroblasts. The same conclusion was deduced in [157]

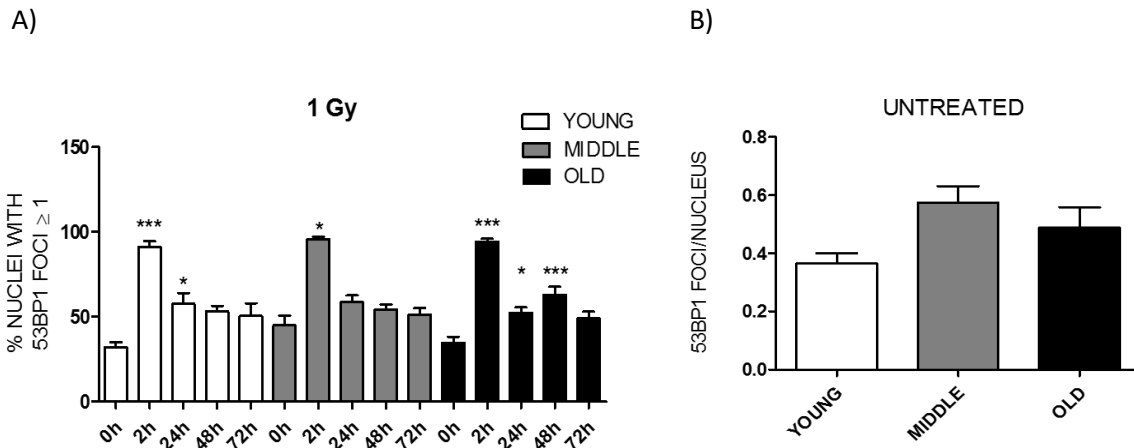


**Figure 40: 53BP1 foci distribution in young, middle and old donors.** A) 53BP1 foci were scored at 2, 24, 48 and 72 hours after damage. Cells with more than 1 focus per nucleus are represented in the graph. Statistical significance is referred to the increase of 53BP1 foci of treated compared to their respective untreated (0 h). B) 53BP1 foci/nucleus in untreated young, middle and old donors. Means +/- s.e.m of two independent experiments are represented in the graph.

The three chronological groups don't show any significant difference in their ability to sense damage (% 53BP1 foci) measured 2h after damage, at least when irradiated with low doses IR. Data are consistent with Kalfalah *et al.* [152]. Despite literature suggests a decline of the DNA damage repair, not significant differences were observed among young, middle or old donors in the present work.

**4.2.2 Absence of MN variation with chronologica age**

To assess the amount of unresolved damage in each chronological-age group after genotoxic stress (1 Gy irradiation dose), we scored micronuclei formation 0, 2, 24, 48 and 72 h after. Statistical analysis was performed comparing treated samples to untreated cells. Scoring MN in each experimental group did not reveal significant difference among young, middle and old donors, at any analysed time point.

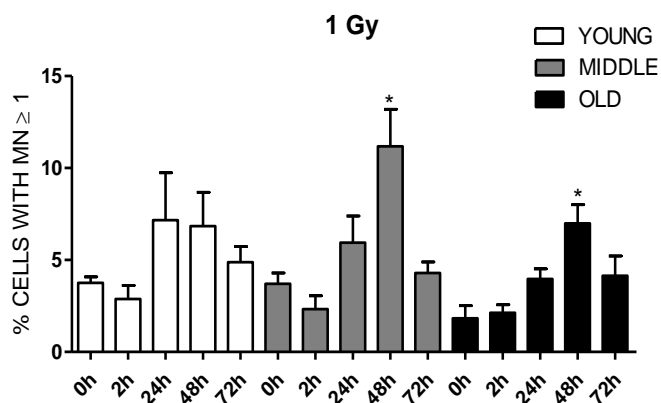


**Figure 41: Absence of significant correlation between MN formation and chronological age.** MN were scored in irradiated fibroblast from young, middle and old donors. Statistical analysis is referred to % MN in treated compared to respective untreated (0 h). Means +/- s.e.m of two independent experiments are represented in the graph.

#### 4.4.3 Higher rate of DNA-SCARS in old donors

Severe and irreparable DNA damage lesions induce cells to senescence, which is accompanied by persistent DNA damage foci, constitutive DDR signalling activation and chronic p53 induction [184]. In this context, it has been recently showed that PMLnb may play a role in stress-induced senescence. In fact it can facilitates p53 activation, the senescence growth arrest [185][186] and DNA-SCARS formation, in senescent cells. As previously mentioned, PMLnb and 53BP1 co-localization are associated to DNA-SCARS. In order to evaluate if the ability to induce senescence in untreated or treated cells is impaired within aging, we scored the percentage of co-localization of persistent 53BP1 damage foci and PMLnb, during the transition to senescence after low and high doses of IR. Analysis of DNA-SCARS has been restricted to young and old groups, in order to reduce a possible confounding factor coming from the middle group of donors. First, unsynchronized fibroblast from young and old donors were seeded one day prior to treatment and then irradiated with increasing IR doses (1 and 10 Gy). Treated cells were allowed to recover for 48h, time point at which cells were fixed and analysed. Co-localization of DNA-SCARS and PMLnb is complete 48 hours after irradiation [121].

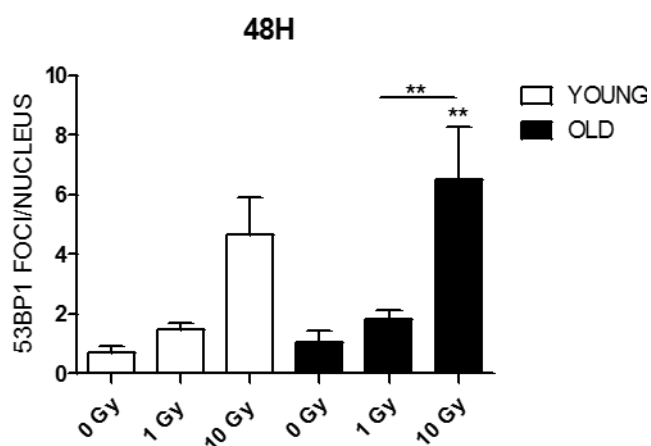


**Figure 42: Persistent 53BP1 foci/ nucleus increase in old donors in response to high doses irradiation.** 53BP1 foci/nucleus were scored 48h after 1 and 10 Gy irradiation. Statistical analysis is referred to % 53BP1 foci/nucleus in treated compared to respective untreated (0 Gy). Means +/- s.e.m of two independent experiments are represented in the graph.

## RESULTS

As showed in figure 42, all proliferating cells, exposed to 1 and 10 Gy, developed persistent 53BP1 foci as observed at 48h. The comparison of 53BP1 foci/nuclei, between young and old group, show a small increase of 53BP1 foci/nucleus at 1 Gy, and a higher increase at 10 Gy in the group of old donors. In order to define whether 53BP1 long lasting foci are associated to PMLnb, and therefore identified as DNA- SCARS, the rate of 53BP1 co-localized or overlapped to PMLnb was investigate in the same groups. As showed in figure 43.A, 10 Gy irradiation induces a significant increase of the % 53BP1-PMLnb co-localization. Association of 53BP1 to PMLnb is observed also in controls cells. In fact, it has been showed that 53BP1 foci co-localization to PML , in untreated cells, is approximately 70%, suggesting that DNA-SCARS or TIF in the senescent cells that are present in most normal human cell populations [121]. Moreover, the % of co-localization of 53BP1 foci to PMLnb per nucleus is higher, at higher doses, in old donors, although not significant.

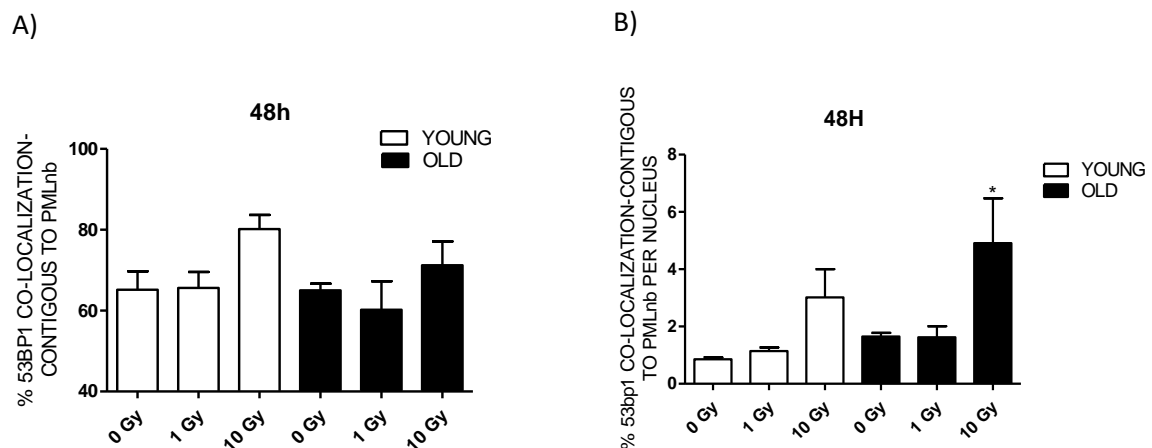


**Figure 43: DNA-SCARS increase in old donors.** 53BP1 co-localization with PMLnb was performed in young and old donors. A) % 53BP1 colocalization-contiguous to PMLnb were scored 48h after 1 and 10 Gy irradiation. 50 nuclei for each experimental treatment were scored. Significant statistical value is referred to % 53BP1 colocalization-contiguous to PMLnb per nucleus in treated compared to respective untreated (0 Gy). Means  $\pm$  s.e.m of two independent experiments are represented in the graph.

## 5. CONCLUSIONS

Despite significant experimental support have been produced for the elaboration of theories which may explain the aging process and the evolution of longevity [3], aging still remains a fascinating field to further explore. The aim of the present work is to investigate mechanisms which may influence lifespan length and partially explain the exceptional longevity of some species, like human.

The mammalian radiation, in evolutionary terms, is a relatively recent event; so since life on the planet has had the form of individual cells for the majority of the evolutionary time, it is plausible to hypothesize that many basic cellular mechanisms are highly conserved among mammals. Then, with a look at the mammalian evolutionary tree, it seems reasonable to investigate if conserved cellular mechanisms show some convergent adaptation to long life. In a comparative analysis of the evolution of longevity, together with lifespan length, maximum adult body size should always be taken in consideration. Both features, in fact, are fundamental traits which may widely vary between species [187] (see figure 44).

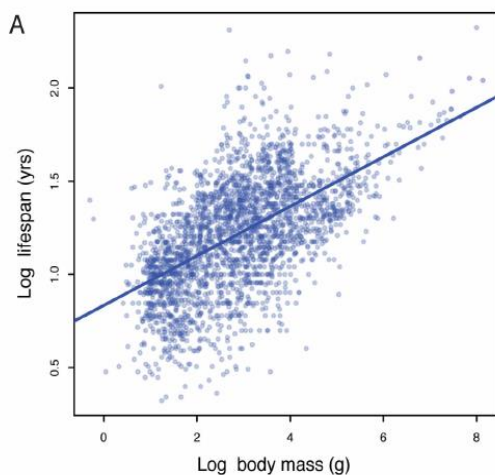


**Figure 44. Body size evolution in vertebrates.** Figure adapted from [188]. Relationship between body mass (g) and lifespan (years) among 2556 vertebrates. Blue line shows the linear regression between log (body mass) and log (lifespan),  $R^2 = 0.32$ .

Assuming that all cells have a similar risk to accumulate mutations, larger and longer-lived animals should have higher risk of developing cancer than smaller and shorter-lived species. But, there are no scientific evidence of the existence of a relationship between the size of an animal and its risk of developing cancer. Consequently, a fundamental question in comparative biology is how very large or long-lived animals protect themselves against diseases (i.e. cancer development) and the accumulation of genomic damage [182].

## CONCLUSIONS

The meta-analysis performed in the present work suggested a possible mechanism which may explain the preferential adaptation for the evolution and achievement of a large body. DNA damage can accumulate both in mitotic and post-mitotic tissues and dividing cells represent a susceptible target. Cell division, in fact, requires DNA synthesis, elevated transcription, and chromosome segregation. All these processes are potentially errors prone and a source of threats, which may impair DNA integrity. In adulthood, during the maintenance of mitotic tissues (gut, skin, blood, etc), but especially during development, there is the need to produce a certain number of cells in a given time, in order to guarantee balanced growth and tissue renewal. Therefore, it has been hypothesized that during the evolution of cellular maintenance mechanisms, time has represented an important constraint [189]. The meta-analysis of published data, performed in the present work, demonstrated the existence of an inverse link between basal MNEF and species body mass; additionally none relationship to longevity has been identified (Figure 38). Large bodies require more cell divisions during development and homeostatic maintenance. Consequently, it is reasonable to propose that together with the evolution of large bodies there was a concurrent improvement in the efficiency of the mitotic apparatus. In a small comparison of six mammals it was showed, in fact, that the fidelity of the spindle assembly check point, a cellular mechanism ensuring proper alignment of chromosomes at the metaphase plate of the mitotic spindle, correlates strictly with species adult body mass [189].

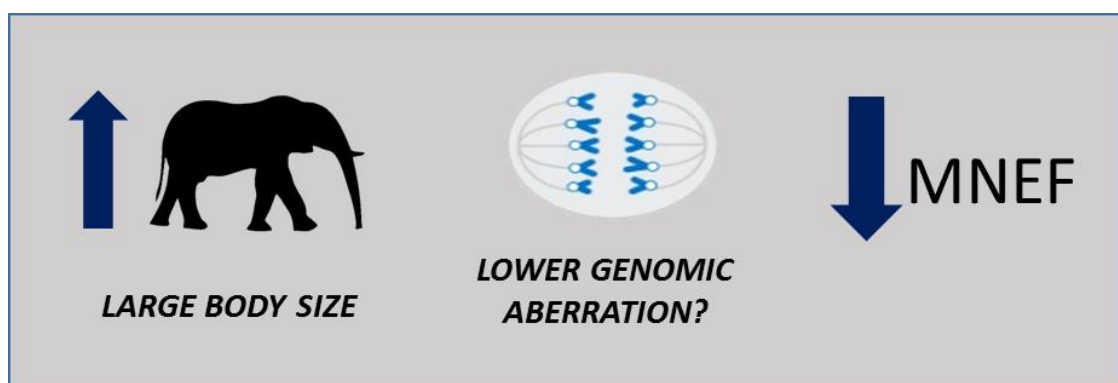


**Figure 45. Micronucleated erythrocytes frequency (MNEF) as improper chromosome segregation.** The meta-analysis showed a clear and inverse link between basal MNEF and species body mass.

Together with the data shown in the meta-analysis, this hypothesis suggests that spontaneous level of MN in circulating erythrocytes could be interpreted as a marker of improper chromosome segregation during erythropoiesis (an hypothesis that could be verified analyzing the presence of centromeres in MN), which is higher in small sized-animals (Figure 45).

On the other hand, the capacity to repair DNA, when damaged by exogenous or endogenous substances or by improper transcription or duplication, might still be an important determinant for longevity. As time passes, healthy cells become more prone to accumulate mutations at DNA level, which in turn can lead to cancerous transformation or accelerated aging. In fact, the DNA damage accumulation theory of aging suggests that “hits” to the genome, acquired over time, may be responsible for the aging process [34]. Support of this theory comes in part from the fact that several human premature aging syndromes are characterized by defects in single genes, coding either for DNA repair proteins or for lamin A, a protein primarily involved in nuclear architecture with the capacity to influence genomic stability. These syndromes dramatically shorten longevity in affected patients (reviewed in [190]). In addition, also the hypothesis that DNA damage repair may be impaired during aging has several experimental support [162][163].

53BP1 protein is a DNA damage marker and a repair orchestrator which accumulates in nuclear foci and activates transcription of genes involved in the cell cycle control in a p53-dependent manner [101] in response to DSBs. Overall, 53BP1 is a fundamental protein for DNA damage detection and maintenance of genomic stability. The presence of persistent 53BP1 foci was analyzed in a large investigation of skin-derived fibroblasts from 100 human donors aged 20 to 90 years. A positive correlation between donor age and 53BP1 foci and a positive correlation between 53BP1 foci and micronuclei were observed in support of the concept that, inside a single species, 53BP1 represents a marker of the endured DNA damage [157]. Considering this last hypothesis, in the present work, an analysis of 53BP1 foci formation in fibroblasts from a small cohort of donors was conducted, in order to measure possible impairment in the repair machinery with aging. In the above mentioned study on 100 human donors, analysis of 53BP1 endured foci was performed after an oxidative damage. While, the focus of the current analysis was orientated on the DNA damage answer after radiation-induced DSBs. The basal number of 53BP1 foci/nucleus increased by the increase of chronological age (although not significantly). Additionally, both young and old group of

donors are still able to induce DNA-SCARS, even though at different grade. Co-localization of 53BP1 and PMLnb results increased in old donors at high irradiation doses, suggesting a small impairment in the repair machinery. Finally, although further investigation might be required, data suggest that chronological aging is associated with an increase of spontaneous 53BP1 foci and 53BP1 DNA-SCARS. Notwithstanding chronological aging seems to be associated to an increase of DNA damage SCARS, Lattanzi et al. suggested instead that the up-regulation of NHEJ recombination pathway in centenarians represents a reshaping of the DNA Damage response rather than a decline in the DNA repair capability [191]. Additionally, they showed that rapamycin increases 53BP1 recruitment in a prelamin-A-accumulation dependent manner in young, old and centenarians donors, hypothesising that these events are part of a defence mechanism against stress events and, therefore, may contribute to lifespan extension.

Then, based on the DNA damage accumulation theory, one plausible hypothesis is that convergent evolution could be at play in the mechanism that protects long-lived species from accumulation of DNA damage. One of this possible mechanism is the efficiency in the detection and repair of DNA damage. In fact, identification of damage is a necessary step in order to proceed with repair or, if the damage is irreparable, with the induction of additional cellular pathways like senescence or apoptosis. The major experimental hypothesis of the present work aimed to test if the efficiency of DNA damage detection and repair could be a potential cellular determinant for the evolution of longevity in mammals. In order to test this latter hypothesis, the focus of the present work was the investigation of the role of 53BP1 in response to DSB, induced by several procedures (genotoxic treatments and IR), as a possible player and determinant factor to explain the wide differences in terms of longevity across five mammals species (mouse, dog, cow, bat, human).

Analysis of the appearance of the number of DNA damage-induced 53BP1 foci in human cells, compared to other four mammal species, surprisingly showed that longer-lived species respond to DSB forming more of this foci. This initial finding was counterintuitive since a higher number of foci are generally interpreted as evidence of a greater amount of damage. However, using direct measurements of DNA damage such as the comet assay (Figure 28) and micronuclei counts (Figure 29), we report here that longevity and, to a lesser extent, adult body size are indeed associated with higher genomic stability. Data about foci abundance in

micronucleated cells suggest that the failure of the cellular mechanism responsible for MN production and for nuclear abnormalities is downstream 53BP1 foci formation (Figures 14 and 15). This hypothesis was strongly confirmed by data on stable 53BP1 knockdown clones. In this model, reduction of 53BP1 level is associated to an evident increase of MN in treated cells, suggesting the direct contribution of 53BP1 in the process which ensures maintenance of genomic stability.

In the present work, species with significant longevity (human and little brown bat) and species with a combination of moderate longevity and large adult body size (cow) showed a higher level of early repair measured by the comet assay. Additionally, mouse, the species in the present study in which short life span associates with a small body mass, shows a significantly higher level of micronuclei, when compared with all other longer-lived or larger species. Thus, analysing data under the lens "53BP1 foci abundance", two interpretation are possible: 1) mouse cells, and to a lesser extent cow cells, produce fewer foci after damage compared with the other species; 2) little brown bat and human, the two species with the longest life span, show the highest level of foci both at shorter (see 5  $\mu$ M ETO treatment) and at longer time points (see 0.13  $\mu$ M NCS treatment).

Rodier and colleagues suggests that persistent foci (i.e., foci that have not resolved in 24 h) should be considered as DNA-SCARS [121], in other words foci associated to stress-induced-senescence. Our data on PML contiguity with 53BP1 in human cells supports the proposal that 53BP1 long lasting foci are gathered to the ability to induce senescence in the case DNA damage is irreparable. To further test, if the ability to induce senescence or apoptosis is also a determinant for lifespan length,  $\beta$ -galactosidase activity and AnnexinV(+) cells abundance were measured in human and mouse or in all the five mammalian species, respectively (Figures 22 and 26). These analysis confirmed that DNA damage induced senescence and apoptosis, in association with more proficient cell cycle checkpoints, could be an effective way to guarantee tissues genomic stability when multiple cellular divisions are required to provide sufficient tissue turnover during a long lifespan or attain a large body size.

Taking together all these considerations, we propose that 53BP1 has a double biological meaning: a) early appearing foci are the sign of an active DNA damage repair and their abundance is related to damage detection efficiency; b) long lasting foci are a sign of residual

and persistent damage. Thus, as we can deduce from up-regulation of 53BP1 in longer lived species, both these features are potentially important in species longevity determination.

The hypothesis that specific cellular functionalities, necessary to guarantee genomic stability, may be upregulated simply by increasing the abundance of key proteins is a straightforward one. Sulak et al., for example, have shown that the Asian and African elephants (among the largest but also the longest-lived mammals species), encodes up to 20 additional gene copies of TP53 [188]. This results in an increased expression of the oncosuppressor following genotoxic stress and a consequent increase in apoptosis in comparison to phylogenetically closely related species (hyrax, armadillo, and armadillo) (Figure 44). Another example comes from the analysis of Parp activity: it varies more than fivefold from short lived to long-lived mammals. Yet, Parp protein abundance across species is not related to its activity level [88]. In a further analysis of proteins involved in NHEJ activation, DNA ligase IV expression was examined using an antibody raised against a peptide conserved between human and rodents. It was found that abundance for this protein is similar among human, hamster, and mouse cells [13].

When one considers these examples it appears that evolutionary changes to improve genomic stability driving also structural modification (which can improve protein functionality) or by the overexpression of key proteins involved in DNA repair, cell cycle control, induction of apoptosis and senescence. Although it will be difficult to disentangle the different aspects of these evolutionary processes, we believe that considering the role of many molecular mechanisms will be more informative rather than focusing on a single alteration as a driver of genomic stability. Albeit the investigation conducted in the present work, included a small number of species, selection was performed according to strict criteria which need to be respected for a comparative analysis: selection included species with a wide range in maximum life span and adult body mass, with the attempt to dissociate the potential effects of these two parameters on genome stability. Species longevity and body mass are known to correlate with each other [189] and it is reasonable to expect that they both correlate positively with genome stability. The following model is proposed as a possible explanation of the differences we observed among the species (Figure 45):

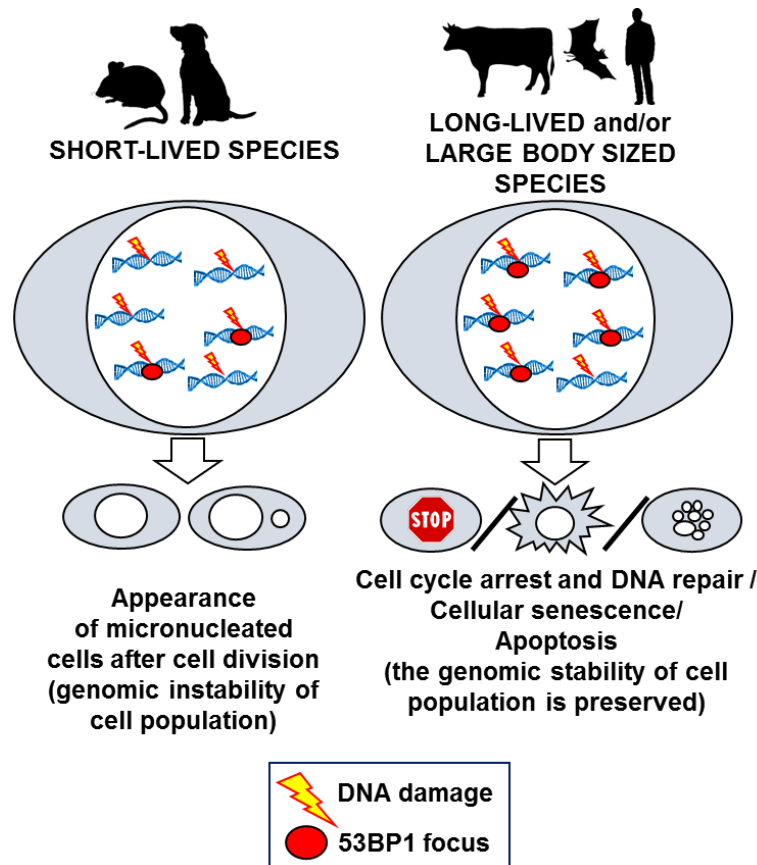


**Figure 45: Proposed model.** Red dots represent 53BP1 foci while lightning images represent DNA damage. See discussion for model explanation

“In mammals, DNA and associated proteins (histones) are chemically equivalent and similarly fragile if exposed to the same amount of genotoxic damage. In a single species, 53BP1 foci abundance is proportional to the amount of damage. However, the differences observed in foci abundance among species are not due to different quantity of damage but rather to different ability to detect it. We suggest that foci represent a primary DNA damage response. Thus, within each species, an increasing amount of damage correlates with a growing number of foci. But, when species are compared, longer-lived or larger species induce the formation of a higher number of foci for a similar content of DNA damage suggesting their higher efficiency in the primary DNA damage response. A potential downstream consequence of this difference is that long-lived or larger species may be more prone to activate cell cycle arrest, DNA repair, apoptosis, or senescence. The choice between these options will likely depend on the interactions between the level of damage and other cellular and extracellular conditions.”

## **CONCLUSIONS**

---

In the context of our previous observation on DNA-end binding [13], we believe that improving DNA damage detection could be an evolutionary conserved mechanism to provide the increased genomic stability required in long-lived and large species to prevent respectively early life tissue dysfunctions and tumors development. The relevance of this observation goes beyond the aging field since scientists: DNA damage foci are widely studied, in the clinical field, as potential markers for radiosensitivity of tumors [192] and in patients' normal tissues [193]. Clinicians, therefore, will have to interpret correctly data obtained by researcher using different species to design the most adapt therapy for humans.

In conclusion we propose that the evolution of longevity is the result of the concurrently improved efficiency in different cellular machineries and that DNA damage detection driven by 53BP1 is actively contributing to this improvement.

## 6. List of references

- [1] P. Sen, P. P. Shah, R. Nativio, and S. L. Berger, “Epigenetic Mechanisms of Longevity and Aging,” *Cell*, vol. 166, no. 4, pp. 822–839, Aug. 2016.
- [2] M. J. Rae *et al.*, “The demographic and biomedical case for late-life interventions in aging,” *Sci. Transl. Med.*, vol. 2, no. 40, p. 40cm21, Jul. 2010.
- [3] C. López-Otín, M. A. Blasco, L. Partridge, M. Serrano, and G. Kroemer, “The hallmarks of aging,” *Cell*, vol. 153, no. 6, pp. 1194–217, Jun. 2013.
- [4] L. HAYFLICK and P. S. MOORHEAD, “The serial cultivation of human diploid cell strains,” *Exp. Cell Res.*, vol. 25, pp. 585–621, Dec. 1961.
- [5] A. M. Olovnikov, “Telomeres, telomerase, and aging: Origin of the theory,” *Exp. Gerontol.*, vol. 31, no. 4, pp. 443–448, 1996.
- [6] A. G. Bodnar, “Extension of Life-Span by Introduction of Telomerase into Normal Human Cells,” *Science (80-. )*, vol. 279, no. 5349, pp. 349–352, Jan. 1998.
- [7] M. A. Blasco, “Telomere length, stem cells and aging,” *Nat. Chem. Biol.*, vol. 3, no. 10, pp. 640–649, Oct. 2007.
- [8] M. Armanios and E. H. Blackburn, “The telomere syndromes,” *Nat. Rev. Genet.*, vol. 13, no. 10, pp. 693–704, Sep. 2012.
- [9] M. Armanios, J. K. Alder, E. M. Parry, B. Karim, M. A. Strong, and C. W. Greider, “Short Telomeres are Sufficient to Cause the Degenerative Defects Associated with Aging,” *Am. J. Hum. Genet.*, vol. 85, no. 6, pp. 823–832, Dec. 2009.
- [10] K. L. Rudolph *et al.*, “Longevity, stress response, and cancer in aging telomerase-deficient mice,” *Cell*, vol. 96, no. 5, pp. 701–12, Mar. 1999.
- [11] A. Tomás-Loba *et al.*, “Telomerase Reverse Transcriptase Delays Aging in Cancer-Resistant Mice,” *Cell*, vol. 135, no. 4, pp. 609–622, Nov. 2008.
- [12] A. Seluanov *et al.*, “Telomerase activity coevolves with body mass not lifespan,” *Aging*

- Cell*, vol. 6, no. 1, pp. 45–52, Feb. 2007.
- [13] A. Lorenzini *et al.*, “Significant correlation of species longevity with DNA double strand break recognition but not with telomere length,” *Mech. Ageing Dev.*, vol. 130, no. 11–12, pp. 784–92, Nov. 2009.
- [14] N. M. V Gomes *et al.*, “Comparative biology of mammalian telomeres: hypotheses on ancestral states and the roles of telomeres in longevity determination,” *Aging Cell*, vol. 10, no. 5, pp. 761–8, Oct. 2011.
- [15] J. A. Stuart *et al.*, “A comparative cellular and molecular biology of longevity database,” *Age (Dordr.)*, vol. 35, no. 5, pp. 1937–47, Oct. 2013.
- [16] R. Peto, “Quantitative implications of the approximate irrelevance of mammalian body size and lifespan to lifelong cancer risk,” *Philos. Trans. R. Soc. Lond. B. Biol. Sci.*, vol. 370, no. 1673, p. 20150198, Jul. 2015.
- [17] C. H. Waddington, “The Epigenotype,” *Int. J. Epidemiol.*, vol. 41, no. 1, pp. 10–13, Feb. 2012.
- [18] M. F. Fraga and M. Esteller, “Epigenetics and aging: the targets and the marks,” *Trends Genet.*, vol. 23, no. 8, pp. 413–418, Aug. 2007.
- [19] S. Han and A. Brunet, “Histone methylation makes its mark on longevity,” *Trends Cell Biol.*, vol. 22, no. 1, pp. 42–49, Jan. 2012.
- [20] B. A. Benayoun, E. A. Pollina, and A. Brunet, “Epigenetic regulation of ageing: linking environmental inputs to genomic stability,” *Nat. Rev. Mol. Cell Biol.*, vol. 16, no. 10, pp. 593–610, Sep. 2015.
- [21] E. A. Pollina and A. Brunet, “Epigenetic regulation of aging stem cells,” *Oncogene*, vol. 30, no. 28, pp. 3105–26, Jul. 2011.
- [22] L. Liu *et al.*, “Chromatin modifications as determinants of muscle stem cell quiescence and chronological aging,” *Cell Rep.*, vol. 4, no. 1, pp. 189–204, Jul. 2013.
- [23] A. D. Goldberg *et al.*, “Epigenetics: A Landscape Takes Shape,” *Cell*, vol. 128, no. 4, pp. 635–638, Feb. 2007.

- [24] Y. Kanfi *et al.*, "SIRT6 protects against pathological damage caused by diet-induced obesity," *Aging Cell*, vol. 9, no. 2, pp. 162–173, Apr. 2010.
- [25] R. Mostoslavsky *et al.*, "Genomic Instability and Aging-like Phenotype in the Absence of Mammalian SIRT6," *Cell*, vol. 124, no. 2, pp. 315–329, Jan. 2006.
- [26] L. Lapasset *et al.*, "Rejuvenating senescent and centenarian human cells by reprogramming through the pluripotent state.," *Genes Dev.*, vol. 25, no. 21, pp. 2248–53, Nov. 2011.
- [27] S. Mahmoudi and A. Brunet, "Aging and reprogramming: a two-way street.," *Curr. Opin. Cell Biol.*, vol. 24, no. 6, pp. 744–56, Dec. 2012.
- [28] G.-H. Liu *et al.*, "Recapitulation of premature ageing with iPSCs from Hutchinson-Gilford progeria syndrome.," *Nature*, vol. 472, no. 7342, pp. 221–5, Apr. 2011.
- [29] T. A. Rando and H. Y. Chang, "Aging, rejuvenation, and epigenetic reprogramming: resetting the aging clock.," *Cell*, vol. 148, no. 1–2, pp. 46–57, Jan. 2012.
- [30] A. Ocampo *et al.*, "In Vivo Amelioration of Age-Associated Hallmarks by Partial Reprogramming.," *Cell*, vol. 167, no. 7, p. 1719–1733.e12, Dec. 2016.
- [31] J. H. J. Hoeijmakers, "DNA damage, aging, and cancer.," *N. Engl. J. Med.*, vol. 361, no. 15, pp. 1475–85, Oct. 2009.
- [32] S. Q. Gregg *et al.*, "A mouse model of accelerated liver aging caused by a defect in DNA repair," *Hepatology*, vol. 55, no. 2, pp. 609–621, Feb. 2012.
- [33] M. Murga *et al.*, "A mouse model of ATR-Seckel shows embryonic replicative stress and accelerated aging," *Nat. Genet.*, vol. 41, no. 8, pp. 891–898, Aug. 2009.
- [34] A. A. Moskalev *et al.*, "The role of DNA damage and repair in aging through the prism of Koch-like criteria.," *Ageing Res. Rev.*, vol. 12, no. 2, pp. 661–84, Mar. 2013.
- [35] F. Faggioli, T. Wang, J. Vijg, and C. Montagna, "Chromosome-specific accumulation of aneuploidy in the aging mouse brain.," *Hum. Mol. Genet.*, vol. 21, no. 24, pp. 5246–53, Dec. 2012.
- [36] L. A. Forsberg *et al.*, "Age-related somatic structural changes in the nuclear genome of

- human blood cells," *Am. J. Hum. Genet.*, vol. 90, no. 2, pp. 217–228, Feb. 2012.
- [37] A. Musacchio and E. D. Salmon, "The spindle-assembly checkpoint in space and time.," *Nat. Rev. Mol. Cell Biol.*, vol. 8, no. 5, pp. 379–93, May 2007.
- [38] D. J. Baker *et al.*, "BubR1 insufficiency causes early onset of aging-associated phenotypes and infertility in mice.," *Nat. Genet.*, vol. 36, no. 7, pp. 744–9, Jul. 2004.
- [39] D. J. Baker *et al.*, "Increased expression of BubR1 protects against aneuploidy and cancer and extends healthy lifespan," *Nat. Cell Biol.*, vol. 15, no. 1, pp. 96–102, Dec. 2012.
- [40] A. Kowald and T. B. Kirkwood, "A network theory of ageing: the interactions of defective mitochondria, aberrant proteins, free radicals and scavengers in the ageing process.," *Mutat. Res.*, vol. 316, no. 5–6, pp. 209–36, May 1996.
- [41] V. N. Gladyshev, "The origin of aging: imperfectness-driven non-random damage defines the aging process and control of lifespan.," *Trends Genet.*, vol. 29, no. 9, pp. 506–12, Sep. 2013.
- [42] O. R. Jones *et al.*, "Diversity of ageing across the tree of life," *Nature*, vol. 505, no. 7482, pp. 169–173, Dec. 2013.
- [43] T. Bilinski, A. Bylak, and R. Zadrag-Tecza, "Principles of alternative gerontology.," *Aging (Albany. NY)*, vol. 8, no. 4, pp. 589–602, Apr. 2016.
- [44] D. HARMAN, "Aging: a theory based on free radical and radiation chemistry.," *J. Gerontol.*, vol. 11, no. 3, pp. 298–300, Jul. 1956.
- [45] K. B. Beckman and B. N. Ames, "The free radical theory of aging matures.," *Physiol. Rev.*, vol. 78, no. 2, pp. 547–81, Apr. 1998.
- [46] S. Miwa, K. Riyahi, L. Partridge, and M. D. Brand, "Lack of correlation between mitochondrial reactive oxygen species production and life span in *Drosophila*," *Ann. N. Y. Acad. Sci.*, vol. 1019, no. 1, pp. 388–91, Jun. 2004.
- [47] A. K. BRUNET ROSSINNI, "Testing the Free Radical Theory of Aging in Bats," *Ann. N. Y. Acad. Sci.*, vol. 1019, no. 1, pp. 506–508, Jun. 2004.

- [48] T. R. Golden, D. A. Hinerfeld, and S. Melov, "Oxidative stress and aging: beyond correlation.," *Aging Cell*, vol. 1, no. 2, pp. 117–23, Dec. 2002.
- [49] T. T. Huang, E. J. Carlson, A. M. Gillespie, Y. Shi, and C. J. Epstein, "Ubiquitous overexpression of CuZn superoxide dismutase does not extend life span in mice.," *J. Gerontol. A. Biol. Sci. Med. Sci.*, vol. 55, no. 1, pp. B5-9, Jan. 2000.
- [50] E. Dufour and N.-G. Larsson, "Understanding aging: revealing order out of chaos.," *Biochim. Biophys. Acta*, vol. 1658, no. 1–2, pp. 122–32, Jul. 2004.
- [51] V. N. Gladyshev, "The origin of aging: imperfectness-driven non-random damage defines the aging process and control of lifespan.," *Trends Genet.*, vol. 29, no. 9, pp. 506–12, Sep. 2013.
- [52] G. FAILLA, "The aging process and cancerogenesis.," *Ann. N. Y. Acad. Sci.*, vol. 71, no. 6, pp. 1124–40, Sep. 1958.
- [53] G. M. Martin, A. C. Smith, D. J. Ketterer, C. E. Ogburn, and C. M. Disteché, "Increased chromosomal aberrations in first metaphases of cells isolated from the kidneys of aged mice.," *Isr. J. Med. Sci.*, vol. 21, no. 3, pp. 296–301, Mar. 1985.
- [54] T. Lu *et al.*, "Gene regulation and DNA damage in the ageing human brain.," *Nature*, vol. 429, no. 6994, pp. 883–91, Jun. 2004.
- [55] M. Hyun, J. Lee, K. Lee, A. May, V. A. Bohr, and B. Ahn, "Longevity and resistance to stress correlate with DNA repair capacity in *Caenorhabditis elegans*.," *Nucleic Acids Res.*, vol. 36, no. 4, pp. 1380–9, Mar. 2008.
- [56] G. M. Martin and J. Oshima, "Lessons from human progeroid syndromes.," *Nature*, vol. 408, no. 6809, pp. 263–6, Nov. 2000.
- [57] A. A. Freitas, O. Vasieva, and J. P. de Magalhães, "A data mining approach for classifying DNA repair genes into ageing-related or non-ageing-related.," *BMC Genomics*, vol. 12, no. 1, p. 27, Jan. 2011.
- [58] R. Zoncu, A. Efeyan, and D. M. Sabatini, "mTOR: from growth signal integration to cancer, diabetes and ageing.," *Nat. Rev. Mol. Cell Biol.*, vol. 12, no. 1, pp. 21–35, Jan. 2011.

## List of references

- [59] T. Misteli and E. Soutoglou, "The emerging role of nuclear architecture in DNA repair and genome maintenance," *Nat. Rev. Mol. Cell Biol.*, vol. 10, no. 4, pp. 243–254, Apr. 2009.
- [60] R. D. Kornberg, "Structure of Chromatin," *Annu. Rev. Biochem.*, vol. 46, no. 1, pp. 931–954, Jun. 1977.
- [61] M. Kulis and M. Esteller, "DNA Methylation and Cancer," in *Advances in genetics*, vol. 70, 2010, pp. 27–56.
- [62] T. Kouzarides, "Chromatin Modifications and Their Function," *Cell*, vol. 128, no. 4, pp. 693–705, Feb. 2007.
- [63] E. P. Rogakou, D. R. Pilch, A. H. Orr, V. S. Ivanova, and W. M. Bonner, "DNA double-stranded breaks induce histone H2AX phosphorylation on serine 139.," *J. Biol. Chem.*, vol. 273, no. 10, pp. 5858–68, Mar. 1998.
- [64] S. E. Polo and S. P. Jackson, "Dynamics of DNA damage response proteins at DNA breaks: a focus on protein modifications.," *Genes Dev.*, vol. 25, no. 5, pp. 409–33, Mar. 2011.
- [65] S. Panier and S. J. Boulton, "Double-strand break repair: 53BP1 comes into focus.," *Nat. Rev. Mol. Cell Biol.*, vol. 15, no. 1, pp. 7–18, Jan. 2014.
- [66] C. B. Bennett, A. L. Lewis, K. K. Baldwin, and M. A. Resnick, "Lethality induced by a single site-specific double-strand break in a dispensable yeast plasmid.," *Proc. Natl. Acad. Sci. U. S. A.*, vol. 90, no. 12, pp. 5613–7, Jun. 1993.
- [67] L. L. Sandell and V. A. Zakian, "Loss of a yeast telomere: arrest, recovery, and chromosome loss.," *Cell*, vol. 75, no. 4, pp. 729–39, Nov. 1993.
- [68] M. R. Lieber, "The mechanism of double-strand DNA break repair by the nonhomologous DNA end-joining pathway.," *Annu. Rev. Biochem.*, vol. 79, no. 1, pp. 181–211, Jun. 2010.
- [69] A. Kakarougkas and P. A. Jeggo, "DNA DSB repair pathway choice: an orchestrated handover mechanism.," *Br. J. Radiol.*, vol. 87, no. 1035, p. 20130685, Mar. 2014.

- [70] K. Rothkamm, I. Krüger, L. H. Thompson, and M. Löbrich, "Pathways of DNA double-strand break repair during the mammalian cell cycle.," *Mol. Cell. Biol.*, vol. 23, no. 16, pp. 5706–15, Aug. 2003.
- [71] Z. MAO, M. BOZZELLA, A. SELUANOV, and V. GORBUNOVA, "Comparison of nonhomologous end joining and homologous recombination in human cells," *DNA Repair (Amst)*, vol. 7, no. 10, pp. 1765–1771, Oct. 2008.
- [72] M. R. Lieber, "The Mechanism of Double-Strand DNA Break Repair by the Nonhomologous DNA End-Joining Pathway," *Annu. Rev. Biochem.*, vol. 79, no. 1, pp. 181–211, Jun. 2010.
- [73] M. McVey and S. E. Lee, "MMEJ repair of double-strand breaks (director's cut): deleted sequences and alternative endings," *Trends Genet.*, vol. 24, no. 11, pp. 529–538, Nov. 2008.
- [74] A. Decottignies, "Alternative end-joining mechanisms: a historical perspective," *Front. Genet.*, vol. 4, p. 48, 2013.
- [75] M. Wang *et al.*, "PARP-1 and Ku compete for repair of DNA double strand breaks by distinct NHEJ pathways," *Nucleic Acids Res.*, vol. 34, no. 21, pp. 6170–6182, Oct. 2006.
- [76] J. Della-Maria *et al.*, "Human Mre11/Human Rad50/Nbs1 and DNA Ligase III /XRCC1 Protein Complexes Act Together in an Alternative Nonhomologous End Joining Pathway," *J. Biol. Chem.*, vol. 286, no. 39, pp. 33845–33853, Sep. 2011.
- [77] H. Wang *et al.*, "DNA Ligase III as a Candidate Component of Backup Pathways of Nonhomologous End Joining," *Cancer Res.*, vol. 65, no. 10, pp. 4020–4030, May 2005.
- [78] M. Audebert, B. Salles, and P. Calsou, "Involvement of Poly(ADP-ribose) Polymerase-1 and XRCC1/DNA Ligase III in an Alternative Route for DNA Double-strand Breaks Rejoining," *J. Biol. Chem.*, vol. 279, no. 53, pp. 55117–55126, Dec. 2004.
- [79] L. N. Truong *et al.*, "Microhomology-mediated End Joining and Homologous Recombination share the initial end resection step to repair DNA double-strand breaks in mammalian cells," *Proc. Natl. Acad. Sci.*, vol. 110, no. 19, pp. 7720–7725, May 2013.

- [80] Z. Mao *et al.*, "SIRT6 Promotes DNA Repair Under Stress by Activating PARP1," *Science* (80- ), vol. 332, no. 6036, pp. 1443–1446, Jun. 2011.
- [81] J. Oshima, S. Huang, C. Pae, J. Campisi, and R. H. Schiestl, "Lack of WRN results in extensive deletion at nonhomologous joining ends.," *Cancer Res.*, vol. 62, no. 2, pp. 547–51, Jan. 2002.
- [82] J. R. Walker, R. A. Corpina, and J. Goldberg, "Structure of the Ku heterodimer bound to DNA and its implications for double-strand break repair.," *Nature*, vol. 412, no. 6847, pp. 607–14, Aug. 2001.
- [83] P. Grob *et al.*, "Electron microscopy visualization of DNA–protein complexes formed by Ku and DNA ligase IV," *DNA Repair (Amst.)*, vol. 11, no. 1, pp. 74–81, Jan. 2012.
- [84] M. B. Kastan and D. S. Lim, "The many substrates and functions of ATM.," *Nat. Rev. Mol. Cell Biol.*, vol. 1, no. 3, pp. 179–86, Dec. 2000.
- [85] I. M. Ward, K. Minn, K. G. Jorda, and J. Chen, "Accumulation of checkpoint protein 53BP1 at DNA breaks involves its binding to phosphorylated histone H2AX.," *J. Biol. Chem.*, vol. 278, no. 22, pp. 19579–82, May 2003.
- [86] S. J. Collis, T. L. DeWeese, P. A. Jeggo, and A. R. Parker, "The life and death of DNA-PK.," *Oncogene*, vol. 24, no. 6, pp. 949–61, Feb. 2005.
- [87] G. J. Williams, M. Hammel, S. K. Radhakrishnan, D. Ramsden, S. P. Lees-Miller, and J. A. Tainer, "Structural insights into NHEJ: building up an integrated picture of the dynamic DSB repair super complex, one component and interaction at a time.," *DNA Repair (Amst.)*, vol. 17, pp. 110–20, May 2014.
- [88] R. C. Getts and T. D. Stamato, "Absence of a Ku-like DNA end binding activity in the xrs double-strand DNA repair-deficient mutant.," *J. Biol. Chem.*, vol. 269, no. 23, pp. 15981–4, Jun. 1994.
- [89] K. Grube and A. Bürkle, "Poly(ADP-ribose) polymerase activity in mononuclear leukocytes of 13 mammalian species correlates with species-specific life span.," *Proc. Natl. Acad. Sci. U. S. A.*, vol. 89, no. 24, pp. 11759–63, Dec. 1992.
- [90] R. W. Hart and R. B. Setlow, "Correlation between deoxyribonucleic acid excision-

- repair and life-span in a number of mammalian species.," *Proc. Natl. Acad. Sci. U. S. A.*, vol. 71, no. 6, pp. 2169–73, Jun. 1974.
- [91] G. A. Cortopassi and E. Wang, "There is substantial agreement among interspecies estimates of DNA repair activity.," *Mech. Ageing Dev.*, vol. 91, no. 3, pp. 211–8, Nov. 1996.
- [92] D. E. Promislow, "DNA repair and the evolution of longevity: a critical analysis.," *J. Theor. Biol.*, vol. 170, no. 3, pp. 291–300, Oct. 1994.
- [93] Y. Gu *et al.*, "Growth retardation and leaky SCID phenotype of Ku70-deficient mice.," *Immunity*, vol. 7, no. 5, pp. 653–65, Nov. 1997.
- [94] H. Vogel, D. S. Lim, G. Karsenty, M. Finegold, and P. Hasty, "Deletion of Ku86 causes early onset of senescence in mice.," *Proc. Natl. Acad. Sci. U. S. A.*, vol. 96, no. 19, pp. 10770–5, Sep. 1999.
- [95] R. A. Busuttill *et al.*, "Effect of Ku80 Deficiency on Mutation Frequencies and Spectra at a LacZ Reporter Locus in Mouse Tissues and Cells," *PLoS One*, vol. 3, no. 10, p. e3458, Oct. 2008.
- [96] H. Li, H. Vogel, V. B. Holcomb, Y. Gu, and P. Hasty, "Deletion of Ku70, Ku80, or Both Causes Early Aging without Substantially Increased Cancer," *Mol. Cell. Biol.*, vol. 27, no. 23, pp. 8205–8214, Dec. 2007.
- [97] A. Ozgenc and L. A. Loeb, "Current advances in unraveling the function of the Werner syndrome protein," *Mutat. Res. Mol. Mech. Mutagen.*, vol. 577, no. 1–2, pp. 237–251, Sep. 2005.
- [98] A. Vaidya, Z. Mao, X. Tian, B. Spencer, A. Seluanov, and V. Gorbunova, "Knock-in reporter mice demonstrate that DNA repair by non-homologous end joining declines with age.," *PLoS Genet.*, vol. 10, no. 7, p. e1004511, Jul. 2014.
- [99] J. E. FitzGerald, M. Grenon, and N. F. Lowndes, "53BP1: function and mechanisms of focal recruitment," *Biochem. Soc. Trans.*, vol. 37, no. 4, 2009.
- [100] K. Iwabuchi, P. L. Bartel, B. Li, R. Marraccino, and S. Fields, "Two cellular proteins that bind to wild-type but not mutant p53.," *Proc. Natl. Acad. Sci. U. S. A.*, vol. 91, no. 13,

- pp. 6098–102, Jun. 1994.
- [101] R. Cuella-Martin, C. Oliveira, H. E. Lockstone, S. Snellenberg, N. Grolmusova, and J. R. Chapman, “53BP1 Integrates DNA Repair and p53-Dependent Cell Fate Decisions via Distinct Mechanisms,” *Mol. Cell*, vol. 64, no. 1, pp. 51–64, Oct. 2016.
- [102] S. Difilippantonio *et al.*, “53BP1 facilitates long-range DNA end-joining during V(D)J recombination,” *Nature*, vol. 456, no. 7221, pp. 529–33, Nov. 2008.
- [103] J. P. Manis, J. C. Morales, Z. Xia, J. L. Kutok, F. W. Alt, and P. B. Carpenter, “53BP1 links DNA damage-response pathways to immunoglobulin heavy chain class-switch recombination,” *Nat. Immunol.*, vol. 5, no. 5, pp. 481–487, May 2004.
- [104] I. M. Ward *et al.*, “53BP1 is required for class switch recombination,” *J. Cell Biol.*, vol. 165, no. 4, pp. 459–464, May 2004.
- [105] J. P. Manis, J. C. Morales, Z. Xia, J. L. Kutok, F. W. Alt, and P. B. Carpenter, “53BP1 links DNA damage-response pathways to immunoglobulin heavy chain class-switch recombination,” *Nat. Immunol.*, vol. 5, no. 5, pp. 481–7, May 2004.
- [106] A. Fradet-Turcotte *et al.*, “53BP1 is a reader of the DNA-damage-induced H2A Lys 15 ubiquitin mark,” *Nature*, vol. 499, no. 7456, pp. 50–4, Jul. 2013.
- [107] H. Pei *et al.*, “MMSET regulates histone H4K20 methylation and 53BP1 accumulation at DNA damage sites,” *Nature*, vol. 470, no. 7332, pp. 124–8, Feb. 2011.
- [108] J. C. Morales *et al.*, “53BP1 and p53 synergize to suppress genomic instability and lymphomagenesis,” *Proc. Natl. Acad. Sci. U. S. A.*, vol. 103, no. 9, pp. 3310–5, Feb. 2006.
- [109] I. M. Ward *et al.*, “53BP1 Cooperates with p53 and Functions as a Haploinsufficient Tumor Suppressor in Mice,” *Mol. Cell. Biol.*, vol. 25, no. 22, pp. 10079–10086, Nov. 2005.
- [110] I. M. Ward, K. Minn, J. van Deursen, and J. Chen, “p53 Binding protein 53BP1 is required for DNA damage responses and tumor suppression in mice,” *Mol. Cell. Biol.*, vol. 23, no. 7, pp. 2556–63, Apr. 2003.

- [111] L. B. Schultz, N. H. Chehab, A. Malikzay, and T. D. Halazonetis, "p53 binding protein 1 (53BP1) is an early participant in the cellular response to DNA double-strand breaks.," *J. Cell Biol.*, vol. 151, no. 7, pp. 1381–90, Dec. 2000.
- [112] T. Nikolova *et al.*, "The  $\gamma$ H2AX assay for genotoxic and nongenotoxic agents: comparison of H2AX phosphorylation with cell death response.," *Toxicol. Sci.*, vol. 140, no. 1, pp. 103–17, Jul. 2014.
- [113] R. A. DiTullio *et al.*, "53BP1 functions in an ATM-dependent checkpoint pathway that is constitutively activated in human cancer.," *Nat. Cell Biol.*, vol. 4, no. 12, pp. 998–1002, Dec. 2002.
- [114] E. Marková, N. Schultz, and I. Y. Belyaev, "Kinetics and dose-response of residual 53BP1/gamma-H2AX foci: co-localization, relationship with DSB repair and clonogenic survival.," *Int. J. Radiat. Biol.*, vol. 83, no. 5, pp. 319–29, May 2007.
- [115] M. Podhorecka, A. Skladanowski, and P. Bozko, "H2AX Phosphorylation: Its Role in DNA Damage Response and Cancer Therapy," *J. Nucleic Acids*, vol. 2010, pp. 1–9, Aug. 2010.
- [116] U. Herbig, M. Ferreira, L. Condell, D. Carey, and J. M. Sedivy, "Cellular senescence in aging primates.," *Science*, vol. 311, no. 5765, p. 1257, Mar. 2006.
- [117] R. Carbone, M. Pearson, S. Minucci, and P. G. Pelicci, "PML NBs associate with the hMre11 complex and p53 at sites of irradiation induced DNA damage.," *Oncogene*, vol. 21, no. 11, pp. 1633–40, Mar. 2002.
- [118] Z.-X. Xu, A. Timanova-Atanasova, R.-X. Zhao, and K.-S. Chang, "PML colocalizes with and stabilizes the DNA damage response protein TopBP1.," *Mol. Cell. Biol.*, vol. 23, no. 12, pp. 4247–56, Jun. 2003.
- [119] N. Stuurman, A. M. Meijne, A. J. van der Pol, L. de Jong, R. van Driel, and J. van Renswoude, "The nuclear matrix from cells of different origin. Evidence for a common set of matrix proteins.," *J. Biol. Chem.*, vol. 265, no. 10, pp. 5460–5, Apr. 1990.
- [120] R. Bernardi and P. P. Pandolfi, "Structure, dynamics and functions of promyelocytic leukaemia nuclear bodies," *Nat. Rev. Mol. Cell Biol.*, vol. 8, no. 12, pp. 1006–1016,

- Dec. 2007.
- [121] F. Rodier *et al.*, “DNA-SCARS: distinct nuclear structures that sustain damage-induced senescence growth arrest and inflammatory cytokine secretion.,” *J. Cell Sci.*, vol. 124, no. Pt 1, pp. 68–81, Jan. 2011.
- [122] F. Rodier *et al.*, “Persistent DNA damage signalling triggers senescence-associated inflammatory cytokine secretion.,” *Nat. Cell Biol.*, vol. 11, no. 8, pp. 973–9, Aug. 2009.
- [123] C. Rosefort, E. Fauth, and H. Zankl, “Micronuclei induced by aneugens and clastogens in mononucleate and binucleate cells using the cytokinesis block assay.,” *Mutagenesis*, vol. 19, no. 4, pp. 277–84, Jul. 2004.
- [124] S. Sellappa, M. Balakrishnan, S. Raman, and S. Palanisamy, “Induction of micronuclei in buccal mucosa on chewing a mixture of betel leaf, areca nut and tobacco.,” *J. Oral Sci.*, vol. 51, no. 2, pp. 289–92, Jun. 2009.
- [125] O. Torres-Bugarín, R. Covarrubias-Bugarín, A. L. Zamora-Perez, B. M. G. Torres-Mendoza, M. García-Ulloa, and F. G. Martínez-Sandoval, “Anabolic androgenic steroids induce micronuclei in buccal mucosa cells of bodybuilders.,” *Br. J. Sports Med.*, vol. 41, no. 9, p. 592–6; discussion 596, Sep. 2007.
- [126] H. Tinwell and J. Ashby, “Micronucleus morphology as a means to distinguish aneugens and clastogens in the mouse bone marrow micronucleus assay.,” *Mutagenesis*, vol. 6, no. 3, pp. 193–8, May 1991.
- [127] P. Thomas and M. Fenech, “Cytokinesis-block micronucleus cytome assay in lymphocytes.,” *Methods Mol. Biol.*, vol. 682, pp. 217–34, 2011.
- [128] M. Fenech and A. A. Morley, “Measurement of micronuclei in lymphocytes.,” *Mutat. Res.*, vol. 147, no. 1–2, pp. 29–36.
- [129] K. Rothkamm, S. Barnard, J. Moquet, M. Ellender, Z. Rana, and S. Burdak-Rothkamm, “DNA damage foci: Meaning and significance.,” *Environ. Mol. Mutagen.*, vol. 56, no. 6, pp. 491–504, Jul. 2015.
- [130] N. Dimitrova, Y.-C. M. Chen, D. L. Spector, and T. de Lange, “53BP1 promotes non-homologous end joining of telomeres by increasing chromatin mobility.,” *Nature*, vol.

- 456, no. 7221, pp. 524–8, Nov. 2008.
- [131] O. Fernandez-Capetillo *et al.*, “DNA damage-induced G2-M checkpoint activation by histone H2AX and 53BP1.,” *Nat. Cell Biol.*, vol. 4, no. 12, pp. 993–7, Dec. 2002.
- [132] B. Wang, S. Matsuoka, P. B. Carpenter, and S. J. Elledge, “53BP1, a mediator of the DNA damage checkpoint.,” *Science*, vol. 298, no. 5597, pp. 1435–8, Nov. 2002.
- [133] R. Cescutti, S. Negrini, M. Kohzaki, and T. D. Halazonetis, “TopBP1 functions with 53BP1 in the G1 DNA damage checkpoint,” *EMBO J.*, vol. 29, no. 21, pp. 3723–3732, Nov. 2010.
- [134] L. S. Fink *et al.*, “53BP1 contributes to a robust genomic stability in human fibroblasts.,” *Aging (Albany. NY).*, vol. 3, no. 9, pp. 836–45, Sep. 2011.
- [135] S. Soubeyrand, L. Pope, and R. J. G. Haché, “Topoisomerase IIalpha-dependent induction of a persistent DNA damage response in response to transient etoposide exposure.,” *Mol. Oncol.*, vol. 4, no. 1, pp. 38–51, Feb. 2010.
- [136] I. H. Goldberg, “Free radical mechanisms in neocarzinostatin-induced DNA damage.,” *Free Radic. Biol. Med.*, vol. 3, no. 1, pp. 41–54, 1987.
- [137] L. Dostál, W. M. Kohler, J. E. Penner-Hahn, R. A. Miller, and C. A. Fierke, “Fibroblasts from long-lived rodent species exclude cadmium.,” *J. Gerontol. A. Biol. Sci. Med. Sci.*, vol. 70, no. 1, pp. 10–9, Jan. 2015.
- [138] D. G. Gibson *et al.*, “Creation of a bacterial cell controlled by a chemically synthesized genome.,” *Science*, vol. 329, no. 5987, pp. 52–6, Jul. 2010.
- [139] A. Bürkle, “In memoriam Bernard Strehler--genomic instability in ageing: a persistent challenge.,” *Mech. Ageing Dev.*, vol. 123, no. 8, pp. 899–906, Apr. 2002.
- [140] M. Soffritti *et al.*, “Life-span carcinogenicity studies on Sprague-Dawley rats exposed to  $\gamma$ -radiation: design of the project and report on the tumor occurrence after post-natal radiation exposure (6 weeks of age) delivered in a single acute exposure.,” *Am. J. Ind. Med.*, vol. 58, no. 1, pp. 46–60, Jan. 2015.
- [141] R. D. Wood, M. Mitchell, and T. Lindahl, “Human DNA repair genes, 2005.,” *Mutat.*

- Res.*, vol. 577, no. 1–2, pp. 275–83, Sep. 2005.
- [142] A. Kaya, A. V. Lobanov, and V. N. Gladyshev, “Evidence that mutation accumulation does not cause aging in *Saccharomyces cerevisiae*,” *Aging Cell*, vol. 14, no. 3, pp. 366–371, Jun. 2015.
- [143] J. P. de Magalhães, J. Costa, and G. M. Church, “An analysis of the relationship between metabolism, developmental schedules, and longevity using phylogenetic independent contrasts.,” *J. Gerontol. A. Biol. Sci. Med. Sci.*, vol. 62, no. 2, pp. 149–60, Feb. 2007.
- [144] A. Lorenzini, T. Stamato, and C. Sell, “The disposable soma theory revisited: time as a resource in the theories of aging.,” *Cell Cycle*, vol. 10, no. 22, pp. 3853–6, Nov. 2011.
- [145] R. Tacutu *et al.*, “Human Ageing Genomic Resources: Integrated databases and tools for the biology and genetics of ageing,” *Nucleic Acids Res.*, vol. 41, no. D1, pp. D1027–D1033, Jan. 2013.
- [146] S. N. Austad, “Comparative Biology of Aging,” *Journals Gerontol. Ser. A Biol. Sci. Med. Sci.*, vol. 64A, no. 2, pp. 199–201, Feb. 2009.
- [147] S. Bonassi *et al.*, “The HUman MicroNucleus project on exfoLIated buccal cells (HUMN(XL)): the role of life-style, host factors, occupational exposures, health status, and assay protocol.,” *Mutat. Res.*, vol. 728, no. 3, pp. 88–97, Nov. 2011.
- [148] L. Abramsson-Zetterberg, J. Grawé, and G. Zetterberg, “Spontaneous and radiation-induced micronuclei in erythrocytes from four species of wild rodents: a comparison with CBA mice.,” *Mutat. Res.*, vol. 393, no. 1–2, pp. 55–71, Sep. 1997.
- [149] W. Schmid, “The micronucleus test.,” *Mutat. Res.*, vol. 31, no. 1, pp. 9–15, Feb. 1975.
- [150] G. Krishna and M. Hayashi, “In vivo rodent micronucleus assay: protocol, conduct and data interpretation.,” *Mutat. Res.*, vol. 455, no. 1–2, pp. 155–66, Nov. 2000.
- [151] R. Schlegel and J. T. MacGregor, “The persistence of micronuclei in peripheral blood erythrocytes: detection of chronic chromosome breakage in mice.,” *Mutat. Res.*, vol. 104, no. 6, pp. 367–9, Jul. 1982.

- [152] F. Kalfalah *et al.*, "Structural chromosome abnormalities, increased DNA strand breaks and DNA strand break repair deficiency in dermal fibroblasts from old female human donors.," *Aging (Albany. NY)*, vol. 7, no. 2, pp. 110–22, Feb. 2015.
- [153] J. Tigges *et al.*, "The hallmarks of fibroblast ageing.," *Mech. Ageing Dev.*, vol. 138, pp. 26–44, Jun. 2014.
- [154] D. M. Waldera Lupa *et al.*, "Characterization of Skin Aging-Associated Secreted Proteins (SAASP) Produced by Dermal Fibroblasts Isolated from Intrinsically Aged Human Skin.," *J. Invest. Dermatol.*, vol. 135, no. 8, pp. 1954–68, Aug. 2015.
- [155] H. Takai *et al.*, "DNA damage foci at dysfunctional telomeres.," *Curr. Biol.*, vol. 13, no. 17, pp. 1549–56, Sep. 2003.
- [156] B. E. Peace and P. Succop, "Spontaneous micronucleus frequency and age: what are normal values?," *Mutat. Res.*, vol. 425, no. 2, pp. 225–30, Apr. 1999.
- [157] M. E. C. Waaijer *et al.*, "DNA damage markers in dermal fibroblasts in vitro reflect chronological donor age.," *Aging (Albany. NY)*, vol. 8, no. 1, pp. 147–157, Jan. 2016.
- [158] A. Lorenzini, M. Tresini, S. N. Austad, and V. J. Cristofalo, "Cellular replicative capacity correlates primarily with species body mass not longevity.," *Mech. Ageing Dev.*, vol. 126, no. 10, pp. 1130–3, Oct. 2005.
- [159] G. E. Gibson, B. Tofel-Grehl, K. Scheffold, V. J. Cristofalo, and J. P. Blass, "A reproducible procedure for primary culture and subsequent maintenance of multiple lines of human skin fibroblasts.," *Age (Omaha)*, vol. 21, no. 1, pp. 7–14, Jan. 1998.
- [160] F. M. Kalfalah *et al.*, "Spatio-temporal regulation of the human licensing factor Cdc6 in replication and mitosis.," *Cell Cycle*, vol. 14, no. 11, pp. 1704–15, Jun. 2015.
- [161] W. Gorczyca, J. Gong, B. Ardelt, F. Traganos, and Z. Darzynkiewicz, "The cell cycle related differences in susceptibility of HL-60 cells to apoptosis induced by various antitumor agents.," *Cancer Res.*, vol. 53, no. 13, pp. 3186–92, Jul. 1993.
- [162] P. L. Olive and J. P. Banáth, "The comet assay: a method to measure DNA damage in individual cells," *Nat. Protoc.*, vol. 1, no. 1, pp. 23–29, Jun. 2006.

- [163] B. M. Gyori, G. Venkatachalam, P. S. Thiagarajan, D. Hsu, and M.-V. Clement, "OpenComet: An automated tool for comet assay image analysis," *Redox Biol.*, vol. 2, pp. 457–465, 2014.
- [164] T. Mosmann, "Rapid colorimetric assay for cellular growth and survival: application to proliferation and cytotoxicity assays.," *J. Immunol. Methods*, vol. 65, no. 1–2, pp. 55–63, Dec. 1983.
- [165] L. Cong *et al.*, "Multiplex Genome Engineering Using CRISPR/Cas Systems," *Science (80-. )*, vol. 339, no. 6121, 2013.
- [166] J. D. Sander and J. K. Joung, "CRISPR-Cas systems for editing, regulating and targeting genomes," *Nat. Biotechnol.*, vol. 32, no. 4, pp. 347–355, Mar. 2014.
- [167] N. A. P. Franken, H. M. Rodermond, J. Stap, J. Haveman, and C. van Bree, "Clonogenic assay of cells in vitro.," *Nat. Protoc.*, vol. 1, no. 5, pp. 2315–9, Dec. 2006.
- [168] G. M. Zúñiga-González *et al.*, "Micronucleated erythrocyte frequencies in old and new world primates: measurement of micronucleated erythrocyte frequencies in peripheral blood of *Callithrix jacchus* as a model for evaluating genotoxicity in primates.," *Environ. Mol. Mutagen.*, vol. 46, no. 4, pp. 253–9, Dec. 2005.
- [169] S. B. Dass, S. F. Ali, R. H. Heflich, and D. A. Casciano, "Frequency of spontaneous and induced micronuclei in the peripheral blood of aging mice.," *Mutat. Res.*, vol. 381, no. 1, pp. 105–10, Nov. 1997.
- [170] E. Croco, S. Marchionni, and A. Lorenzini, "Genetic instability and aging under the scrutiny of comparative biology: a meta-analysis of spontaneous micronuclei frequency," *Mech. Ageing Dev.*, vol. 156, pp. 34–41, Jun. 2016.
- [171] G. Zúñiga *et al.*, "Spontaneous micronuclei in peripheral blood erythrocytes from 35 mammalian species.," *Mutat. Res.*, vol. 369, no. 1–2, pp. 123–7, Jul. 1996.
- [172] M. P. Ramírez-Muñoz *et al.*, "Evaluation of the micronucleus test in peripheral blood erythrocytes by use of the splenectomized model.," *Lab. Anim. Sci.*, vol. 49, no. 4, pp. 418–20, Aug. 1999.
- [173] G. M. Zúñiga-González *et al.*, "Micronucleated erythrocyte frequencies in old and new

- world primates: measurement of micronucleated erythrocyte frequencies in peripheral blood of *Callithrix jacchus* as a model for evaluating genotoxicity in primates.," *Environ. Mol. Mutagen.*, vol. 46, no. 4, pp. 253–9, Dec. 2005.
- [174] M. Cristaldi, L. Anna Ieradi, I. Udroui, and R. Zilli, "Comparative evaluation of background micronucleus frequencies in domestic mammals.," *Mutat. Res.*, vol. 559, no. 1–2, pp. 1–9, Apr. 2004.
- [175] J. R. Meier, P. Wernsing, and J. Torsella, "Feasibility of micronucleus methods for monitoring genetic damage in two feral species of small mammals.," *Environ. Mol. Mutagen.*, vol. 33, no. 3, pp. 219–25, 1999.
- [176] G. P. Dimri *et al.*, "A biomarker that identifies senescent human cells in culture and in aging skin in vivo.," *Proc. Natl. Acad. Sci. U. S. A.*, vol. 92, no. 20, pp. 9363–7, Sep. 1995.
- [177] C. L. Nguyen, R. Possemato, E. L. Bauerlein, A. Xie, R. Scully, and W. C. Hahn, "Nek4 regulates entry into replicative senescence and the response to DNA damage in human fibroblasts.," *Mol. Cell. Biol.*, vol. 32, no. 19, pp. 3963–77, Oct. 2012.
- [178] P.-O. Mari *et al.*, "Dynamic assembly of end-joining complexes requires interaction between Ku70/80 and XRCC4.," *Proc. Natl. Acad. Sci. U. S. A.*, vol. 103, no. 49, pp. 18597–602, Dec. 2006.
- [179] M. Hayashi *et al.*, "In vivo erythrocyte micronucleus assay III. Validation and regulatory acceptance of automated scoring and the use of rat peripheral blood reticulocytes, with discussion of non-hematopoietic target cells and a single dose-level limit test.," *Mutat. Res.*, vol. 627, no. 1, pp. 10–30, Feb. 2007.
- [180] I. Udroui, "Feasibility of conducting the micronucleus test in circulating erythrocytes from different mammalian species: an anatomical perspective.," *Environ. Mol. Mutagen.*, vol. 47, no. 9, pp. 643–6, Dec. 2006.
- [181] J. R. Speakman, "Correlations between physiology and lifespan--two widely ignored problems with comparative studies.," *Aging Cell*, vol. 4, no. 4, pp. 167–75, Aug. 2005.
- [182] A. Seluanov, D. Mittelman, O. M. Pereira-Smith, J. H. Wilson, and V. Gorbunova, "DNA

- end joining becomes less efficient and more error-prone during cellular senescence,” *Proc. Natl. Acad. Sci.*, vol. 101, no. 20, pp. 7624–7629, May 2004.
- [183] C. Garm *et al.*, “Age and gender effects on DNA strand break repair in peripheral blood mononuclear cells,” *Aging Cell*, vol. 12, no. 1, pp. 58–66, Feb. 2013.
- [184] F. d’Adda di Fagagna *et al.*, “A DNA damage checkpoint response in telomere-initiated senescence,” *Nature*, vol. 426, no. 6963, pp. 194–198, Nov. 2003.
- [185] G. Ferbeyre, E. de Stanchina, E. Querido, N. Baptiste, C. Prives, and S. W. Lowe, “PML is induced by oncogenic ras and promotes premature senescence.,” *Genes Dev.*, vol. 14, no. 16, pp. 2015–27, Aug. 2000.
- [186] M. Pearson *et al.*, “PML regulates p53 acetylation and premature senescence induced by oncogenic Ras.,” *Nature*, vol. 406, no. 6792, pp. 207–10, Jul. 2000.
- [187] K. Healy *et al.*, “Ecology and mode-of-life explain lifespan variation in birds and mammals.,” *Proceedings. Biol. Sci.*, vol. 281, no. 1784, p. 20140298, Jun. 2014.
- [188] M. Sulak *et al.*, “Correction: TP53 copy number expansion is associated with the evolution of increased body size and an enhanced DNA damage response in elephants,” *Elife*, vol. 5, Dec. 2016.
- [189] A. Lorenzini, L. S. Fink, T. Stamato, C. Torres, and C. Sell, “Relationship of spindle assembly checkpoint fidelity to species body mass, lifespan, and developmental rate,” *Aging (Albany. NY.)*, vol. 3, no. 12, pp. 1206–1212, Dec. 2011.
- [190] A. A. Freitas and J. P. de Magalhães, “A review and appraisal of the DNA damage theory of ageing,” *Mutat. Res. Mutat. Res.*, vol. 728, no. 1–2, pp. 12–22, Jul. 2011.
- [191] G. Lattanzi *et al.*, “Lamins are rapamycin targets that impact human longevity: a study in centenarians.,” *J. Cell Sci.*, vol. 127, no. Pt 1, pp. 147–57, Jan. 2014.
- [192] H. Willers *et al.*, “DNA Damage Response Assessments in Human Tumor Samples Provide Functional Biomarkers of Radiosensitivity.,” *Semin. Radiat. Oncol.*, vol. 25, no. 4, pp. 237–50, Oct. 2015.
- [193] C. Bourcier *et al.*, “Late side-effects after curative intent radiotherapy: Identification

of hypersensitive patients for personalized strategy.," *Crit. Rev. Oncol. Hematol.*, vol. 93, no. 3, pp. 312–9, Mar. 2015.

- [194] Sato *et al.*, "Effect of aging on spontaneous micronucleus frequencies in peripheral blood of nine mouse strains: the results of the 7th collaborative study organized by CSGMT/JEMS.MMS". Collaborative Study Group for the Micronucleus Test. Environmental Mutagen Society, 1995.